

MICROBIAL ECOLOGY AND GENETICS OF BENZALKONIUM CHLORIDE
BIOTRANSFORMATION IN THE ENVIRONMENT

by

Emine Ertekin

B.S. in Biology, Marmara University, 2008

M.S. in Environmental Sciences, Bogazici University, 2011

Submitted to the Institute of Environmental Sciences in partial fulfillment of

the requirements for the degree of

Doctor

of

Philosophy

Boğaziçi University

2017

ACKNOWLEDGEMENTS

MICROBIAL ECOLOGY AND GENETICS OF BENZALKONIUM CHLORIDE BIOTRANSFORMATION IN THE ENVIRONMENT

Contamination of the environment with biocides such as quaternary ammonium compounds (QACs) has been associated with many public health and environmental hazards such as proliferation of antimicrobial resistance and ecotoxicity. The biodegradation of benzalkonium chloride (BAC), the most commonly used type of QAC biocides, is initiated with the conversion of BAC to benzyldimethyl amine (BDMA) via an N-dealkylation reaction. This reaction removes the biocidal activity of the BAC thus eliminates its impact in the environment. Although BAC N-dealkylation is the major bioreaction that detoxifies the QACs in the environment, structure of BAC degrading microbial communities are not fully understood. In addition, BAC degrading microorganisms along with the genes underlying the BAC degradation pathway remain poorly elucidated.

In this study, the common structure of BAC degrading enrichment communities originating from different environments has been characterized. A novel species named *Pseudomonas* sp. BIOMIG1, which degrades BACs, was predominant in all of these communities. Whole genomes of four BIOMIG1 phenotypes differ from each other with respect to the steps achieved in BAC degradation pathway, i.e., a complete BAC degrader, a BDMA accumulator, a BDMA degrader and a non degrader, were sequenced and compared. The results revealed that a gene cluster specific to the former two strains was likely involved in converting BAC to BDMA, which is the key step in the pathway. This gene cluster consisted of genes encoding two major facilitator superfamily (MFS) type transport proteins, a transcriptional regulator, a Rieske oxygenase, a sterol binding protein, two hypothetical proteins, and an integrase. The identified Rieske oxygenase was the only catabolic gene that was homologous to those transforming QAC-like compounds. Nonetheless this enzyme had low sequence identity (~30% amino acid identity) to its closest biochemically characterized relatives and was named oxyBAC. *E. coli* transformed with oxyBAC could transform BAC into equimolar amounts of BDMA, confirming its function as a novel enzyme catalyzing an unusual dealkylation reaction.

ÇEVREDE BENZALKONYUM BİLEŞİĞİ BİYODEGRADASYONUNUN MİKROBİYAL EKOLOJİSİ VE GENETİK ALTYAPISI

Antimikrobiyal özellikte olan dördüncül amonyum bileşiklerinin (DAB) çevreye salınmaları ekotoksisite ve antimikrobiyal direncinin yayılması gibi problemlere sebep olmaktadır. DAB ların en sık kullanılan alt grubu benzalkonyum klorürlerin (BAK) biyodegradasyonu sırasında BAK önce bir N-dealkilasyonu ile benzil dimetil amine (BDA) dönüşür daha sonra dimetil amin ve metil amin oluşur. Bu reaksiyon sonucunda BAK lar antimikrobiyal özelliklerini ve dolayısıyla çevreye olan etkilerini kaybederler. BAK biyodegradasyonu biyokimyasal olarak bilinmekle birlikte, çevrede biyodegradasyonu gerçekleştiren mikrobiyal komuniteler ilgili çok az şey bilinmektedir. Buna ek olarak, biyodegradasyonu gerçekleştiren bakteriler ile biyodegradasyonun altında yatan genler hâlâ tam olarak anlaşılamamıştır.

Bu çalışmada, dört farklı ortamdan alınıp BAK ile zenginleştirilen ve BAK ları degrade edebilen mikrobiyal komunitelerdeki ortak yapı ortaya çıkartılmıştır. Bu komunitelerde BAK degradasyonunu gerçekleştiren yeni bir *Pseudomonas* türü baskın hale gelmiştir. Bu *Pseudomonas* türü “BIOMIG1” olarak adlandırılmıştır. BAK biyodegradasyonunun gerçekleşmesinde rol oynayan genleri tespit edebilmek için, önce biyodegradasyonun farklı kademelerini gerçekleştirebilen ya da hiçbirini gerçekleştiremeyen dört BIOMIG1 fenotipi elde edilmiştir. Daha sonra bu bakterilerin tüm genomları sekanslanmış ve karşılaştırılmışlardır. Karşılaştırmanın sonucunda içinde iki tane taşıyıcı (transporter), bir transkripsiyon regülatörü bir Rieske tipi oksijenaz, bir integraz ve üç tane fonksiyonu tam bilinmeyen gen olan gen kümesinin BAK ı BDA ya dönüştürdüğü tespit edilmiştir. Bu gen kümesi içindeki Rieske oksijenaz tek katabolik gen olup ürettiği enzim diğer DAB ları degrade eden enzimlerle düşük seviyede homoloji göstermektedir (~30% amino asit benzerliği). Bu enzim oxyBAC olarak adlandırılmış ve *E.coli* içerisine transfer edilmiştir. oxyBAK ı eksprese eden *E.coli* nin BAKı eşit oranda BDA ya dönüştürdüğü gösterilerek, fonksiyonu deneysel olarak da kanıtlanmıştır.

TABLE OF CONTENTS

1.	BACKGROUND	1
1.1.	Biodegradation of Xenobiotics	5
1.1.1.	Catabolic Genes and Enzymes.....	5
1.1.2.	Microbial Diversity of Xenobiotic Biodegradation	19
1.1.3.	Biotransformation of Quaternary Ammonium Compounds	23
2.	MICROBIAL COMPOSITION AND FUNCTIONS IN BENZALKONIUM CHLORIDE DEGRADING COMMUNITIES	30
2.1.	Introduction.....	30
2.2.	Materials and Methods.....	32
2.2.1.	Chemicals.....	32
2.2.2.	Analytical Methods.....	33
2.2.3.	Enrichment of BAC Degrading Microbial Communities	33
2.2.4.	Metagenome Sequencing and Analysis of the Enrichment Communities 35	
2.2.5.	Identification of Functions Specific to BAC Degradation in the Enriched Community Metagenomes	38
2.3.	Result and Discussion	41
2.3.1.	Phylogenetic Diversity of BAC-Enriched Microbial Communities	41
2.3.2.	Core Functions in BAC Degrading Microbial Consortia and Distinct Functions Related to BAC Degradation.....	48
3.	PHYLOGENETIC AND GENOMIC CLASSIFICATION OF A NOVEL PSEUDOMONAS THAT DEGRADES BENZALKONIUM CHLORIDES	56
3.1.	Introduction.....	56
3.2.	Materials and Methods.....	58
3.2.1.	Isolation and Characterization of BAC Degrading Microorganisms.....	58
3.2.2.	Scanning Electron Microscopy of <i>Pseudomonas</i> sp. BIOMIG1	60
3.2.3.	Determination of the Carbon Utilization Patterns of Microorganisms using BIOLOG GENIII™ Micro Plates	61

3.2.4.	Sequencing the Draft Genome of <i>Pseudomonas</i> sp. BIOMIG1 and Bioinformatics analysis	61
3.3.	Results and Discussion	63
3.3.1.	<i>Pseudomonas</i> sp. BIOMIG1 is the Prevalent BAC Degradator in the Environment.....	63
3.3.2.	Phenotypic Characterization of <i>Pseudomonas</i> sp. BIOMIG1	65
3.3.3.	Genome features of <i>Pseudomonas</i> sp. BIOMIG1	78
4.	CHARACTERIZATION OF THE GENES INVOLVED IN BENZALKONIUM CHLORIDE BIOTRANSFORMATION	90
4.1.	Introduction.....	90
4.2.	Materials and Methods.....	91
4.2.1.	Microorganisms	91
4.2.2.	Identification of the Genes Involved in BAC Biotransformation Pathway	92
4.2.3.	BAC Biotransformation Experiments with <i>Pseudomonas</i> sp. BIOMIG1	94
4.2.4.	Heterologous Expression of Genes in <i>E. coli</i>	94
4.3.	Results and Discussion	96
4.3.1.	Potential Genetic Determinants of BAC Biotransformation	96
4.3.2.	Phylogenetic Analysis and Classification of the Genes Involved in BAC Degradation Pathway	101
4.3.3.	<i>Pseudomonas</i> sp. BIOMIG1 with <i>oxyBAC</i> grows on BACs	105
4.3.4.	<i>E. coli</i> overexpressing <i>oxyBAC</i> gene converts BACs to BDMA.....	107
4.3.5.	<i>OxyBAC</i> is a unique N-dealkylating RO	109
5.	CONCLUSIONS AND PERSPECTIVES	112

LIST OF FIGURES

Figure 1.1. Typical reactions catalyzed by different ROs. (A) Dioxygenation of the benzene ring (B) Direct removal of the substituting group by dioxygenation (C) Monooxygenation	8
Figure 1.2. Classification of Rieske oxygenases according to the oxygenase subunit. Proteins were aligned using ClustalW and tree was constructed using Neighbour Joining method. Adapted from Nam et al. (2001)	10
Figure 1.3. Representative catabolic operon structure encoding ROs involved in the degradation xenobiotics.	14
Figure 1.4. Abundance of species involved in different pathways as represented in EAWAG-BBD	21
Figure 1.5. Taxonomic tree of the bacteria with groups heavily represented in the	22
Figure 1.6. QAC biodegradation pathways	24
Figure 1.7. Adaptation of microbial communities to QAC exposure. (A) QAC exposure kills susceptible bacteria (B) QAC resistance emerges. (C) QAC degradation genes evolve and they are integrated into MGEs. (D) Recruitment of degradation determinants enables bacteria to use QACs as a C and energy source and provides fitness advantage. (E) Assembly of complete QAC degradation pathway occurs.	28
Figure 2.1. Chemical structure of BACs used in this study. “n” is 12, 14 or 16	33
Figure 2.2. Illustration of dilution to extinction method used for enrichment of the communities. Pink bacteria indicate BAC degraders.	35
Figure 2.3. Pipeline used for processing metagenomic datasets	40
Figure 2.4. BAC degradation profiles in (A) Control and (B) AS, (C) SEW, (D) SOIL and (E) SEA enrichment communities	43
Figure 2.5. Relative abundance of bacterial genera present in the enriched microbial communities recovered by pyro- and shotgun sequencing of the genomic DNA	44

Figure 2.6. Phylogenetic relationship of the detected OTUs and their relative abundance in the communities. The abundance of an OTU in each community was summed up and this value was considered 100%. The abundance of that OTU in each community was divided by this total value and the result was represented as the relative percentage of that OTU in a particular community.....	45
Figure 2.7. Profiles of BAC utilization in (A) AS, (B) SEW, (C) SOIL and (D) SEA enrichment communities.....	46
Figure 2.8. Relationship between the biotransformation rate of enrichment communities and abundance of <i>Pseudomonas</i> spp. AS (yellow) SEW (green) SOIL (red) SEA (blue).....	47
Figure 2.9. Venn diagram showing the number common and distinct functions in enrichment cultures.....	49
Figure 2.10. Relative abundance of the functional categories in enriched microbial communities identified in SEED database.....	50
Figure 2.11. Unique functions of each community	51
Figure 2.12. Differentially abundant functions in BAC-enriched microbial communities compared to the controls: (A) Antimicrobial resistance; (B) Oxidative stress response; (C) Gene expression regulation; (D) Horizontal gene transfer; (E) Catabolic reactions; (F) Transport and (G) Protein metabolism. The log ₂ fold change was estimated as the log ₂ ratio of normalized counts between BAC-enriched and control samples. Significant differences in the relative abundance of proteins were determined with a negative binomial test.	52
Figure 3.1. Phylogenetic relationship of <i>P. sp.</i> BIOMIG1 (blue) with other QAC degrading species (red)	64
Figure 3.2. Scanning Electron Micrograph of <i>Pseudomonas</i> sp. BIOMIG1	65
Figure 3.3. Profiles of (A) C ₁₄ BDMA-Cl utilization and (B) O ₂ utilization and CO ₂ formation by <i>Pseudomonas</i> sp. BIOMIG1 under O ₂ limiting conditions in a closed serum bottle. Arrows show the y-axis of data points.	67
Figure 3.4. Correlation of O ₂ consumption with (A) BAC utilization and (B) CO ₂ formation by <i>Pseudomonas</i> sp. BIOMIG1	68

Figure 3.5. Profile of benzyl dimethyl amine (BDMA) utilization and dimethyl amine (DMA) formation by <i>Pseudomonas sp.</i> BIOMIG1	69
Figure 3.6. Pathway of BACs biodegradation by <i>Pseudomonas sp.</i> BIOMIG1.....	70
Figure 3.7. BAC degradation kinetics of <i>Pseudomonas. sp.</i> BIOMIG1 isolates. (A) <i>P. sp.</i> BIOMIG1-AS ^{BAC1} (B) <i>P.sp.</i> BIOMIG1-AS ^{BAC2} (C) <i>P.sp.</i> BIOMIG1-SEW ^{BAC} (D) <i>P.sp.</i> BIOMIG1-SEW ^{BDMA} (E) <i>P.sp.</i> BIOMIG1-SOIL ^{BAC} (F) <i>P.sp.</i> BIOMIG1-SOIL ^{BDMA} (G) <i>P.sp.</i> BIOMIG1-SEA ^{BAC} (H) <i>P.sp.</i> BIOMIG1-SEA ^{BDMA}	72
Figure 3.8. Dendogram showing the hierarchical clustering made according to the carbon utilization profiles of BIOMIG1.....	78
Figure 3.9. Phylogenetic tree constructed with the genome sequences of <i>P. sp.</i> BIOMIG1 and related microorganisms	80
Figure 3.10. Relative abundance of Level 1 and level 2 functional categories in the genome of BIOMIG1	83
Figure 3.11. Distinct proteins of BIOMIG1 that are related to (A) Multidrug efflux pumps (B) Oxidative stress response	86
Figure 3.12. Distinct proteins of BIOMIG1 related to (A) Catabolism of organics (B) Transfer of solutes (C) Regulation of gene expression.....	87
Figure 3.13. Distinct proteins of BIOMIG1 that are related with horizontal gene transfer.	89
Figure 4.1. Plasmid map used in the heterologous expression experiments.....	95
Figure 4.2. Comparison of (A) Contig_BAC1 with a similar contig in metagenome datasets of (B) SEW, SOIL and SEA, (C) AS and (D) river sediment (Contig B _{43d} _01683) communities. Genes are: (1) Hypothetical protein; (2) Single strand DNA binding protein; (3) Hypothetical protein; (4) IS21 family transposase; (5) IS21 family transposase; (6) Amine oxidase; (7) MFS transporter; (8) MFS transporter; (9) TetR family transcriptional regulator; (10) Rieske oxygenase; (11) Sterol binding domain protein; (12) Hypothetical protein; (13) LysR family transcriptional regulator and (14) Phage integrase family protein	97

Figure 4.3. Relationship between the abundance of <i>Pseudomonas</i> sp. and abundance of Contig_BAC1 represented as coverage. (Red) AS (Yellow) SEW (Green) SOIL (Blue) SEA	98
Figure 4.4. Contigs involved in BDMA degradation.....	100
Figure 4.5. Phylogenetic relationship of oxyBAC, ttmao, aox-bac, microbial Rieske type terminal oxygenases (Groups I-IV) and eukaryotic Rieske type choline monooxygenases. Benzylsuccinate synthase was used as the outgroup. Reactions show generalized mechanisms of oxidation of substrates by Rieske type oxygenases.	103
Figure 4.6. Reactions catalyzed by QAC degrading enzymes.....	104
Figure 4.7. Amplification of <i>oxy-BAC</i> from <i>P. sp.</i> BIOMIG1 phenotypes.	106
Figure 4.8. Profile of C ₁₂ BDMA-Cl utilization, BDMA formation and cell growth by (A) BIOMIG1 ^{BAC} , (B) BIOMIG1 ^{BDMA} , (C) BIOMIG1 ^{BD} and (D) BIOMIG1 ^N (Error bars represent one standard deviation of the means, <i>n</i> = 3).....	106
Figure 4.9. (A) <i>oxyBAC</i> PCR amplicons of two <i>E. coli</i> phenotypes on agarose gel. Profile of C ₁₂ BDMA-Cl utilization and BDMA formation by (B) <i>E. coli</i> ^N and <i>E. coli</i> ^{oxyBAC} (Error bars represent one standard deviation of the means, <i>n</i> = 3).....	108
Figure 4.10. Multiple sequence alignment of (A) Rieske domain and (B) mononuclear iron center of oxyBAC with other Group V Rieske oxygenases and oxyBAC of <i>Novosphingobium sp.</i> B7. ↑ and Δ denote amino acid insertion and substitution, respectively	110

LIST OF TABLES

Table 1.1. The most important chemicals by volume, manufactured in the USA (EPA, 2012)	2
Table 1.2. Environmental concentrations of some representative xenobiotics.....	2
Table 1.3. Representation of EC Enzyme classes in the EAWAG-BBD database as of November (2016).....	5
Table 1.4. Examples of different types of mobile genetic elements.....	15
Table 1.5. Transposons that encode ROs involved in xenobiotic degradation.....	17
Table 2.1. Assembly statistics of the metagenomic datasets used in this study	37
Table 2.2. Accession numbers of the metagenomic datasets used in this study.....	39
Table 3.1. Accession numbers of the genome sequences used in phylogenetic analysis	62
Table 3.2. Description of the abbreviations used for isolate labeling.....	63
Table 3.3. C utilization and chemical sensitivity patterns of BIOMIG1 and P.putida. + Indicates a positive and - indicates a negative result.	74
Table 3.4. Genome features of sequenced Pseudomonads and BIOMIG1.....	79
Table 3.5. SEED categories represented in the genome of BIOMIG1	81
Table 4.1. Strains, plasmids and primers used in this study	92
Table 4.2. Assembly statistics of the whole genomes used in this study	93

1. BACKGROUND

Xenobiotics are chemicals that are synthetically produced generally through an abiotic process. Xenobiotics are valuable to humans since they are either used as precursors in the production of commercial products or directly as the active ingredients of many consumer goods. There are over fifty categories that xenobiotics are classified based on their activity, such as preservatives, food additives, pesticides, herbicides, pharmaceuticals, disinfectants, fertilizers and explosives (Neilson and Allard, 2008; Iovdijova and Benchko, 2010).

Most of the xenobiotics are high production volume (HPV) chemicals, meaning the average production rate exceeds 1000 tons per year (Harbers et al., 2006) (Table 1.1). After used, a substantial portion of xenobiotics is carried to sewer systems and wastewater treatment plants that are not designed to eliminate them, therefore they finally end-up in the environment (Rieger et al., 2002; Loos et al., 2013). In the environment xenobiotics are detected at low concentrations (less than 1 ppb to 10 ppm) (Rieger et al., 2002; Janssen et al., 2005; Kolvenbach et al., 2014). However, even at low concentrations, xenobiotics can be toxic to humans and the ecosystem. (Rieger et al., 2002; Iovdijova and Benchko, 2010; Fatta-Kassinos et al., 2011). Environmental concentrations of some important xenobiotic chemicals are given in Table 1.2. As of today, most of the xenobiotic chemicals are classified as emerging micropollutants (von der Ohe et al., 2011). Consequently, actions have been undertaken to accurately assess the fate of xenobiotics in the environment and discover new methods to eliminate contamination.

Table 1.1. The most important chemicals by volume, manufactured in the USA (EPA, 2012)

Chemical	Production volume (tons/year)
Alkyldimethyl ammonium chlorides	4,535.9
Toluene	1,119,407.1
Naphtalene	72,388.4
Benzene	10,755,792.4
Ethylene	1,155,481.7
Phenol	2,371,748.8
Ethylene dichloride	113,398.0
Biphenyl	7,966.0

Table 1.2. Environmental concentrations of some representative xenobiotics

Functional class	Compound	Concentration range ($\mu\text{g/L}$)	Sampling site	Reference
Disinfectant	triclosan	0.001-2.3	surface water	Brausch and Rand, 2011
Disinfectant	benzyl alkyl ammonium salts	1.9	surface water	Martinez Carballo et al., 2007
Explosive	2-nitrotoluene	2-700,000 (mg/kg)	sediments	Godejehann et al., 1998 ; Fuchs et al., 2001 ; SAIC, 2001
Pesticide	2,4-D	0.04-18,600	surface water	Orton et al., 2009
Pesticide	atrazine	0.05	surface water	Sass and Colangelo, 2013
Preservative	triclocarban	0.019-1.5	surface water	Brausch and Rand, 2011
Industrial by-product	polychlorobiphenyls	14×10^{-6}	surface water	Srogi, 2008
Organic solvent	trichloroethene	$10-1 \times 10^6$	contaminated groundwater	Hunkeler et al., 2004
Organic solvent	tetrachloroethene	2500*	contaminated groundwater	Witt et al., 2006

*Highest measured concentration

Biodegradation is the microbial modification of a chemical, which converts it into non-toxic end products in order to provide carbon and energy to microorganisms. This process can be used as a promising tool for eliminating xenobiotics in the environment (Alexander, 1981). Xenobiotic, as a term, refers to a chemical that cannot be biochemically synthesized therefore it is neither present in the environment nor structurally similar to naturally occurring compounds (Rieger et al., 2002). As a result, microbial enzymes have not evolved to use these synthetic compounds as carbon and energy sources. For example aromatics and aliphatics with ortho-dimethyl and vicinal-trimethyl substitutions, branched aliphatic compounds and compounds containing halo, azo and nitro groups are amongst xenobiotic structures. These structures are extremely electrophilic therefore resistant to be attacked by microbial enzyme systems (Kolvenbach et al., 2014). Therefore, many xenobiotic chemicals are not readily biodegradable by the vast majority of microorganisms in the environment (Rieger et al., 2002; Kolvenbach et al., 2014). However, there are certain microorganisms, which are rare in the environment, that have evolved to express necessary enzymes for breaking down such compounds and using them as carbon and energy sources.

When microorganisms get exposed to xenobiotic chemicals, they develop strategies to adapt and exploit these compounds. This is the outcome of an evolutionary process in which catabolic genes and regulatory elements play a key role. Essentially, if a catabolic gene provides a selective advantage to a microorganism and let it use the chemical to gain energy, it is integrated into the genome and biodegradation pathways are generated. However, the dynamics of these mechanisms is not fully understood (Janssen et al., 2005; Kolvenbach et al., 2014). Extensive sequencing of environmental DNA has shown that a large number of recovered gene sequences cannot be assigned to known metabolic pathways (Ufarte et al., 2015). This shows that only a small fraction of the genes and pathways underlying xenobiotic biodegradation are known. Better understanding of the context would not only enable more efficient utilization of biodegradation for wastewater treatment and on-site bioremediation, but would also provide information on the insights of microbial evolution.

Quaternary ammonium compounds (QACs) are cationic biocides that are used to sanitize environments in close contact to humans such as hospitals and indoor surfaces, as well as used as preservatives in consumer goods (Buffet-Bataillon et al., 2012a; Tezel and Pavlostathis, 2012). They are prominent members of the HPV xenobiotic chemicals described above (Table 1.1) and frequently detected in the environment (Table 1.2). Contamination of the environment with QACs causes toxicity to ecosystem and promotes dissemination of antimicrobial resistance (Tezel and Pavlostathis, 2012). Some unique microorganisms can biotransform QACs and convert them to harmless end products, which is the ultimate mechanism to alleviate their impact on the environment. Although this process is biochemically characterized, how microbial communities adapt to QAC exposure in the environment as well as how QAC biodegradation pathways assemble and the specific genes underlying the biotransformation process remain unknown. Therefore, the aim of this study was to identify the community structure of benzalkonium chloride (BAC, a QAC homolog) degrading microbial communities originating from natural environments, as well as to identify the key BAC degrader microorganisms and catabolic genes involved in the BAC biodegradation pathway.

1.1. Biodegradation of Xenobiotics

1.1.1. Catabolic Genes and Enzymes

Microorganisms have been evolving for the last 3.6 billion years; therefore they harbor the most diverse set of catabolic genes and enzymes providing an enormous biodegradation potential (Wackett and Hershberger, 2001). Catabolic enzymes are crucial for the environment since they are used for extracting electrons and carbon from all kinds of organic compounds. This not only maintains biogeochemical cycles that are essential for life but also biotransforms human introduced industrial chemicals into harmless intermediates (Alexander, 1981; Kolvenbach et al., 2014).

Currently, the total number of identified catabolic enzymes in Eawag Biocatalysis/Biodegradation Database (EAWAG-BBD) is 993, involved in 219 pathways, and these numbers are rapidly expanding (<http://eawag-bbd.ethz.ch>). According to the enzyme commission (EC) (<http://enzyme.expasy.org>), which was established for categorizing enzymes into classes according to the type of reactions they catalyze, there are six major divisions of enzymes as shown in Table 1.3. However, oxidoreductases are significantly overrepresented in EAWAG-BBD. Hydrolases and lyases follow them, with isomerases and transferases being the least abundant (Table 1.3).

Table 1.3. Representation of EC Enzyme classes in the EAWAG-BBD database as of November (2016).

EC no.	Enzyme Class	Number of class in EAWAG-BBD
1	Oxidoreductase	597
2	Transferase	57
3	Hydrolase	185
4	Lyase	99
5	Isomerase	35
6	Ligase	39

Dehydrogenases and oxygenases are the most abundant subgroups of oxidoreductases. Dehydrogenases can directly transfer hydrogen to electron acceptors such as nicotinamide adenine dinucleotide (NAD)/nicotinamide adenine dinucleotide phosphate (NADP), without utilizing molecular oxygen (Wackett and Hershberger, 2001). Since they do not require oxygen, dehydrogenases function also under anaerobic and anoxic conditions. Some important pathways that involve dehydrogenases include biodegradation of synthetic polymers such as poly vinyl alcohol and polyethylene glycol (Kawai and Hu, 2009) and aminopolycarboxylic acids (Bucheli-Witschel and Egli, 2001). On the other hand, oxygenases insert oxygen into the substrate and create hydroxylated intermediates, which then become more suitable for subsequent degradation (Wackett and Hershberger, 2001). They mainly operate on the compounds that have the benzene ring, the double bonds in aliphatic substances or halo-, nitro- or azo-substitutions, which are otherwise resistant to biodegradation.

Oxygenases oxidize reduced substrates by incorporating molecular oxygen (O_2) to the substrate by utilizing flavin adenine dinucleotide (FAD), NADH or NADPH as coenzyme. There are two main classes of oxygenases: monooxygenases which incorporate one oxygen and dioxygenases which incorporate two oxygen atoms into the substrate. Monooxygenases can act on a variety of substrates due to their high region-selectivity (preference to break a bond from one direction) and stereo-selectivity (tendency to form a certain metabolite isomer). They are divided into two subgroups based on the cofactor they utilize; flavin-dependent monooxygenases and P450 dependent monooxygenases. Flavin-dependent monooxygenases contain flavin as prosthetic group and require NADP or NADPH as coenzyme. An example to this group is flavoprotein 1,2-monooxygenases that are used for the insertion of an atom of oxygen into the ring that is the first step in the degradation of both cyclopentanone and cyclohexanone (Neilson and Allard, 2008). P450 monooxygenases are heme containing oxygenases that exist in both eukaryotic and prokaryotic organisms. Some example reactions catalyzed by this group are hydroxylation of *n*-octane by *Gordonia* sp. 7E1C and transformation of benzene, toluene, naphthalene,

biphenyl, and benzo[*a*]pyrene to the corresponding phenol by *Streptomyces griseus*. (Neilson and Allard, 2008).

Dioxygenases are two or three component enzymes that add two oxygen atoms into their substrate. Bacterial Rieske non-heme iron dependent dioxygenases (ROs) constitute a large family among dioxygenase. They are two or three component enzymes composed of a reductase, a ferredoxin (in three component systems) and an oxygenase. Oxygenase component contains the Rieske cluster [2Fe-2S] and the catalytic mononuclear iron center which is the active site. The reductase transfers electrons from an electron donor (NADPH or NADH) to oxygen, and further to ferredoxin if there is one. The Rieske cluster accepts electrons, and passes them to the mononuclear iron center for catalysis. (Ferraro et al., 2005). This type of coordination has made electron transfer so efficient that ROs can perform complicated reactions.

ROs have been characteristically associated with attacking the benzene ring. The produced hydroxyl groups are either dehydrogenated by a dehydrogenase to produce catechol or elimination of CO₂H, NH₃, Hal⁻, NO²⁻, and SO₃²⁻ or exceptionally OH⁻ produces catechols directly without dehydrogenation (Ferraro et al., 2005; Neilson and Allard, 2008; Barry and Challis, 2013). Representative reactions are shown in Figure 1.1. They have been identified in the degradation pathways of many human-introduced, toxic organic chemicals such as carbazole and dioxin pesticides, solvents like toluene, benzene, explosives like 2- and 3-nitrotoluene and industrial chemicals like polychlorobiphenyls (PCBs) (Ferraro et al., 2005). These structures include linked and fused aromatics with halo and nitro groups substitutions and hetero-aromatics, many of which are known to be toxic and/or carcinogenic in nature (McKinney et al., 1985; van den Berg et al., 1998).

ROs have been traditionally classified either according to the number of subunits they have, the type of reductase they utilize or the character of the reaction they catalyze (Ferraro et al., 2005). However, as the number of newly discovered ROs expanded, it became difficult to comply with the existing classification system. Some recently discovered ROs catalyze reactions that are unprecedented (Zhu et al., 2014). In addition, due to the

and three component enzymes. Vanillate demethylase of *Pseudomonas* sp. and toluene sulfonate monooxygenase of *Comamonas testosteroni* are example monooxygenases and carbazole 1,9 dioxygenase of *Pseudomonas stutzeri* OM, phenoxybenzoate dioxygenase of *P.pseudoalcaligenes* and phthalate 4,5 dioxygenase of *P.putida* are example dioxygenases for Group I ROs (Nam et al., 2001).

ROs from Group II are heterodimeric meaning that they contain two subunits (α and β) in the oxygenase component. They are two component enzymes that catalyze only dioxygenations. Aniline dioxygenase of *Acinetobacter* sp. and, trichlorophenoxyacetic acid oxygenase of *Burkholderia capecica* are among Group II ROs. Group III and IV ROs are also heterodimeric, but are three component enzymes that catalyze strictly dioxygenation reactions. Naphtalene 1,2 dioxygenases of various *Pseudomonas* species are characteristic Group III ROs whereas isopropylbenzene dioxygenases, biphenyl dioxygenases, benzene dioxygenases of *Pseudomonas* species and dioxin dioxygenase of *Sphingomonas* RW1 are representative Group IV ROs (Nam et al., 2001).

Group V ROs have been recently recognized. As appose to other groups, they catalyze monooxygenations, and they have been explicitly associated with demethylations and dealkylations of quaternary ammonium compounds. Although there are not as much information compared to other groups, it can be suggested that they are mainly composed of two component enzymes. Choline monooxygenase, carnitine oxygenase and stachydrine demethylase are example Group V ROs (Rathinasabapathi et al., 1997; Daughtry et al., 2012; Zhu et al., 2014).

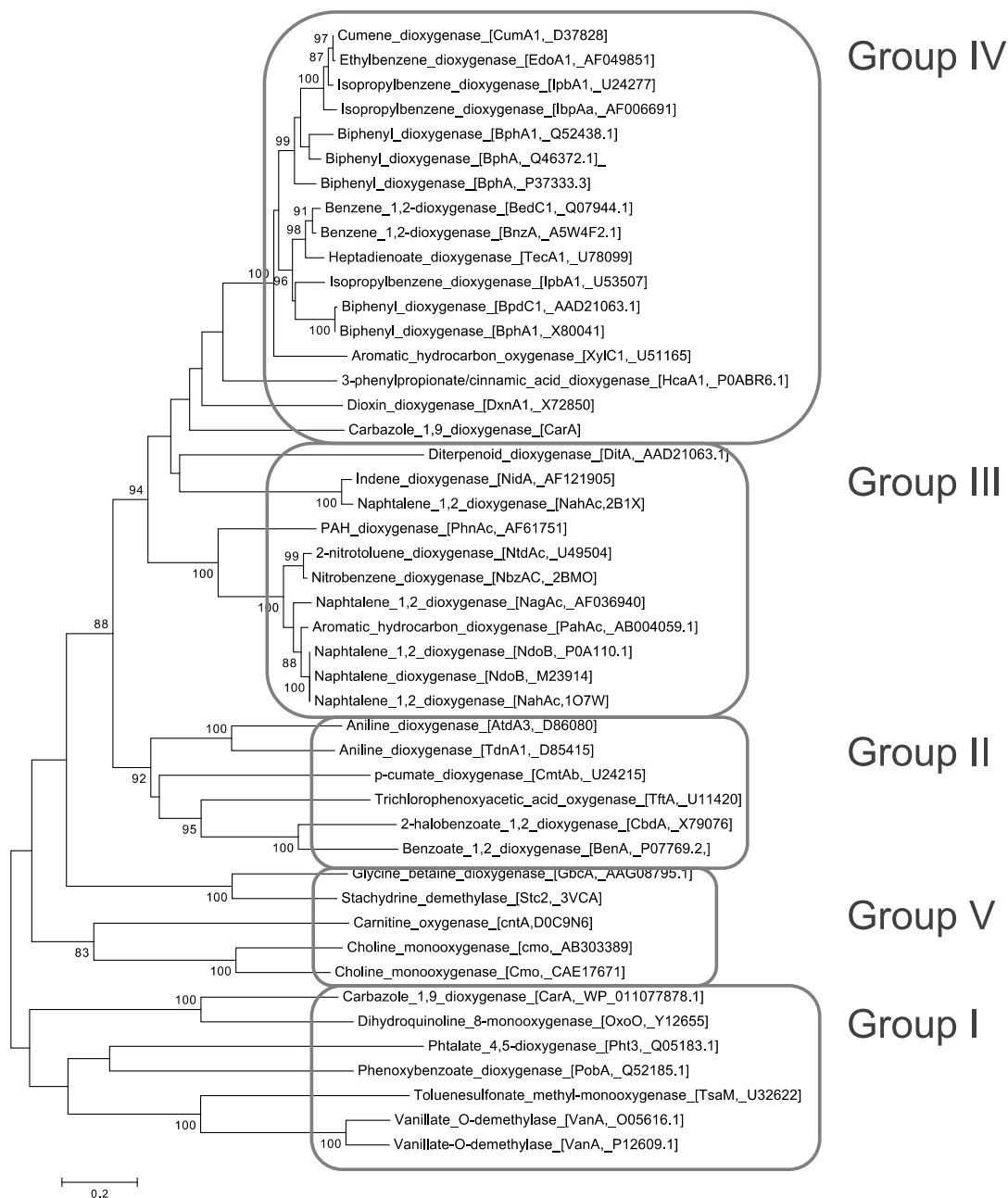


Figure 1.2. Classification of Rieske oxygenases according to the oxygenase subunit. Proteins were aligned using ClustalW and tree was constructed using Neighbour Joining method. Adapted from Nam et al. (2001)

Biodegradation pathways of xenobiotic chemicals consist of peripheral and central pathways (Pieper et al., 2010; Fuchs et al., 2011; Diaz et al., 2013). The peripheral (upper) pathway encodes for enzymes that converts the substrate into intermediates which are channeled into the central pathway where the intermediates are further transformed to enter the tricarboxylic acid (TCA) cycle (Diaz et al., 2013). ROs are explicitly part of peripheral pathways, where they catalyze the initial hydroxylation of substituted (fused) benzenes that removes the functional groups and produce catechol as an intermediate. (Gibson and Parales, 2000; Wackett, 2002). Catechol is then degraded by a series of reactions initiated by catechol 1,2 dioxygenase or catechol 2,3 dioxygenase which is a part of the central pathway (Ferraro et al., 2005). The genes encoding ROs are located within a gene cluster that is expressed under one promoter, which is called a catabolic operon. These catabolic operons have a common structure and gene organization (Diaz et al., 2013). Genes encoding subunits of the oxygenase component, ferredoxin and reductase are found next to each other. Other catabolic genes involved in subsequent degradation of the metabolites such as dehydrogenases are located next to the former gene cluster. A gene expression regulator is found upstream of these genes, controlling their expression. Finally, genes encoding auxiliary functions such as transporters for substrate and metabolite uptake are identified next to the catabolic genes (Johri et al., 1999; Jimenez et al., 2002; Gai et al., 2010; Zhu et al., 2014) (Figure 1.3).

The operon structures described above gives information on the evolutionary stage of the pathway and affect the characteristics of the degradation process. In a primitive pathway, genes are scattered, poorly regulated and interspaced by remnants of genetic material from lateral gene transfer or directly mobile genetic elements (Johnson and Spain, 2003). Such pathways have low degradation efficiency and may require multiple microorganisms for mineralization. In developed pathways, genes are closely clustered and are under tight regulatory control. These pathways are highly efficient and specialized for certain chemicals. Understanding these issues is crucial for implementing degradation for bioremediation and wastewater treatment as well as predicting the outcomes (Copley, 2000; Kivisaar, 2011).

In the environment, assembly of xenobiotic degradation pathways occur in a “patchwork” manner, meaning that enzymes with preexisting functions come together to form a new pathway (Copley, 2000). In a number of cases, it has been shown that a gene cluster encoding a hydroxylating RO with a broad substrate range and dihydrodiol dehydrogenase, was inserted next to an operon encoding a central ring-cleavage pathway (Johnson and Spain, 2003). Genetic evidence suggests that mobile genetic elements (MGE) such as transposons, phages and integrases played a significant role in bringing these gene clusters together (Tan, 1999; van der Meer et al., 2001). Once assembled, xenobiotic degradation pathways are integrated into plasmids and disseminated among microorganisms (Top and Springael, 2003; Dennis, 2005). Some example MGEs associated with environmentally relevant xenobiotics are given in Table 1.4 and

Table 1.5.

Several examples can be given to illustrate how xenobiotic degradation pathways evolved as explained in the above paragraph. Degradation pathways of many xenobiotics such as toluene, benzene, and chlorinated phenols require two distinct gene clusters. The first gene cluster encodes the hydroxylating ROs that produce catechol from the specified compound and the second gene cluster encodes the catechol biodegradation pathway. For example the gene cluster encoding the toluene 2,3 dioxygenase which converts toluene to catechol came together with the genes encoding the catechol degradation pathway by the transposition of transposon Tn4660 and formed the toluene degradation pathway. This pathway was further integrated into various plasmids such as pWW53, pDK1, pTK0 and pGB known as the TOL plasmids and disseminated within microorganisms. Likewise, the chlorobenzene dioxygenase (TcbA) and a dihydrodiol dehydrogenase were inserted next to the chlorocatechol degradation operon by transposon Tn5280 to form the chlorobenzene degradation pathway. This pathway was mobilized and disseminated after integration into plasmid pP51. 22% of the genes encoding ROs in Figure 1.2 have been identified on plasmids suggesting horizontal gene transfer (HGT) played an important part for their dissemination.

The recruitment of a RO provides fitness advantage to a microorganism in presence of a xenobiotic, as it would be able to alleviate the toxicity and use it as a energy source (Kolvenbach et al., 2014). Rapid adaptation of microbial communities to xenobiotics upon dissemination of ROs has been reported (Top and Springael, 2003). The chlorobenzene degradation genes described on the paragraph above have been identified on a genomic island called the “clc element” (Springael et al., 2002). observed that in a bioreactor treating influent contaminated with chlorobenzoate, the original inoculum that contained the clc element was being replaced by another chlorobenzoate degrading bacteria. Since control reactors without inoculum did not develop a chlorobenzoate degrading microbial community or a detectable degradation activity, the authors concluded that contaminant bacteria had acquired the clc element from the inoculum strain and became more competitive under the implied bioreactor conditions (Springael et al., 2002). In another study, a soil microbial community associated with the rhizosphere environment acquired the self transmissible TOL plasmid from *Pseudomonas fluorescence*. This microbial community could degrade meta-toluate therefore protecting the rhizosphere from this xenobiotic (Sarand et al., 2000).

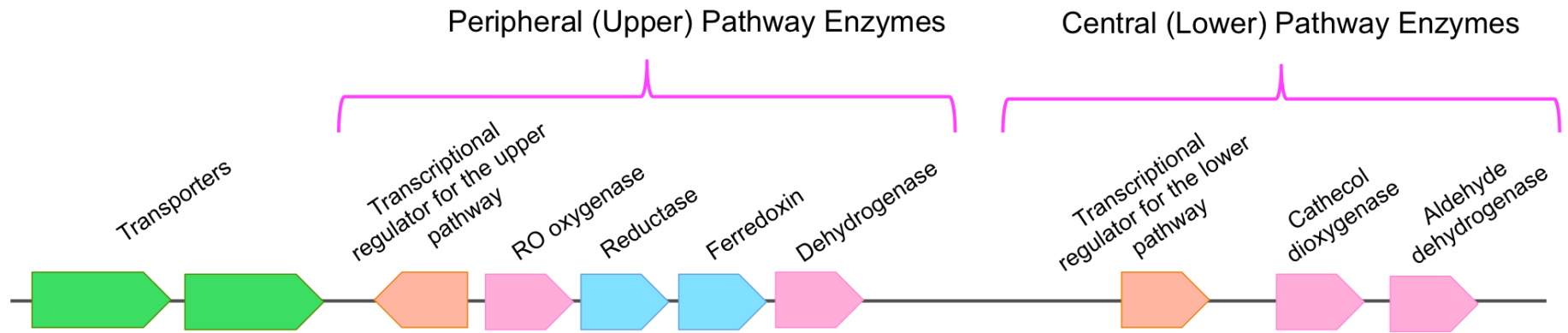


Figure 1.3. Representative catabolic operon structure encoding ROs involved in the degradation xenobiotics.

Table 1.4. Examples of different types of mobile genetic elements

Mobile element	Strain	Substrates	Size of MGE (kb)	Relevant Remarks
Plasmids				
pSS60	<i>Achromobacter</i> sp. LBS1C1	4-Chlorobenzoate	53	Recruitment of a 4-chlorobiphenyl (4CBP) degradative gene cluster present on a chromosomally located mobile element by pSS60 has been observed, creating plasmid-encoded mineralization of 4CBP
pBRC60	<i>Alcaligenes</i> sp. BR60	3-Chlorobenzoate	75	Contains Tn5271 carrying chlorobenzoate catabolic genotype <i>cba</i> Carries chlorocatechol catabolic composite transposon Tn5707 (see below) with a gene module evolutionarily related to the
pENH91	<i>Ralstonia eutropha</i> NH9	3-Chlorobenzoate	78	chlorocatechol degradation gene modules present on the CB degradation plasmids pP51 and pPS12-1, on the <i>clc</i> element, and on the 2,4-D degradative plasmid pJP4

Table 1.4. Continued

Plasmids	Strain	Substrate	Size of MGE (kb)	Relevant Remarks
pTSA	<i>Comamonas testosteroni</i> T-2	p-Toluenesulfonic acid	85	Carries two copies of a <i>tsa</i> gene cluster encoding p-toluenesulfonic acid degradation. These are flanked by two IS1071 elements, constituting a putative composite transposon; <i>tsa</i> genes were also found in other organisms from distant locations present on the same composite transposon, but only one strain contained a plasmid-encoded <i>tsa</i> gene
pP51	<i>Pseudomonas</i> sp. P51	Chlorobenzene	85	Carries a chlorocatechol degradation gene module similar to that of pPS12-1, the <i>clc</i> element and pENH91. In addition, this plasmid encodes a composite transposon Tn5280 (see below) carrying <i>tcbAB</i> genes for the degradation of CB into chlorocatechol. Thus, this pathway is a clear example of natural pathway assembly
pPS12-1	<i>Burkholderia</i> sp. PS12	1,2,4,5- Tetrachlorobenzene	85	Carries a chlorocatechol degradation gene module similar to that of pP51, the <i>clc</i> element and pENH91. It encodes a transposon carrying <i>tecAB</i> genes for the degradation of CB into chlorocatechol. These <i>tecAB</i> genes are similar to the <i>tcbAB</i> genes of strain P51, but are flanked by remnants of the toluene pathway

Table 1.5. Transposons that encode ROs involved in xenobiotic degradation

Transposon	Organism	Substrate	Size (kb)	Description
Tn5280	<i>Pseudomonas</i> sp. P51	Chlorobenzene	85	Present on pP51 (see above), carries the tcbAB genes responsible for CB transformation into chorocatechol. The tcbAB genes are clearly derived from a toluene degradation pathway on the basis of the presence of gene relics belonging to the toluene degradation genes, which flank the tcbAB genes
Tn5271	<i>Alcaligenes</i> sp. BR60 (pBRC60)	Chlorobenzene	17	Present on pBRC60 (see above). Carries chlorobenzoate catabolic genotype cba. Homologous transposons have been found in other chlorobenzoate degraders from different geographical origins. In some cases these transposons carry gene relics of other pathways
Tn5707	<i>Ralstonia eutropha</i> NH9	3-Chlorobenzoate	15	Present on pENH91 (see above). Carries genes evolutionarily related to the chlorocatechol degradation genes on plasmids pP51 and pPS12-1, on the clc element and on pJP4
DEH	<i>Pseudomonas putida</i> PP3	Chlorinated aliphatic acids	9.74	This transposon contains a dehalogenase gene and is bordered by two copies of the IS element ISPpu12, which has also been found flanking other catabolic genes

Table 1.5 Continued

Transposon				
	Organism	Substrate	Size (Kb)	Description
Tn4651	<i>Pseudomonas putida</i> mt-2 (pWWO)	Toluene, xylene	56	Carries gene modules for toluene/xylene degradation via catechol, located between two IS elements. The transposon is located within another transposon Tn4663. The genes are similarly organized in many other TOL plasmids
Tn4653	<i>Pseudomonas putida</i> mt-2 (pWWO)	Toluene, xylene	70	Carries Tn4661
Tn4655	<i>Pseudomonas putida</i> G7 (NAH7)	Naphtalene	38	Carries three gene modules for naphthalene degradation via catechol. The module encoding catechol degradation is similar in organization to that of the pWWO plasmid
Other elements				
Tn4371	<i>Ralstonia oxalatica</i> A5	Biphenyl/4-chlorobiphenyl	55	This element is an unusual combination of phage-like genes (including an integrase), catabolic genes and genes for plasmid transfer. Similar elements have been found in other polychlorinated biphenyl degraders
Clc element	<i>Pseudomonas</i> sp. B13	Chlorocatechol	105	Carries a chlorocatechol degradation gene module similar to that of pP51, pPS12-1 and pENH9

1.1.2. Microbial Diversity of Xenobiotic Biodegradation

In the environment, microorganisms thrive in complex microbial communities, which are shaped by syntrophic and competitive interactions. Therefore, microbial community structure significantly affects the dynamics and efficiency of biodegradation processes (Alexander, 1981). Understanding the relationship between community structure and dynamics of biodegradation is crucial to exploit these processes in both engineered and natural systems.

Most of the knowledge on the structure of xenobiotic degrading microbial communities is derived from generating enrichment cultures coupled by sequencing the phylogenetic marker genes. Recent developments in sequencing methods allow sequencing of all genes from all organisms that enable accurate functional and taxonomic profiling of xenobiotic degrading microbial communities (He et al., 2010; Eren et al., 2013; Luo et al., 2013). This methodology is useful since enrichment selects for a core microbiome enduring the stress caused by the xenobiotic compound, and magnifies the interactions between community members under the implied conditions. Following enrichment, primary biodegrader microorganisms can be isolated to be used in biotechnology applications. Despite their practicality, enrichment cultures may suppress actual diversity and more realistic schemes may be required to predict the long-term effect of a xenobiotic compound in natural microbial communities (Dunbar et al., 1997). Microcosm experiments along with in-situ monitoring of natural microbial communities exposed to xenobiotics are alternative methods to achieve such goals.

Unraveling the relationship between microbial community structure and biodegradation has been used for monitoring natural attenuation of polluted ecosystems. Kleindienst et al. (2015) investigated the on-site community composition before, during and after the petroleum hydrocarbon exposure from the Deepwater Horizon oil spill in the Gulf of Mexico. The authors demonstrated that native hydrocarbon degraders adapted to slow natural oil seepage was outcompeted and previously unrecognized taxa affiliated with *Cycloclasticus*, *Colwellia* and *Oceanospirillaceae* became predominant after the spillage.

Microcosm experiments confirmed that this microbial consortium could efficiently mineralize the hydrocarbon mixture at high concentrations. In the same study, it was shown that dispersant addition to make hydrocarbons more available for biodegradation disturbed the hydrocarbon degrading community and promoted proliferation of another microbial group that degraded dispersants. It can therefore be concluded that dispersant addition is not an effective strategy if natural degradation of oil hydrocarbons is wanted.

In another study, it was shown that in a groundwater bioremediation site contaminated with uranium, indigenous bacteria affiliated with *Desulfovibrio*, *Geobacter*, *Anaeromyxobacter* and *Shewanella*, along with *Rhodopseudomonas* and *Pseudomonas* became highly abundant (Xu et al., 2010). With addition of ethanol, these populations could reduce uranium and decrease soluble uranium concentrations to drinking water standards level. The authors concluded that the abundance of functional genes significantly changed according to pH, temperature, and sulfate concentration that affected performance of bioremediation. Hence hydrological and geochemical conditions could be adjusted for optimal bioremediation by natural communities in the future.

The examples described above present how important it is to understand the relationship between microbial community structure and biodegradation processes to use those communities for monitoring and bioremediation of polluted sites. Another strategy is to identify key biodegrader microorganisms and isolate them for further characterization and bioaugmentation applications. Within this context, it is often questioned if certain taxa have exceptional metabolic capability. As of November 2016, 20% of the microorganisms in EAWAG-BBD are affiliated to genus *Pseudomonas*, involved in 90 different pathways followed by *Rhodococcus*, *Arthrobacter*, *Sphingomonas*, and *Burkholderia* (Wackett and Hershberger, 2001) (Figure 1.4).

The compounds metabolized by *Pseudomonas* include aliphatic and aromatic hydrocarbons with chloro, cyano, nitro, and phosphoryl groups substituted; aliphatic and aromatic acids; and cycloaliphatic compounds. Naturally, this picture is considered biased, since the assignment of biodegradation activity to specific strains requires their isolation and

characterization. Currently adopted isolation techniques select for fast growing, generalist microorganisms with few nutrition requirements such as *Pseudomonas* and *Burkholderia*. However, with the advance of genome sequencing projects, it has been shown that these taxa were indeed equipped with the necessary genetic infrastructure, characteristically having huge genomes and mega-plasmids. This suggests that their designations as “exceptional biodegraders” may not be an isolation bias after all. Deep sequencing technologies reveals numerous unidentified taxa in microbial communities exposed to human-introduced organic chemicals. Physiology of these organisms needs to be characterized in order to affiliate them with metabolic pathways. In fact, with our increased ability to culture organisms or identify an organism's metabolism without isolating it (Wackett and Hershberger, 2001), biodegradative capabilities in new branches of the tree of life are quickly emerging (Figure 1.5).

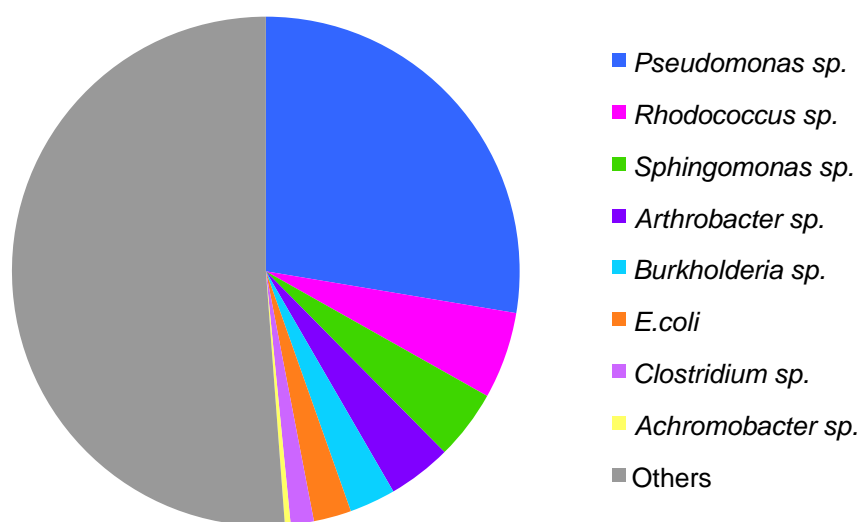


Figure 1.4. Abundance of species involved in different pathways as represented in EAWAG-BBD

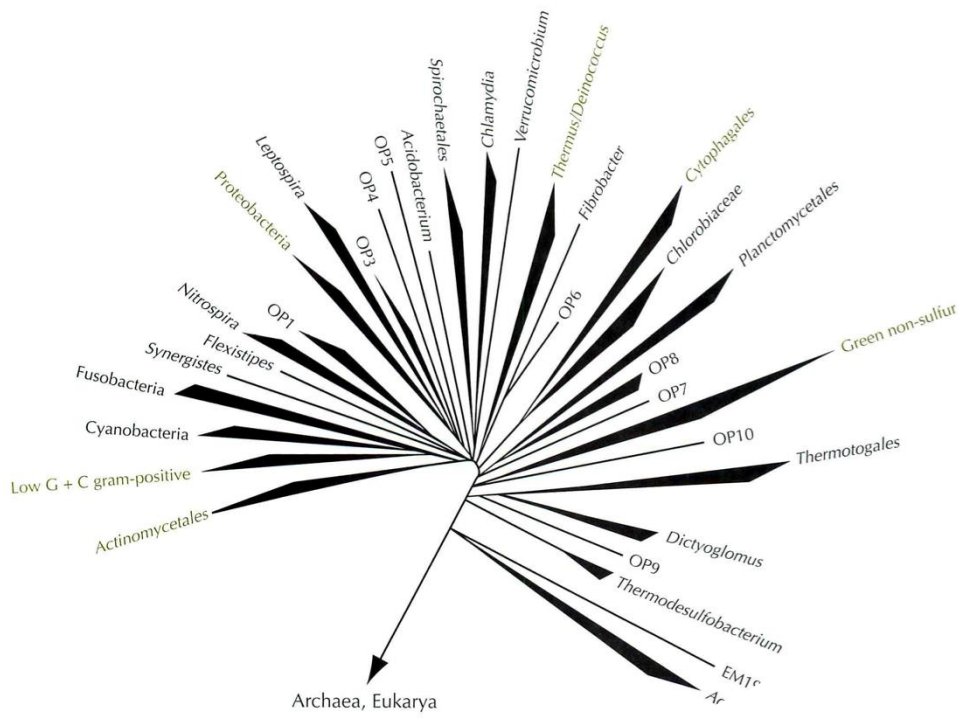
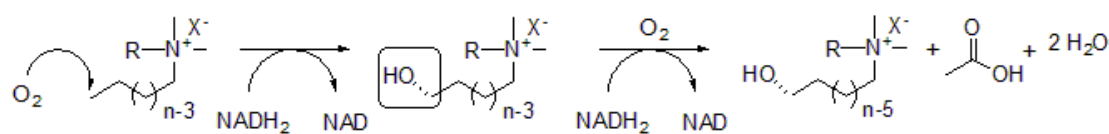


Figure 1.5. Taxonomic tree of the bacteria with groups heavily represented in the UM-BBD highlighted in green (Wackett and Hershberger, 2001)

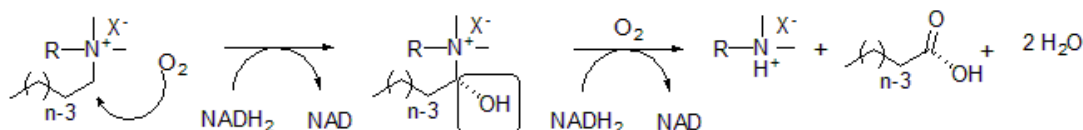
1.1.3. Biotransformation of Quaternary Ammonium Compounds

Quaternary ammonium compounds (QACs) are antimicrobials used in various consumer products since the 1930s (Tezel and Pavlostathis, 2011) to prevent contamination. Thus, they are considered prominent micropollutants in the environment. QACs contain four functional groups that are attached covalently to a central nitrogen atom (R_4N^+). The functional groups (R) include at least one long-chain alkyl group and the rest are methyl, benzyl, or ester groups (Tezel and Pavlostathis, 2011). To date, a number of microorganisms capable of QAC biotransformation have been isolated such as *Xanthomonas* sp. (Dean-Raymond and Alexander, 1977), *Pseudomonas* spp. B1 (van Ginkel et al., 1992), *Pseudomonas fluorescens* strain TN4 (Nishihara et al., 2000), *Pseudomonas fluorescens* strains F7 and F2 (Nishiyama and Nishihara, 2002), *Aeromonas hydrophila* sp. K (Patrauchan and Oriol, 2003), *Pseudomonas* spp. strain 7-6 (Takenaka et al., 2007), *Pseudomonas putida* A ATCC 12633 (Liffourrena et al., 2008, 2009) and *Pseudomonas nitroreducens* B/DPB (Oh et al., 2013).

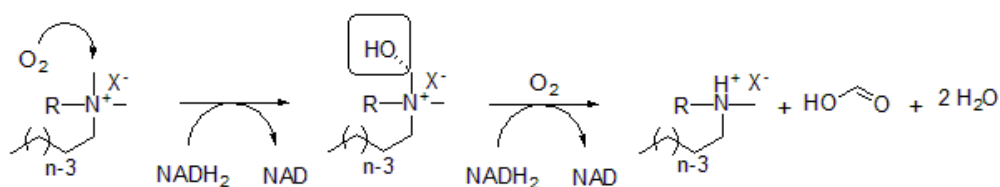
Three QAC biotransformation pathways have been defined for monoalkonium, dialkonium, and benzalkonium chlorides, which differ in terms of the location of the initial attack on the molecule (Figure 1.6). These pathways are: (A) hydroxylation of the terminal C (ω -hydroxylation), followed by multiple β -oxidation cycles, progressing toward the hydrophilic moiety, (B) hydroxylation of C that is adjacent to the central N (α -hydroxylation), followed by the central fission of the molecule resulting in the separation of the hydrophobic from the hydrophilic moiety and (C) hydroxylation of the methyl-C attached to the central N, followed by the fission of the methyl group from the molecule. Among these pathways, pathway (B) has been shown to be the dominant one. Pure cultures of *Pseudomonas* B1, *Pseudomonas putida* A ATCC 12633 (Liffourrena et al., 2008, 2009) and *Pseudomonas nitroreducens* B/DPB (Oh et al., 2013) biotransformed QACs through pathway (B), where an initial dealkylation reaction took place to break the molecule and a tertiary amine was produced as the intermediate. Interestingly, none of the isolates described above were able to degrade the tertiary amine and consequently mineralize QACs.



Pathway A. Hydroxylation of the terminal C of alkyl group



Pathway B. Alpha hydroxylation of C adjacent to N of alkyl group



Pathway C. Alpha hydroxylation of the C of methyl group

Figure 1.6. QAC biodegradation pathways

Biodegradation stands out as the ultimate mechanism to eliminate disinfectants like QACs in wastewater treatment plants. Nevertheless, there are hardly any information regarding the enzymes and genes specifying QAC biodegradation. Van Ginkel (1992) showed that the initial step that converted a QAC homolog; hexadecyl trimethyl ammonium chloride to trimethyl amine was strictly oxygen dependent and utilized NADPH. Based on the metabolites produced, the authors presumed that the enzyme was a monooxygenase. Recently, Liffourena and Lucchesi (2014) identified and overexpressed the first gene associated with QAC degradation from *Pseudomonas putida*. This enzyme was identified as a monooxygenase that converted tetradecyl dimethyl ammonium chloride (TTABMO) to TMA and utilized NADPH and FAD as cofactors. In parallel, Oh et al. (2014) identified an amine oxidase (AmoBAC) in *Pseudomonas nitroreducens* DPB/B, which could convert benzalkonium chloride (BAC) to benzyldimethyl amine (BDMA). This enzyme was also a FAD utilizing mono oxygenase. Phylogenetically, TTBMO and AmoBAC were distant from each other (~15% amino acid identity), suggesting multiple genes and pathways exist

for QAC degradation. In fact, QAC degradation in the environment is not restricted to human-produced disinfectants. Compounds like N,N-dimethylproline (stachydrine), carnitine, trimethylglycine are naturally occurring QACs, identified in places like the human gastro intestinal track (Koeth et al., 2013) or plant roots (Phillips et al., 1992). Three recent studies reported the discovery of novel enzymes degrading naturally occurring QACs. All of these enzymes were multicomponent Rieske oxygenases (ROs), which catalyzed demethylation and dealkylation of the substrate that resulted with the formation of a tertiaryamine, like in the case of synthetic QACs. GbcA and Stc2 were demethylases, degrading trimethyl glycine and stachydrine, respectively, whereas, CntA was a N-dealkylating oxygenase that degraded carnitine. The intermediate metabolite produced from all of these reactions was a tertiary amine called trimethylamine (TMA). TMA is also produced after dealkylation of synthetic QACs (Liffourrena et al., 2008). Phylogenetically, GbcAB, Stc2 and CntA are more closely related to each other than they are to AOx-BAC and TTBMO. These enzymes belong to the Group V ROs described in the previous section, thus represent a conserved group for QAC degradation in the environment.

QACs are antimicrobial compounds that are toxic to microorganisms. When a microbial community is exposed to QACs, members that are intrinsically resistant or that can biotransform QACs get selected. It was reported that microbial communities subsiding on BAC (community B) or BAC and dextrin-peptone mixture (community DPB) became highly enriched with Pseudomonads compared to a control culture that was fed only with dextrin and peptone (community DP) (Tezel et al., 2012; Oh et al., 2013; Tandukar et al., 2013). The predominant *Pseudomonas* species that emerged upon BAC exposure in DPB and B communities was *Pseudomonas nitroreducens* along with *P. aeruginosa* and *P. putida*. Other minor genera were Citrobacter, Klebsiella, Salmonella, Enterobacter and Achromobacter. It was also demonstrated that the diversity loss was less pronounced in community DPB compared to community B (Oh et al., 2013). In the same enrichment communities, BACs were degraded through dealkylation to BDMA followed by subsequent demethylation reactions that formed dimethylamine and methylamine (Tezel et al., 2012). Combined with complementary data it was concluded that BAC degradation was established

through selection of a *P.nitroreducens* population, which converted BAC to BDMA. BDMA was then mineralized by the rest of the microbial community.

Even though some suggest otherwise (McBain et al., 2004), a number of studies shows that QAC exposure results with a very low level of community-wide susceptibility (Tezel et al., 2012; Oh et al., 2013). Oh et al. (2014) reported that BAC susceptibility of the BAC enriched communities decreased up to five folds compared to control. Main resistance determinants were multidrug efflux pumps from the HlyD secretion protein family and small multidrug resistance (SMR) families. It is clear that a core microbiome dominated by Pseudomonads emerges upon exposure to QACs, which is characterized by low diversity, rapid QAC degradation and low QAC susceptibility. However, the dynamics that contribute to formation of such community structure is unresolved. Oh et al. (2013) reported candidate degradative genes involved in QAC biotransformation were identified next to the IS sequences, which lead to the conclusion that HGT, especially IS21 family transposon encoded elements played a role for QAC biodegradation to emerge in an enrichment culture. Nonetheless, this hypothesis is yet to be tested.

A hypothetical process of how microbial communities adapt to QAC exposure is depicted in Figure 1.7. and can be described as follows. Exposure to QACs generates two types of response in a microbial community. First one is the stress response and second one is the metabolic response. Upon QAC exposure initially susceptible populations are eliminated and intrinsically resistant bacteria with low membrane permeability and rigid cell wall becomes dominant. QAC exposure also induces SOS response in bacteria, which results with error prone DNA replication thus increased mutation rates (Figure 1.6A-B). When such incidents take place at regulatory sites of efflux pump genes, they are overexpressed and protect bacteria by pumping the QACs out of the cell. Furthermore, SOS response also promotes dissemination of multidrug efflux pump determinants with transposons, ICEs and phages. These events allow resistant populations proliferate in a microbial community, however cannot advance their utilization as a carbon and energy source.

Metabolic response is induced independently from the stress response. Since there are genes encoding enzymes degrading natural QACs, it can be suggested that these were the precursors of genes that are involved in the degradation of synthetic QAC disinfectants. The former likely accumulated mutations, which modified the active site in such a way that made the enzyme capable of attacking QAC disinfectants. After this function was established, the gene was mobilized by being integrated into gene cassettes and transposons (Figure 1.6C). Recruitment of QAC degrading genes by bacteria already resistant to QACs would allow them to use QACs as a C source and provide fitness advantage to them. It would also protect the microbial community by converting QACs to non-toxic tertiary amines (Figure 1.6D). The second step of the pathway which is degradation of the tertiary amines most likely evolved separately from the first stage since it is known that there are microorganisms that accomplish different steps of the pathway (van Ginkel et al., 1992; Oh et al., 2014). Tertiary amines like trimethylamine (TMA) are ubiquitous in the environment, which are either produced from the degradation of natural QACs (Chen et al., 2011), or through reactions of organic nitrogen (Selbes et al., 2013). TMA is also an intermediate in the degradation pathway of QAC disinfectants along with BDMA (Liffourrena et al., 2008). It has been shown that TMA monooxygenases that convert TMA to TMA oxides are widespread in the environment (Chen et al., 2011). Therefore Assembly of a complete QAC degradation pathway would involve mobilization of enzymes such as TMA monooxygenases and integrating them next to the genes encoding the first part of the pathway in suitable microorganisms (Figure 1.6E).

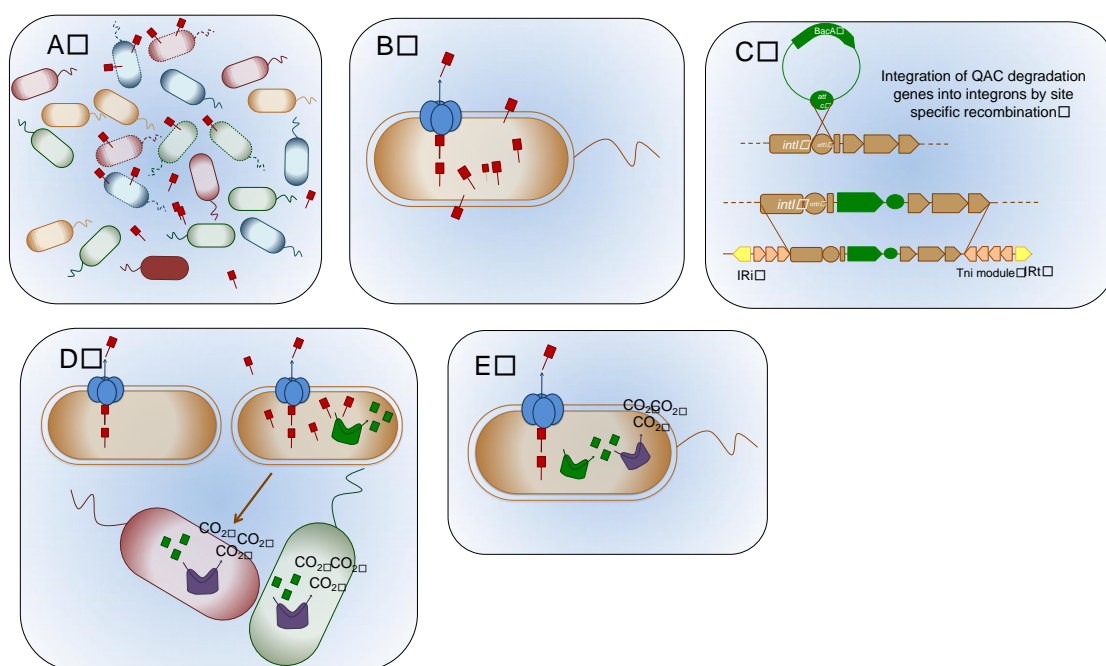


Figure 1.7. Adaptation of microbial communities to QAC exposure. (A) QAC exposure kills susceptible bacteria (B) QAC resistance emerges. (C) QAC degradation genes evolve and they are integrated into MGEs. (D) Recruitment of degradation determinants enables bacteria to use QACs as a C and energy source and provides fitness advantage. (E) Assembly of complete QAC degradation pathway occurs.

BACs are one of the most commonly used types of QACs. BAC biotransformation pathways in the environment have been biochemically characterized. However there is little information on the structure of BAC degrading microbial communities in the environment as well as the underlying genes of the pathway. The only community structure associated with BAC degradation originates from a single polluted river sediment (Tezel and Pavlostathis, 2012; Oh et al., 2013; Tandukar et al., 2013; Oh et al., 2014). Expanding this knowledge would lead to the identification of key role player microorganisms for BAC degradation in the environment and isolation of new, potentially more efficient BAC degraders. Comparing the metagenomic datasets originating from BAC degrading enrichment cultures with cultures unexposed to BACs would yield the functions specific to BAC degradation. Similarly, comparing the genomes of BAC degrader microorganisms with BAC non degraders would reveal the specific genes in the pathway which could be

used in biotechnology applications. Unfortunately, the genome of a BAC degrader has not been sequenced yet. In the light of this information, there were two main objectives of this study. The first one was to identify the core microbiome in BAC degrading microbial communities originating from different environments as well as isolating key BAC degrader microorganisms. The second one was to characterize the genes involved in each step of the BAC degradation pathway and verify their activity.

2. MICROBIAL COMPOSITION AND FUNCTIONS IN BENZALKONIUM CHLORIDE DEGRADING COMMUNITIES

This chapter was partially published in “Environmental Science and Technology” journal entitled “Similar Microbial Consortia and Genes are Involved in the Biodegradation of Benzalkonium Chlorides in Different Environments (Ertekin et al. 2016)” Disclosure of article is permitted by Konstantinidis, K. T. and Tezel, U.

2.1. Introduction

Quaternary ammonium compounds (QACs) are cationic biocides, which are active ingredients of many commercial disinfectants. QACs are especially preferred for sanitization of indoor surfaces, primarily in domestic environments and hospitals. Moreover, they are frequently used in human hygiene products such as contact lens solutions and eye drops to prevent microbial contamination (Buffet-Bataillon et al., 2012b). The typical application concentration of QACs is between 400 and 500 mg/L, and almost always below 1000 mg/L. Due to their unconstrained use, QACs are continuously released into the environment, and therefore classified as emerging pollutants (Tezel and Pavlostathis, 2012). The average concentration of QACs in domestic wastewater treated effluent, sewage sludge and surface water has been reported to be around 0.5 mg/L, 0.05 mg/L, 5000 mg/kg dry weight, and 0.04 mg/L, respectively (Tezel and Pavlostathis, 2012; Tezel and Pavlostathis, 2015).

Environmental QAC concentrations are sub-inhibitory, and therefore exposure to QACs trigger acquirement and dissemination of resistance, which is mediated by intrinsic and acquired resistance mechanisms. Intrinsic resistance involves enhanced cell wall and cell membrane permeability barrier as well as chromosomally encoded multidrug-efflux pumps. The efflux pump determinants include resistance nodulation division (RND) family such as SdeXY, AcrAB-TolC, and MexAB-OprM that are significant and have been identified in both clinical and environmental strains. On the other hand, acquired resistance involves horizontal transfer of efflux pump determinants via plasmids, transposons and

integrans. QacE, Qac Δ E, QacF, QacG, QacH, QacI, and QacJ are QAC-specific efflux determinants that have been associated with plasmids and class I integrans and consequently abundant in the environment. When microorganisms are exposed to QACs at environmental levels, SOS response that results in error-prone DNA replication is induced and cause increased mutation rates (Tezel and Pavlostathis, 2015). Such mutations can occur at the regulatory sites of efflux pump determinants which consequently cause overexpression of efflux pumps. Moreover, under the stress conditions induced by QAC exposure, recombinatorial events that enhance transfer of efflux pump determinants via plasmids and integrans are dominated (Blazquez et al., 2012; Tezel and Pavlostathis, 2012).

Despite their antimicrobial properties, some microorganisms can biotransform QACs and convert them into non-toxic intermediates. This is also considered as an adaptation mechanism of microbial communities against QAC induced-stress. Although there is no evidence suggesting that biotransformation directly causes resistance, it potentially reduces QAC concentrations at target environments such as hospitals, therefore decreasing their efficacy and creating habitable hot spots for the microorganisms. Also, by reducing effective QAC concentrations, biotransformation causes microbial communities to get exposed to sub-inhibitory levels that may promote resistance (Mc Cay et al., 2010; Buffet-Bataillon et al., 2012b; Moen et al., 2012; Gillings, 2014). Whether used as a resistance mechanism or not, biotransformation is the ultimate process that alters QAC concentrations in the environment. Understanding the insights of this process is crucial for exploiting it as a treatment tool to clean-up wastewater, and also revealing how such unusual microbial metabolism evolves in the environment.

How microbial communities adapt to QAC exposure has been studied to a limited extent. Most information on this subject comes from enrichment cultures subsiding on QACs as a sole carbon source. Phylogenetic characterization of two microbial communities degrading benzalkonium chlorides (BACs), which are the most commonly used type of QACs, showed that exposure to BACs selected for low diversity microbial consortia (Tezel et al., 2012; Oh et al., 2013; Tandukar et al., 2013). These authors also showed that adaptation to BACs occurred primarily via selective enrichment of BAC degrading

Pseudomonas spp., particularly *P. nitroreducens*, and secondarily via amino acid substitutions and horizontal transfer of selected genes, including a gene encoding a PAS/PAC sensor protein and ring hydroxylating dioxygenase genes. Additionally, multi-drug efflux pump genes like *sugE*, *PmpM*, *mexAB-oprM* and *mexEF-oprN* were enriched in the BAC-degrading community.

Given the fact that QAC biotransformation is important with respect to both human and environmental health, a better understanding on composition and metabolic potential of microbial communities exposed to QACs should be provided. In this chapter, microbial community structures of rapidly BAC degrading microbial communities is described using high throughput sequencing of enrichment cultures originating from different environmental samples. Also, the specific functions that became enriched in BAC degrading communities compared to non-degrading ones have been identified.

2.2. Materials and Methods

2.2.1. Chemicals

The BAC mixture used in this study was obtained from Lonza Inc. (Switzerland). The mixture was composed of the following, with abbreviation, molecular formula and weight indicated in parentheses. 40% (w/w) dodecyl benzyl dimethyl ammonium chloride (C₁₂BDMA-Cl, C₂₁H₃₈NCl, 340 g/mole), 50% (w/w) tetradecyl benzyl dimethyl ammonium chloride (C₁₄BDMA-Cl, C₂₃H₄₂NCl, 368 g/mole), 10% (w/w) hexadecyl benzyl dimethyl ammonium chloride (C₁₆BDMA-Cl, C₂₅H₄₆NCl, 396.1 g/mole) (Figure 2.1). Individual BACs mentioned above were obtained in high purity from TCI Chemicals (Tokyo Chemical Industry Co., Ltd., Tokyo, Japan). Mineral salts and organic solvents used in experiments and instrumental analyses were purchased from Merck and Sigma Aldrich Chemicals Company at the highest purity.

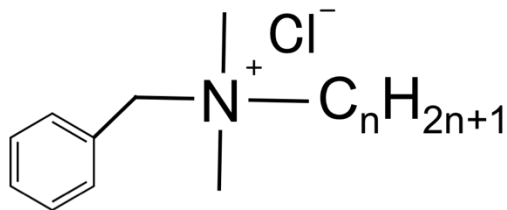


Figure 2.1. Chemical structure of BACs used in this study. “n” is 12, 14 or 16

2.2.2. Analytical Methods

BAC homologues and their chromophoric biotransformation by-products (benzyl amine (BA), benzyl methyl amine (BMA) and benzyl dimethyl amine (BDMA)) were measured using an Agilent 1200 High Pressure Liquid Chromotography (HPLC), equipped with a UV-Vis detector. Briefly, a mobile phase composed of 60% acetonitrile and 40% 50mM phosphate buffer was delivered isocratically at a flow-rate of 1 mL/min. For separation of the compounds, a phenomenex LUNA SCX column serially connected to a Polaris C18 column were used. Prior to analysis, the samples were mixed with equivalent volumes of mobile phase. Samples were then centrifuged at 10,000 rpm for 10 minutes. The supernatant of the sample was used for analysis. The injection volume was 50 μ L and detection of samples was achieved at 210 nm. Temperature was maintained at 35°C throughout the operation.

2.2.3. Enrichment of BAC Degrading Microbial Communities

The samples used as the primary inocula for the enrichment cultures originated from four sites. Activated sludge (AS) and sewage (SEW) samples were obtained from Pasakoy Advanced Wastewater Treatment Plant treating urban wastewater in Istanbul, Turkey. A surface soil sample from an Ataturk arboretum (SOIL) in Belgrad Forest located in a region near Black sea in Istanbul, Turkey and sea sediment sample from Silivri Shore (SEA) were also obtained. 20 grams of each sample were transferred aseptically into 500-mL glass bottles containing 180 mL salt medium (SM) composed of 7.4 g/L K_2HPO_4 , 3.0 g/L KH_2PO_4 , 0.5 g/L NaCl, 1.00 g/L NH_4Cl , 0.25 g/L $MgSO_4 \cdot 7H_2O$, 0.01 g/L $CaCl_2$ and 1 mL/L trace metal solution (0.5 g/L $ZnCl_2$, 0.3 g/L $MnCl_2 \cdot 4H_2O$, 3.0 g/L H_3BO_3 , 2.0 g $CoCl_2 \cdot 6H_2O$,

0.1 g/L $\text{CuCl}_2 \cdot 2\text{H}_2\text{O}$, 0.2 g/L $\text{NiSO}_4 \cdot 6\text{H}_2\text{O}$ and 0.3 g/L $\text{Na}_2\text{MoO}_4 \cdot 2\text{H}_2\text{O}$). The pH was maintained at 7.0 and the bottles were placed on a rotary shaker operated at 130 rpm at room temperature. A mixture of BACs, which served as a sole carbon and energy source, was amended into each bottle aseptically. The initial BAC concentration in each bottle was 50 mg/L and concentration was monitored on a daily basis using HPLC. As soon as all the BACs were consumed, 20 mL sample from each bottle were transferred aseptically into 180 mL sterile SM and re-spiked with 50 mg/L BACs. This serial dilution procedure was repeated 10 times to further enrich for rapidly BAC-degrading microbial communities (Figure 2.2). After about 50 days, BAC degrading microbial communities were maintained by batch-feeding 50 mg/L BACs in SM medium three times a week with a residence time of 5 days (Figure 2.2). After enrichment, BAC biodegradation rate of each enriched community was determined as follows: at the end of the feeding cycle, 100 mL of community sample was transferred into a 250-mL Erlenmeyer Flask. The initial turbidity of the cultures in each flask was 0.25 AU at 600 nm that corresponded to 10^8 CFU/mL. Each flask was then amended with BACs at 50 mg/L initial concentration. After all the BACs were consumed, cultures were re-spiked with 50 mg/L of BACs and BAC concentration was monitored frequently using HPLC. In order to determine the BAC degradation rate constant (k), experimental data was fitted to Michaelis-Menten growth model using Berkeley-Madonna software employing Runge-Kutta 4 integration method.

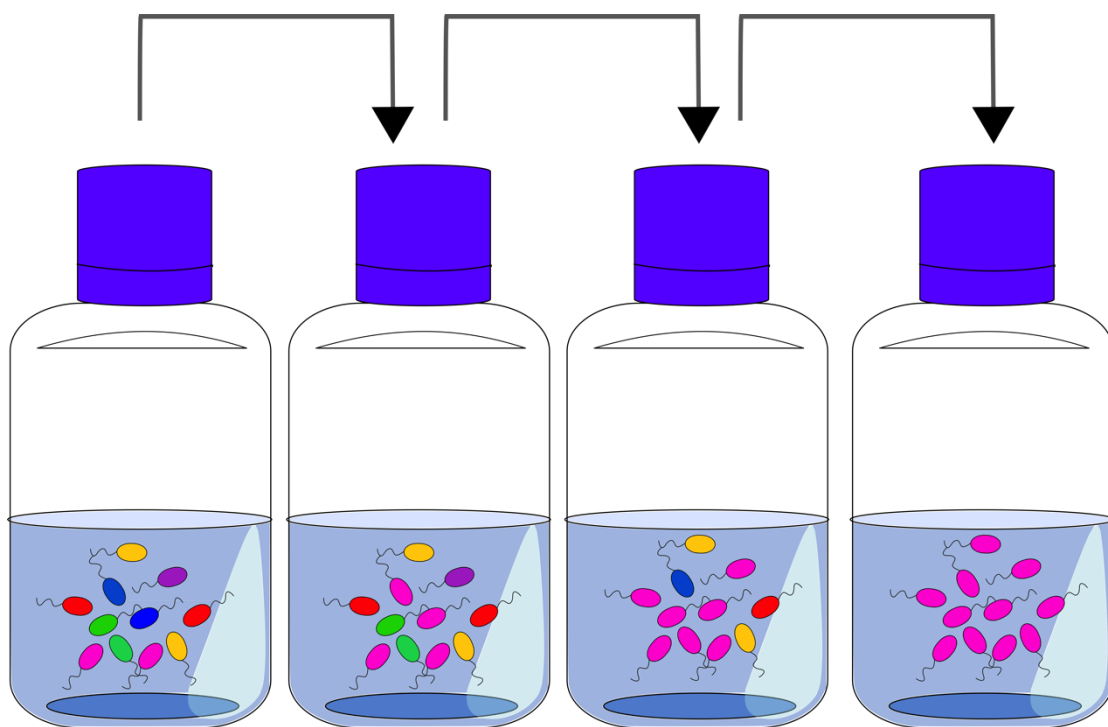


Figure 2.2. Illustration of dilution to extinction method used for enrichment of the communities. Pink bacteria indicate BAC degraders.

2.2.4. Metagenome Sequencing and Analysis of the Enrichment Communities

16S rRNA pyrosequencing and high-throughput shotgun metagenome sequencing were used for revealing the microbial composition and functions in BAC-enriched communities. Briefly, a 20 mL sample from each BAC enriched community developed from SEW, AS, SOIL and SEA was taken, centrifuged at 10,000 rpm and resuspended in 250 μ L saline solution (0.85% NaCl). Genomic DNA in the suspension was extracted with a NucleoSpin™ Soil DNA Extraction Kit (Macherey Nagel, France). Extracted DNA was used for 16S rRNA pyrosequencing and shotgun metagenome sequencing. For pyrosequencing, V1-V3 regions of the 16S rRNA gene were amplified and sequenced with adaptors labeled with 8F and 518R bacterial primers using the Roche FLX 454 platform in MacroGen Inc. (Amsterdam, Netherlands).

For shotgun metagenome sequencing, DNA libraries were prepared using the Nextera XT DNA Library Preparation Kit (Illumina, San Diego, CA, USA) according to manufacturer's instruction except the protocol was terminated after isolation of cleaned double stranded libraries. Library concentrations were determined by fluorescent quantification using a Qubit HS DNA kit and Qubit 2.0 fluorometer (Thermo Fisher Scientific, MA, USA) according to manufacturer's instructions and samples run on a High Sensitivity DNA chip using the Bioanalyzer 2100 instrument (Agilent Technologies, CA, USA) to determine library insert sizes. An equimolar mixture of the libraries (11 pM) was sequenced using a MiSeq reagent v2 kit for 500 cycles (2 x 250 bp paired end run) on an Illumina MiSeq instrument (School of Biology, Georgia Institute of Technology) running the MiSeq Control Software v2.4.0.4 (MCS). Adapter trimming and demultiplexing of sequenced samples was carried out by the MCS.

For community composition analyses, both 16S rRNA pyrosequencing and shotgun sequencing datasets were used separately. 16S rRNA pyrosequences obtained for four community samples were sorted, trimmed and filtered with a Phred average quality score of 34 using Roche GS FLX software (v 2.9) by Macrogen Inc. QIIME package was used for analysis of the resulting sequences, and the following steps were employed: (1) Trimmed sequences were clustered into operational taxonomic units (OTUs) with UCLUST (Edgar, 2010) using a 97% similarity cutoff; (2) Representative sequences from each OTU were taxonomically identified using RDP Classifier (<https://rdp.cme.msu.edu/classifier/classifier.jsp>) and "greengenes" database (<http://greengenes.lbl.gov>); (3) For each community, taxonomy counts were summarized at different levels (phylum, class, genus, etc.) and (4) Using the taxa counts, Shannon diversity indices were calculated.

Raw reads resulting from shotgun sequencing were trimmed using Solexa QA with a Phred quality score cutoff of 30 (Cox et al., 2010). The coverage of the obtained metagenomic dataset was estimated using the Nonpareil algorithm (Rodriguez and Konstantinidis, 2014). Trimmed reads were assembled using a hybrid pipeline (Luo et al., 2013), which uses a combination of Velvet (Zerbino and Birney, 2008), SOAPdenovo (Li et

al., 2010) and Newbler 2.0. MetaGeneMark (Zhu et al., 2010) was used for gene prediction from the assembled contigs. The statistics for the metagenomic dataset is given in Table 2.1.

Table 2.1. Assembly statistics of the metagenomic datasets used in this study

Community	Total Number of Contigs	N50 Contig Length* (bp)	Length of the Largest Contig	Total Number of Base pairs
SEW	9185	3981	175,701	16.9 x 10 ⁶
AS	6701	18,874	147,657	22.3 x 10 ⁶
SOIL	4337	17,164	157,475	17.3 x 10 ⁶
SEA	3072	14,922	130,113	15.9 x 10 ⁶

*N50 is the average length of contigs that account for 50% of the total

Coverage of each gene or contig was determined by mapping the reads onto the assembled sequence using BLASTn, with a minimum identity of 95% and alignment length no less than 50% of the query sequence. Coverage was estimated as the product of the total number of aligned reads multiplied with the average length of the aligned reads and divided by the length of the subject sequence. To identify the relative abundance of distinct functional categories in each community, proteins were first annotated in the uniprot database (December 2015, EMBL/GenBank/DDBJ databases), and then associated functional category was determined using the SEED subsystems (Overbeek et al., 2005). For community composition analyses performed using shotgun sequences, initially 16S rRNA gene sequences in aforementioned metagenome data sets were identified using Parallel-meta (Su et al., 2014) for taxonomic classification. The resulting sequences were then processed following the steps 1-4 described above.

2.2.5. Identification of Functions Specific to BAC Degradation in the Enriched Community Metagenomes

To identify the functions particularly related to BAC degradation, the relative abundances of the protein families in our four metagenomic datasets, along with two extra BAC exposed enrichment community metagenomes, were compared with metagenomes of three microbial communities previously unexposed to BAC which are referred as controls. Aforementioned five microbial community metagenomes were downloaded from the nucleotide database of National Center of Biotechnology Information (NCBI) (<http://www.ncbi.nlm.nih.gov>). Two of these metagenomic datasets were originating from microbial communities enriched with BACs (Oh et al., 2013) whereas the other three metagenomic datasets were originating from environments previously unexposed to BACs, such as a microbial community enriched with dextrin, activated sludge and an estuarine river sediment (Tezel et al., 2012; Oh et al., 2013; Tandukar et al., 2013). Control communities were selected arbitrarily based on the similarity of the source of the samples (activated sludge and estuarine river sediment) to the samples used as inoculum in BAC-enriched communities, as well as the available high quality metagenomic datasets for those communities at the NCBI database. Accession numbers of all metagenomic datasets used in this study are given in Table 2.1. Protein families in all metagenomic datasets were annotated using PFAM database (release 28.0) and HMMER3 (<http://hmmer.janelia.org/>). For each metagenome, total number of proteins from the same protein family were summed and then divided by the total number of proteins to yield “normalized counts”. Averages of normalized counts were taken for BAC related and control environments. The \log_2 fold change was estimated as the \log_2 ratio of average normalized counts between BAC-enriched and control samples and significant differences were identified with a negative binomial distribution test using the NBPSeg package implemented in R (<https://www.r-project.org>). A flowchart of the pipeline is shown in Figure 2.3.

Table 2.2. Accession numbers of the metagenomic datasets used in this study

NCBI Accession Number	Description/Origin	Reference
MCND000000000	BAC enriched/ activated sludge	This study
MCNE000000000	BAC enriched/ sewage	This study
MCNF000000000	BAC enriched/ soil	This study
MCNG000000000	BAC enriched/ sea sediment	This study
SRR643891	BAC enriched/ river sediment	Oh et al., 2013
SRR643892	BAC enriched/ river sediment	Oh et al., 2013
SRR643889	BAC unexposed/ river sediment	Oh et al., 2013
AERA000000000.1	BAC unexposed/ activated sludge	More et al., 2014
AMQJ000000000.1	BAC unexposed/estuarine sediment	Handley et al., 2012

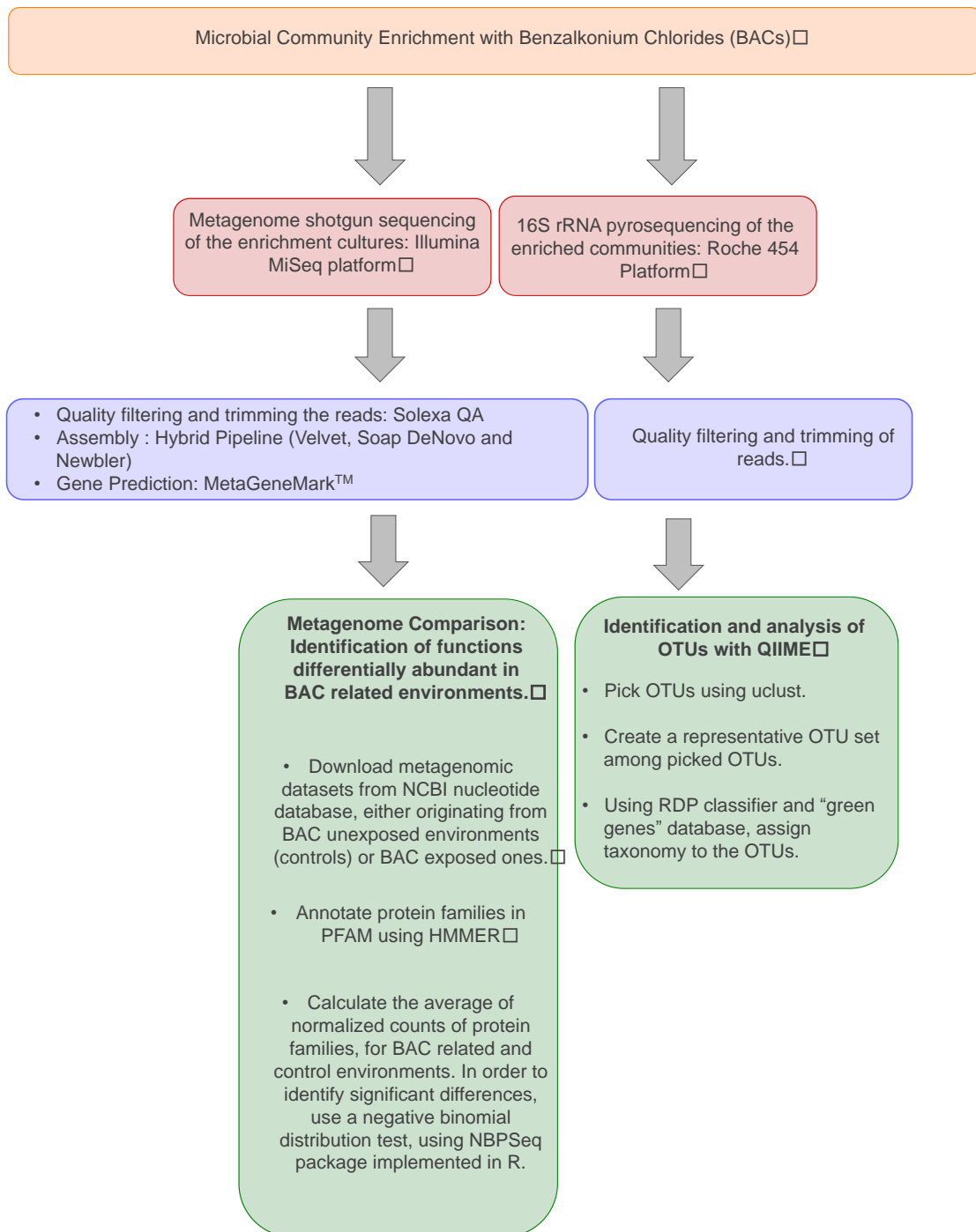


Figure 2.3. Pipeline used for processing metagenomic datasets

2.3. Result and Discussion

2.3.1. Phylogenetic Diversity of BAC-Enriched Microbial Communities

Four rapidly BAC degrading microbial communities enriched from sewage (SEW), activated sludge (AS), soil (SOIL) and sea sediment (SEA) were obtained using the dilution to extinction method. The BAC degradation profiles of those four communities during the course of operation are given in Figure 2.4.

Bacterial composition in BAC-enriched microbial consortia was assessed based on 16S rRNA pyrosequencing. Overall, a total of 148,362 high quality reads were obtained from four BAC-enriched communities, with an average length of 420 bp. 16S rRNA sequence fragments recovered in the shotgun metagenomic datasets of each sample (approximately 10,000 reads per sample), were also used for bacterial composition analysis. Similar results were obtained from analysis of 16S rRNA gene pyrosequences and shotgun sequences (Figure 2.5). More specifically, a total of 15 OTUs were detected in the amplicon datasets from the four enriched microbial communities. In other studies, it has also been shown that exposure to BACs results in reduced diversity in the microbial communities developed from a river sediment. Both Tezel et al. (2012) and Tandukar et al. (2013) identified a total of 9 OTUs in their clone libraries prepared from the DNA obtained from a BAC-degrading microbial community. Moreover, Oh et al. (2013) detected approximately 40 OTUs in the metagenome of a BAC-degrading microbial community. These results along with the ones reported in this study suggest that microbial diversity in BAC-degrading communities is low and comparable to each other.

All OTUs were assigned to the phylum of *Proteobacteria*. Relative abundance of the OTUs identified as *Pseudomonas* spp. was 13.5%, 88.2%, 83.5% and 44.8%, whereas *Achromobacter* spp. was 82.2%, 4.3%, 7.8% and 48.5% in AS, SEW, SOIL and SEA, respectively. Other minor genera, which included members of the *Stenotrophomonas*, *Serratia*, *Comamonas* and *Enterobacter* genera, were present in less than 10% of the total Figure 2.5. In summary, SEW and SOIL were composed mainly of *Pseudomonas* spp.,

whereas AS and SEA were dominated by *Achromobacter* spp. Shannon diversity indices were 1.15, 0.65, 0.77 and 1.29 for AS, SEW, SOIL and SEA, respectively, suggesting that diversity in all consortia was very low.

OTUs 8, 11, 12 and 14 were identified as *Pseudomonas* spp. (Figure 2.6). OTU12 made up the great majority of the *Pseudomonas* population in all consortia and its abundance was 86%, 82%, 43% and 13% of total OTUs in SEW, SOIL, SEA and AS, respectively. OTU12 was closely related to *Pseudomonas* sp. CMR12a (99% identity), a fluorescent bacteria which was isolated from the root of red cocoyam plant and can produce biosurfactants (Perneel et al., 2007). OTUs 2, 4 and 5 were closely related to *Achromobacter* sp., and their total abundances were 8%, 49%, 12% and 82% in SEW, SOIL, SEA and AS communities, respectively (Figure 2.6). OTU5 represented the major *Achromobacter* population in all communities. The closest match to OTU5 was *Achromobacter xylosoxidans* ZSB6 (96.2% similarity). This strain was isolated from a rice rizosphere, and there is no prior knowledge on its biodegradation capability of QACs or any other xenobiotics.

It was recently reported that phylogenetic diversity in two microbial consortia enriched from a river sediment (Calcasieu River, LA, USA), with BACs was significantly decreased compared to a control assay. Those communities were dominated by *Pseudomonas* spp., mainly *P. nitroreducens* and *P. putida* (Tezel et al., 2012; Oh et al., 2013; Tandukar et al., 2013). These results, combined with those reported here suggest that *Pseudomonas* species clearly have an important role in the establishment of BAC degrading microbial consortia. Different than reported, however, *Achromobacter* was the most abundant genus in the AS community. *Achromobacter* species capable of converting dialkyl dimethyl ammonium chlorides to tertiary amines have also been reported earlier (Van Ginkel, 2004).

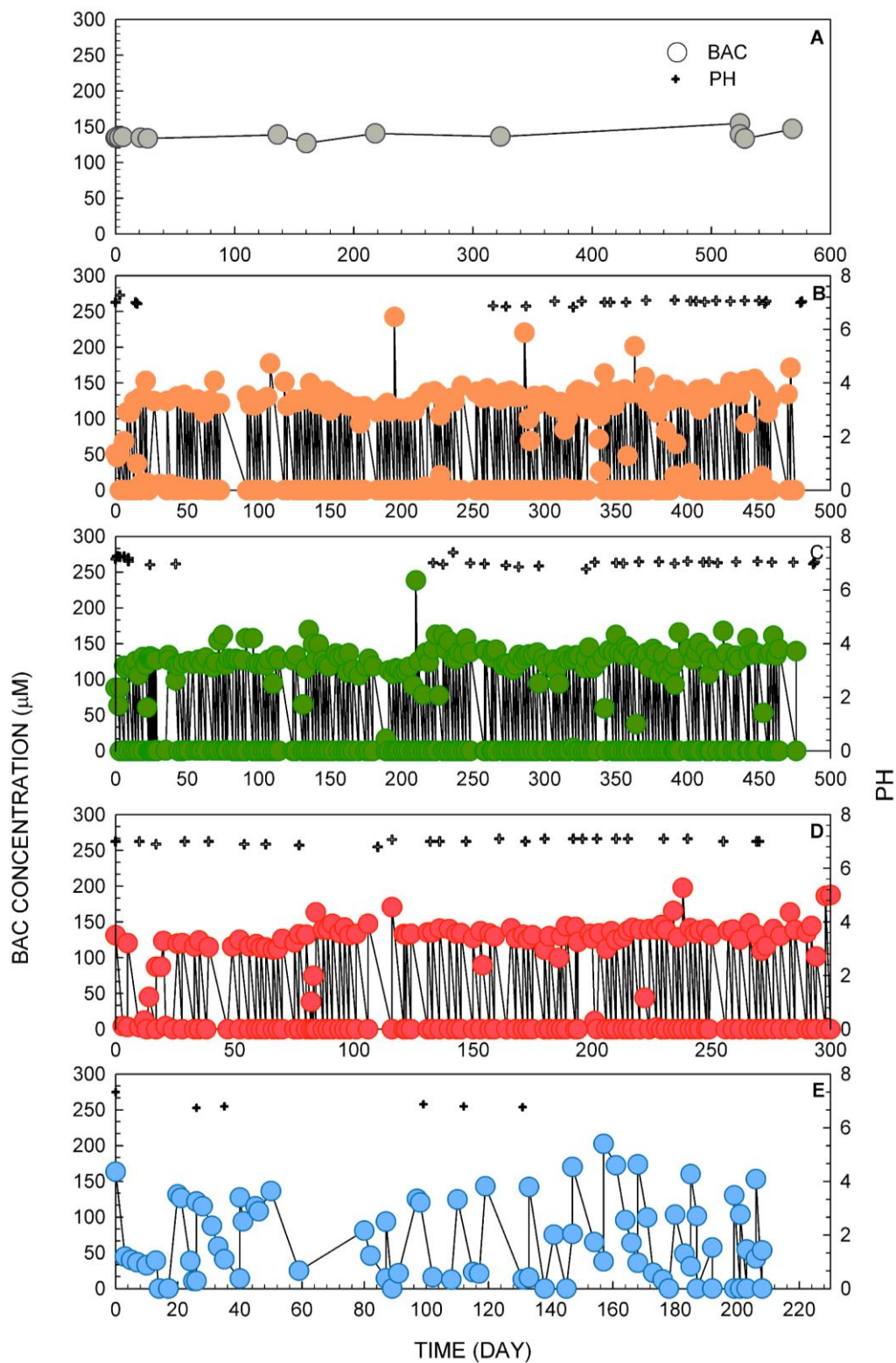


Figure 2.4. BAC degradation profiles in (A) Control and (B) AS, (C) SEW, (D) SOIL and (E) SEA enrichment communities

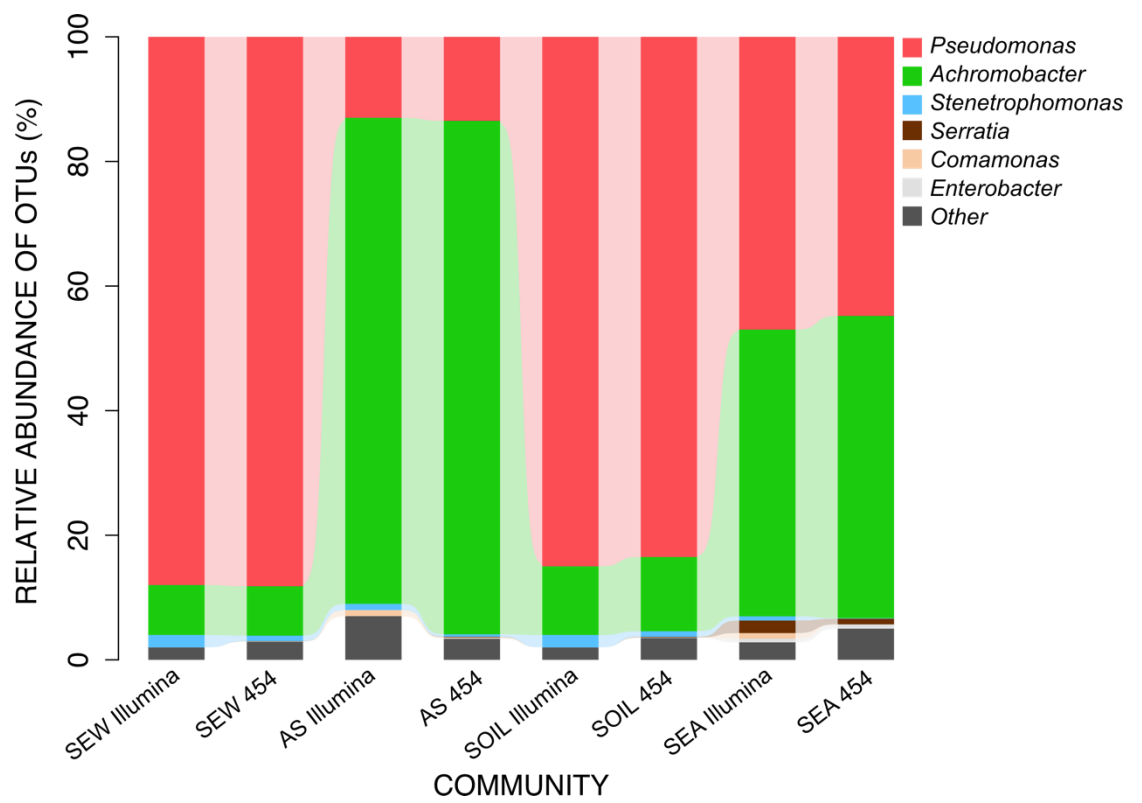


Figure 2.5. Relative abundance of bacterial genera present in the enriched microbial communities recovered by pyro- and shotgun sequencing of the genomic DNA

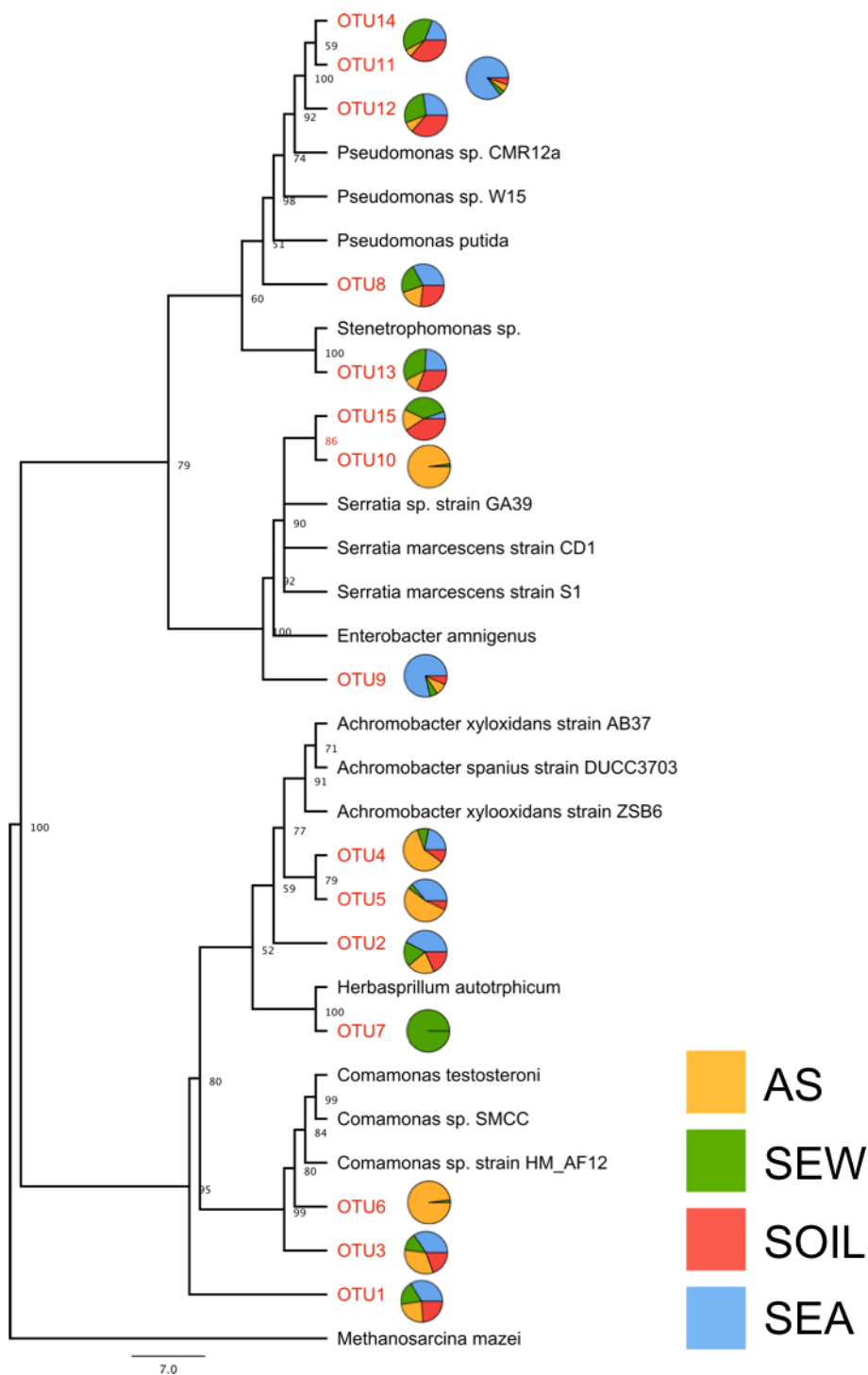


Figure 2.6. Phylogenetic relationship of the detected OTUs and their relative abundance in the communities. The abundance of an OTU in each community was summed up and this value was considered 100%. The abundance of that OTU in each community was divided by

this total value and the result was represented as the relative percentage of that OTU in a particular community.

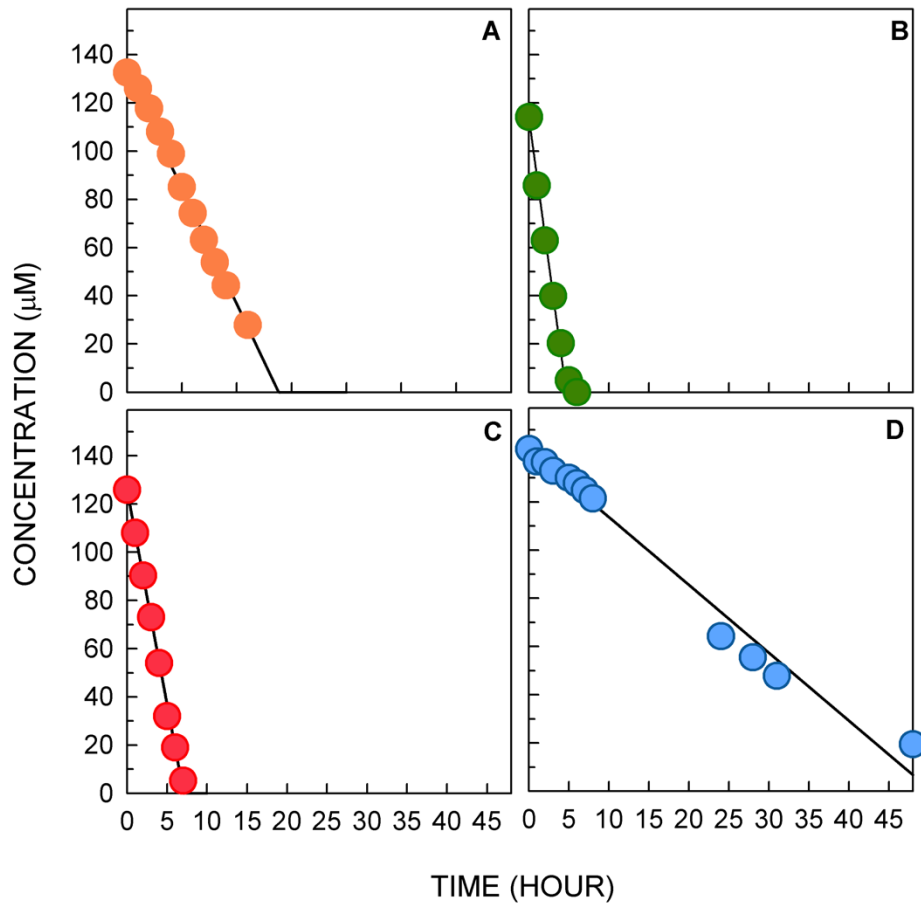


Figure 2.7. Profiles of BAC utilization in (A) AS, (B) SEW, (C) SOIL and (D) SEA enrichment communities

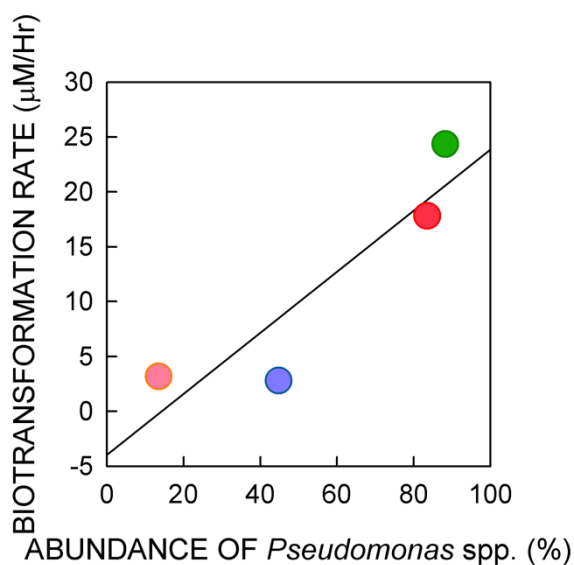


Figure 2.8. Relationship between the biotransformation rate of enrichment communities and abundance of *Pseudomonas* spp. AS (yellow) SEW (green) SOIL (red) SEA (blue)

The results reported here indicate that there are multiple microorganisms in the environment that play a significant role in BAC biotransformation. Moreover, other than OTU6 and 7 which were present only in AS and SEW, all remaining 13 (out of 15 total) OTUs were present in every community but at different relative abundances (Figure 2.6). This suggests that BAC degrading microbial communities were similar; at least at the genus level, and thus highly-overlapping in terms of species present in each community, specialized microbial consortia are responsible for BAC degradation in various environments. The repeated co-occurrence of certain species in microbial communities has been frequently attributed to symbiosis in metabolite exchange (Zelezniak et al., 2015). Symbiosis may have facilitated the syntropic relationship among the bacteria in the community and enhanced the survival by resource sharing and development and dissemination of BAC resistance. BAC-enriched communities in this study mimic oligotrophic environments with BAC as the main carbon source such as those represented by BAC contaminated groundwater, river or soil, and surfaces at homes and hospitals treated with BAC containing disinfectants. Although not all members in the specialized microbial consortia might be a BAC degrader, utilization of by-products such as tertiary, secondary

and primary amines, aliphatic and aromatic acids and aldehydes along with resistance to BACs can facilitate survival of multiple species. Furthermore, some members of these core microbial consortia such as *Serratia* and *Enterobacter* harbor potentially pathogenic species, which can co-exist in BAC-enriched microbial communities originating from environments in close contact to humans.

2.3.2. Core Functions in BAC Degrading Microbial Consortia and Distinct Functions Related to BAC Degradation

For each enriched microbial community, categories of enriched functions were determined using SEED subsystems. Despite the differences in terms of taxonomic composition, 84% of all the functions, which corresponded to a number of 3333 protein families, were shared among four enriched communities (

Figure 2.9). On average, the most abundant core functions were related with amino acid metabolism (12.0 ± 2.5 %), cofactors, vitamins and prosthetic groups (9.8 ± 1.8 %), protein metabolism (8.7 ± 1.4 %) and carbohydrate metabolism (8.6 ± 1.7 %) (Figure 2.10).

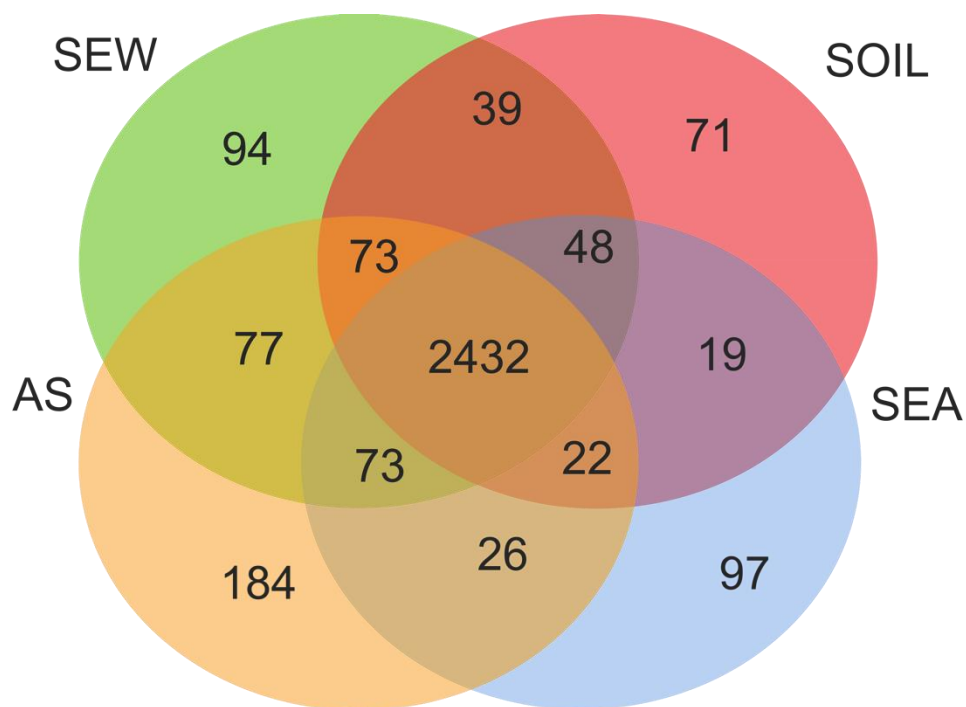


Figure 2.9. Venn diagram showing the number common and distinct functions in enrichment cultures.

A minor fraction of the total genes in enriched communities were unique to each community (Figure 2.9). To identify community specific functions with regard to protein families, unique genes from each community were annotated in the PFAM database. Community with the most unique protein families was AS (142), followed by SEA (86), SOIL (56) and SEW (55). Based on this pattern, it could be argued that as the abundance of *Pseudomonas* decreased, minor microbial groups specific to each environment could survive, leading to the proliferation of unique functions. Interestingly, a major portion of the community specific unique protein families was of uncharacterized function (Figure 2.11). In the AS community, phage related functions constituted a significant fraction of the community-specific functions, which were not abundant in the other three communities. Other than that, different glycosyl hydrolase proteins were comparably abundant among community specific functions. The significance of these proteins for the community structure is unknown, however may play an important role in adaptation to BACs in different ecosystems.

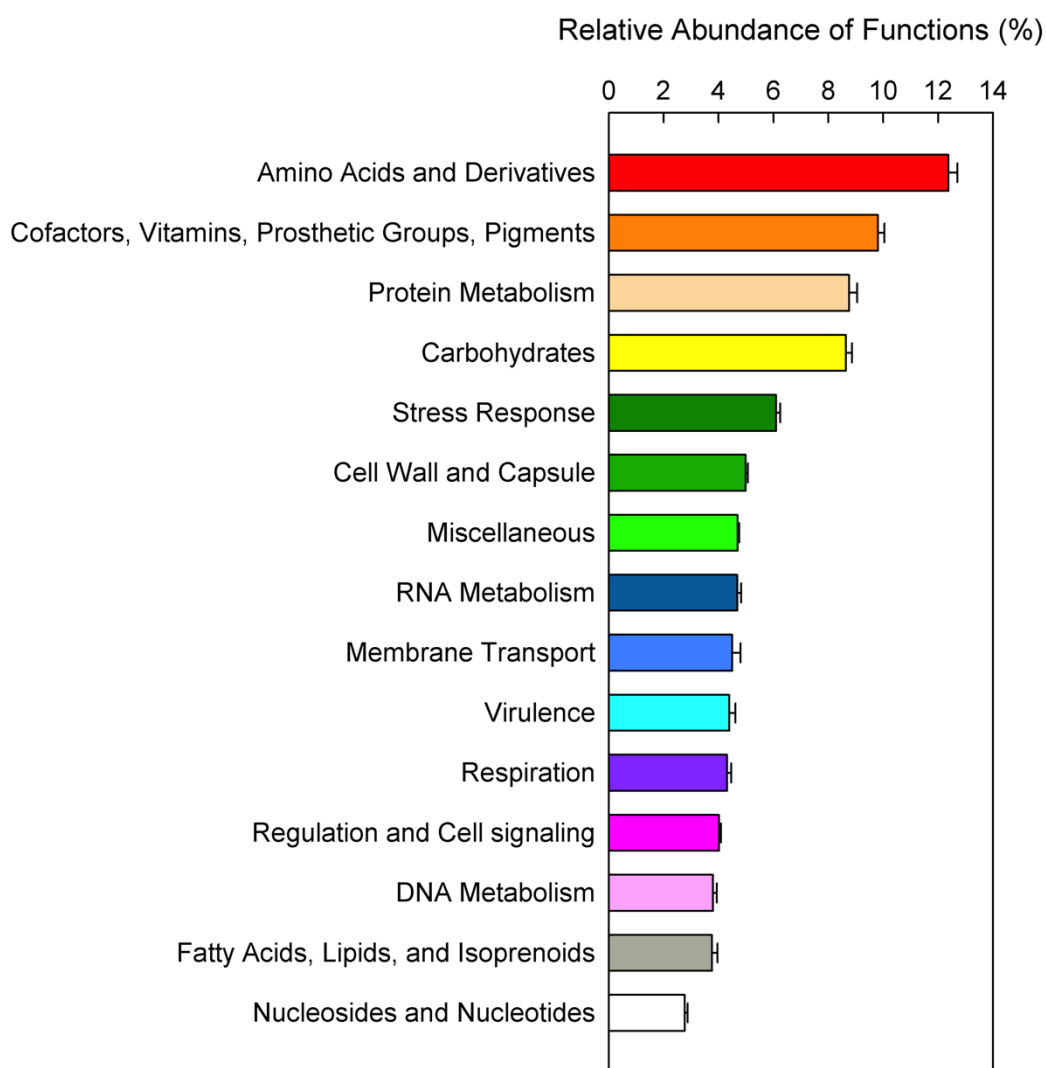


Figure 2.10. Relative abundance of the functional categories in enriched microbial communities identified in SEED database

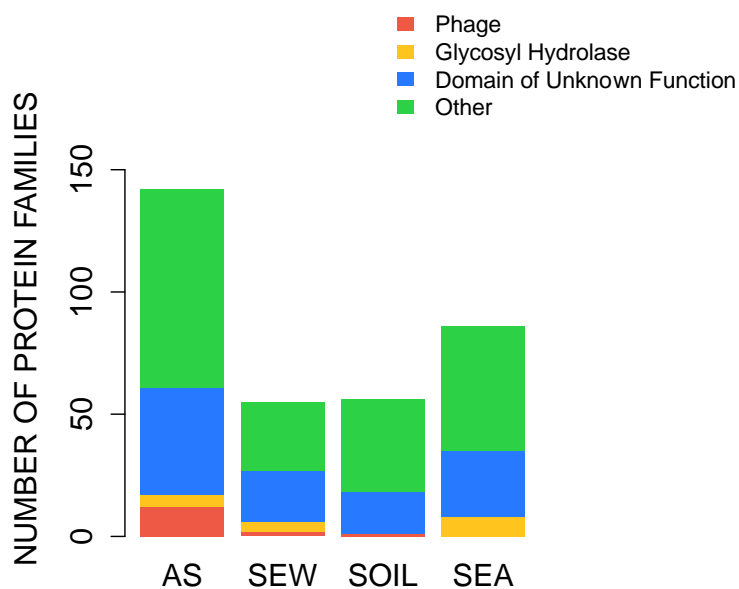


Figure 2.11. Unique functions of each community

In order to identify the specific traits related to BAC degradation, relative abundances of the protein families in BAC degrading microbial communities and in microbial communities unexposed to BAC were compared. Briefly, three microbial community metagenomes unexposed to BACs, originating from environments similar to this study, were obtained from the nucleotide database of NCBI along with two enriched with BACs. These datasets were combined with the metagenomes in this study (AS, SEW, SOIL, SEA). Significant differences in abundance of protein families in each metagenome were determined.

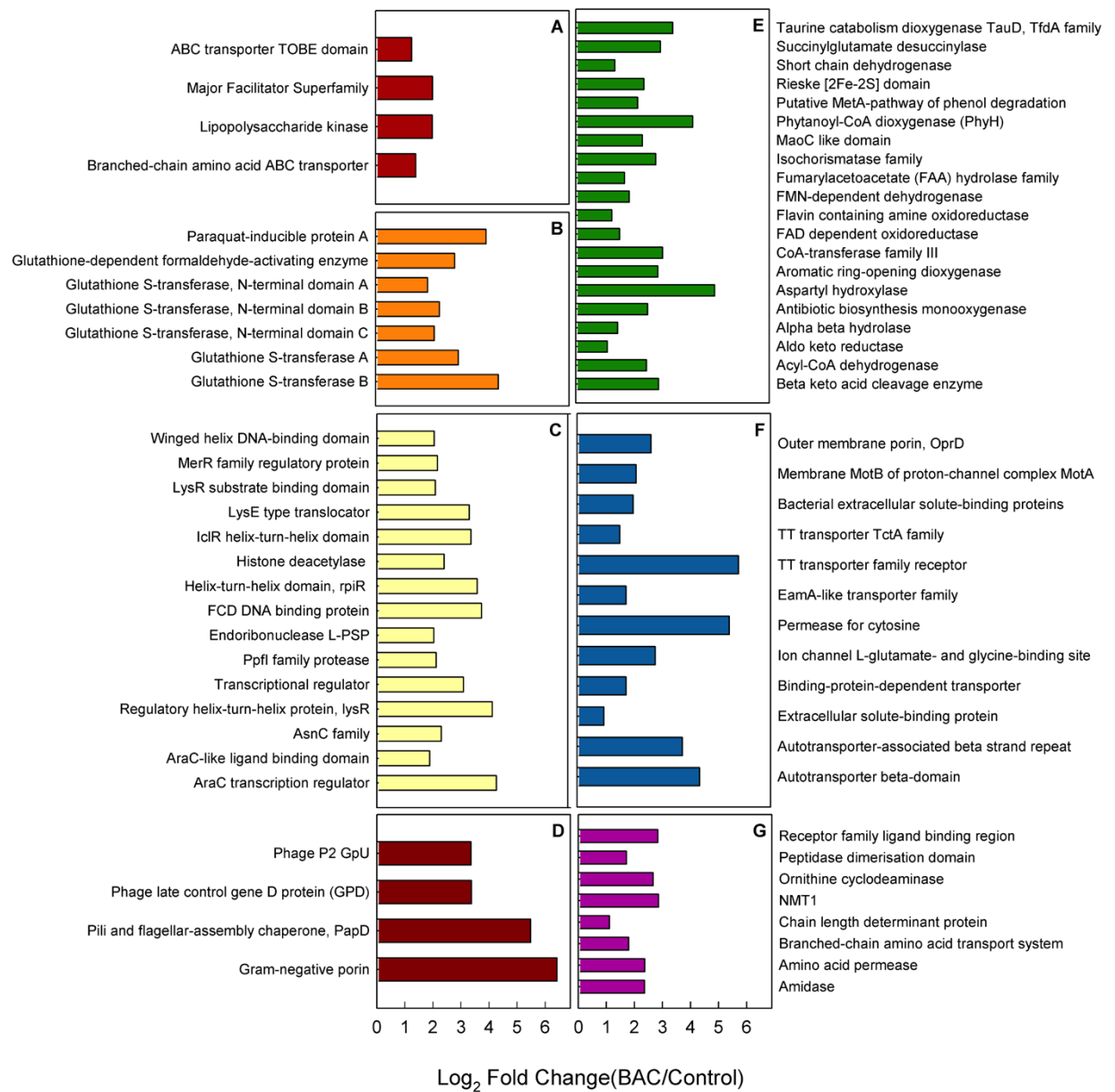


Figure 2.12. Differentially abundant functions in BAC-enriched microbial communities compared to the controls: (A) Antimicrobial resistance; (B) Oxidative stress response; (C) Gene expression regulation; (D) Horizontal gene transfer; (E) Catabolic reactions; (F) Transport and (G) Protein metabolism. The \log_2 fold change was estimated as the \log_2 ratio of normalized counts between BAC-enriched and control samples. Significant differences in the relative abundance of proteins were determined with a negative binomial test.

Overall, the protein families that became significantly abundant in BAC degrading microbial communities ($p < 0.05$) were categorized into seven functional classes i.e. multidrug resistance, oxidative stress response, gene expression regulation, catabolic reactions, protein metabolism, outer cell structure modification and transport (Figure 2.12). In general, these functions were mainly related to antimicrobial resistance (Figure 2.12A-D) and degradation of organics (Figure 2.12D-G). The protein families with putative antimicrobial resistance related functions were mainly multidrug resistance efflux proteins. They were mainly represented by major facilitator superfamily (MFS) transporters, and ATP binding cassette (ABC) superfamily transporters (Figure 2.12F). It has been previously shown that MFS and ABC superfamily transporters facilitate extrusion of QACs from the cell, thus they have been associated with QAC resistance and resistance against several antibiotics (Oh et al., 2013). Therefore, it can be hypothesized that MFS and ABC multidrug efflux systems were the main contributors to BAC resistance in the BAC degrading communities. Similarly, in a recent study it was reported that two multidrug efflux pump related protein families (HlyD secretion and SMR family efflux pump protein, what are they?) became significantly abundant in BAC exposed microbial communities compared to the control (Oh et al., 2013).

Proteins associated with oxidative stress response which are overrepresented in BAC degrading microbial communities, included a group of glutathione S-transferases (Figure 2.12B). These proteins have been previously linked with BAC induced stress response (Nakata et al., 2011), and hence reported as abundant in BAC degrading microbial communities (Oh et al., 2013). A paraquat inducible protein family also became significantly abundant in BAC degrading microbial communities. This protein family has been shown to take part in the regulation of oxidative stress response induced by paraquat, which is also a QAC (Nunoshiba et al., 1992).

A collection of proteins related to gene expression regulation also dominated in BAC degrading communities compared to the controls. Main representatives of these proteins were members of the LysR, LysE, MerR, rpiR, AraC and AsnC families of transcriptional regulators (Figure 2.12). Exposure to QACs and BACs triggers an oxidative stress response,

which can cause mutations and interfere with the regulatory system of the cell. This often results in overexpression of the efflux pump genes and their horizontal transfer via various mobile genetic elements (Tezel and Pavlostathis, 2015). Enrichment of the transcriptional regulators in this study may be linked to such phenomena, although currently this hypothesis lacks experimental verification. Furthermore, a group of proteins likely related to horizontal gene transfer events, mainly two phage proteins (Phage P2 GpU and Phage late control gene D protein), a Gram negative porin protein that can be used as a phage receptor, and a pilin protein that assists conjugation (PapD) (Barnhart et al., 2000) were significantly enriched in BAC degrading communities (Figure 2.12D).

Several protein families with putative catabolic function became significantly enriched in BAC degrading microbial communities. First one was oxygenases mainly consisting of Rieske and phytanoyl-CoA type oxygenases (Figure 2.10E). These enzymes have been associated with the degradation of quaternary ammonium compounds (Zhu et al., 2014) and tertiary amines (Martinez and Hausinger, 2015), respectively. Hence, likely plays a part in transformation of BAC and BDMA. Other significantly enriched catabolic proteins were FAD dependent oxidoreductases, amine oxidases, dehydrogenases and hydrolases. These were probably involved in metabolization of produced metabolites like benzaldehydes, secondary amines and alkanolic acids. (Figure 2.12E).

As expected, another group of proteins that became significantly more abundant in BAC degrading communities were membrane transporters and ion channel proteins, which participate in the transfer of solutes and ionic compounds into the cell (Figure 2.12F). These proteins likely promote uptake of BAC degradation products into the cell. Likewise, proteins associated with amino-acid metabolism and assimilation of nitrogen compounds such as aminotransferases, amidohydrolases and branched chain amino acid transport system were also more abundant in BAC-enriched communities compared to the controls (Figure 2.12G), and therefore they may have a role in the assimilation of nitrogenous compounds resulting from BAC biotransformation.

To further explore the genes that are specific for BAC degradation, a FAD-using amine oxidase (AO_x-BAC) (GenBank Accession Number: KJ911918) that was previously identified as responsible for the initial dealkylation reaction in the QAC biotransformation pathway (Oh et al., 2014) and a tetradecyl trimethyl ammonium bromide monooxygenase (TTABMO) (GenBank Accession Number: JN797595) (Liffourrena and Lucchesi, 2014) were searched within our metagenomic datasets. These genes were not present in our BAC degrading communities, which suggested that there might be other genes responsible for biotransformation of QACs in the environment.

3. PHYLOGENETIC AND GENOMIC CLASSIFICATION OF A NOVEL PSEUDOMONAS THAT DEGRADES BENZALKONIUM CHLORIDES

A part of this chapter was published in “Environmental Science and Technology” journal entitled “Similar Microbial Consortia and Genes Are Involved in the Biodegradation of Benzalkonium Chlorides in Different Environments”. Disclosure of the article is permitted by Hatt, J.; Konstantinidis, K. T. and Tezel, U. The remaining part is being prepared for publication under the working title “A Novel *Pseudomonas* sp. BIOMIG1 is a Predominant BAC Degradation in the Environment”.

3.1. Introduction

Benzalkonium chlorides (BACs) are prominent members of QAC disinfectants. Contamination of the environment with BACs poses a significant threat to both environmental safety and public health. Despite their antimicrobial properties, some microorganisms in the environment can degrade QACs/BACs and convert them to non-toxic end products. QAC degradation commences with a N-dealkylation reaction that results in the formation of a trimethylamine and an alkanaldehyde. This is the key step in the pathway that alleviates the environmental impact of BACs.

Using microorganisms is a promising and efficient tool for eliminating QACs from the environment. Isolating QAC and BAC degraders and revealing their physiological and genomic properties is necessary for their efficient use in wastewater treatment applications. To date, several QAC degraders mainly from the *Pseudomonas* genus has been isolated (Tezel and Pavlostathis, 2012). Most of those microorganisms such as *Pseudomonas putida* ATCC 12633 (Liffourrena and Lucchesi, 2014) and *P. nitroreducens* B (Oh et al., 2014) could not accomplish the whole pathway but stopped at the tertiary amine intermediate (BDMA or TMA). Among them *P. putida* ATCC 12633 immobilized cells could remove 80% of QACs up to 315 mg/L within 48 hours from wastewater effluent (Bergero and Lucchesi, 2015).

Isolation and characterization of QAC degraders is not only important to use them in wastewater treatment applications but also to understand the potential threats they present against public health. A recent study revealed that *Burkholderia caepacia* strains isolated from clinical environments could degrade BACs, which decreased the efficacy of BAC disinfectants in hospitals. (Ahn et al., 2016).

In the environment, QAC degradation is not restricted to disinfectants but there are also microorganisms which degrade naturally occurring QACs. *Sinorhizobium mellioti* is a nitrogen fixing soil bacterium which degrades QACs like stachydrine, which is secreted from the roots and used as osmoprotectant and nitrogen source (Daughtry et al., 2012). Likewise *Acinetobacter baumannii* converts carnitine, a dietary QAC found in the guts of humans, to trimethylamine whereas *Pseudomonas aeruginosa* degrades glycine betaine; a ubiquitous QAC in the environment. It can be argued that pathways for xenobiotic QAC degradation evolved from natural QAC degradation. Isolating and characterizing QAC degraders would unravel how QAC degradation evolved in the environment as well as lead to identification of new and potentially more efficient QAC degraders. Exploring the genomes of these efficient QAC degraders would enable discovery of novel enzymes which could further be used in advanced treatment applications. Unfortunately, the genome of a QAC degrader is yet to be sequenced. In the previous chapter, it was demonstrated that there was a linear relationship between the abundance of a particular *Pseudomonas* population and BAC biodegradation rates of four enrichment cultures (AS, SEW, SOIL, SEA). In this chapter, that *Pseudomonas* was isolated and characterized.

3.2. Materials and Methods

3.2.1. Isolation and Characterization of BAC Degrading Microorganisms

Isolation of *Pseudomonas spp.* in each community was performed using selective agar plating as follows: A 100 μL sample was taken from each microbial community, diluted 10^5 times, and spread onto CHROMAgar *Pseudomonas*TM plates. Blue/green colonies growing on the plates were picked and re-streaked onto fresh CHROMAgar *Pseudomonas*TM. Individual colonies were transferred to Luria Bertani (LB) broth containing 50 mg/L BAC (LB-BAC broth) and incubated overnight at 30°C. About 40 *Pseudomonas* colonies from each community were obtained. In order to determine the biotransformation capabilities of the isolates, single colonies obtained by streaking on LB-BAC agar were suspended in 2 mL SM containing 50 mg/L BAC as the only carbon source in a 10-mL culture tubes. BAC concentration in the culture tubes was monitored for one week using HPLC as previously described (see Chapter 2.2.2).

Phylogenetic identification of the isolates that were able to degrade BACs was made based on their 16S rRNA gene sequences. Briefly, DNA of an overnight grown culture was extracted using BS 434 DNA extraction kit (Bio Basic Inc., Ontario, Canada) following the manufacturer's instructions. 16S rRNA genes were amplified by PCR using TaKaRa Premix TaqTM Kit (TaKaRa Bio, Shiga, Japan) with the following universal primers: 27F forward primer (27F: 5'-AGAGTTTGATCMTGGCTCAG-3') (0.4 μM), and 1492R reverse primer (1492R: 5'-TACGGYTACCTTGTTACGACTT-3') (0.4 μM). The resulting amplicons were then sequenced in Macrogen Inc. (Amsterdam, Netherlands) using the Sanger Sequencing platform. Forward and reverse sequences were trimmed and assembled using Geneious Software to yield about 1350 bp length and above 95% quality 16S rRNA sequence. 16S rRNA sequences of isolates were aligned using MUSCLE. A neighbor joining phylogenetic tree was prepared from a distance matrix created by a maximum likelihood method. Two isolates from each community that could do complete degradation or accumulated BDMA were selected for further analysis.

BAC susceptibility of isolates was determined using a broth dilution method with a concentration range between 1-1024 mg/L BAC. The BAC concentration that inhibited growth was reported as the minimum inhibitory concentration (MIC). Catalase activity of the isolates was determined according to Li and Schellhorn (2007) and oxidase activity was determined by using Bactident® oxidase test strips (Merck Millipore, Merck KGaA Darmstadt, Germany). In order to determine BAC degradation kinetics of the isolates, a batch biotransformation experiment was performed in 250-mL Erlenmeyer flasks. Briefly, isolates were grown overnight in LB-BAC broth and harvested cells were resuspended in 100 mL SM. The cell suspension was spiked with 10 μM C₁₂BDMA-Cl. After all C₁₂BDMA-Cl was consumed, the same amount of C₁₂BDMA-Cl was re-spiked and its concentration was measured at 1-hour intervals. The experiment was performed in triplicate. In order to determine BAC degradation rate constant (*k*), experimental data was fitted to Michaelis-Menten growth model using Berkeley-Madonna software employing Runge-Kutta 4 integration method. Equation 1 was used to simulate the model where *[BAC]* is the C₁₂BDMA-Cl concentration (μM), *k* is the BAC degradation rate constant (μmoles/hour·10¹¹ cells), *K_{BAC}* is the half saturation constant (μM) and *X* is the cell concentration (10¹¹ cells/L).

$$\frac{d[BAC]}{dt} = \frac{k[BAC]X}{K_{BAC} + [BAC]}$$

Equation. 1

A second batch assay was conducted with the strain isolated from SEW community, in order to delineate the biotransformation pathway of C₁₄BDMA-Cl. Briefly; two experiment sets were prepared in 120 mL serum bottles containing either 250 μM C₁₄BDMA-Cl or 1000 μM BDMA dissolved in 80 mL SM. An overnight culture of a BAC degrading isolate was resuspended in SM and inoculated into the serum bottles. The bottles were closed with rubber stoppers and crimped with aluminum seals to prevent intrusion of air into the bottles. Headspaces of the serum bottles were then flushed with nitrogen and 10 mL O₂ were injected into the 20-mL headspace. The assay was performed in triplicates.

C_{14} BDMA-Cl and its biotransformation by-products were monitored daily with HPLC. Non-chromophoric biotransformation by-products dimethyl amine (DMA) and methyl amine (MMA) were analyzed after the sample was derivitized with 7-Chloro-4-nitro-2,1,3-benzoxadiazole (NBD-Cl). Primary and secondary amine derivatives were measured by HPLC equipped with Polaris 18A RP column using a 55:45 % Water:Methanol mobile phase at a flow rate of 1 mL/min. Detection was achieved using a UV-Vis diode array detector set at 490 nm. The headspace gas composition (O_2 and CO_2) in the bottles were determined by an Agilent 6850 Series GC unit (Agilent Technologies Inc., Palo Alto, CA) equipped with a 30 m Carboxen 1010 Plot fused silica, 0.53 mm i.d. column (Supelco Inc.) and a thermal conductivity detector. Helium was used as the carrier gas at a constant flow rate of 6 mL/min. The 10:1 split injector was maintained at 150°C, the oven was set at 40°C and the detector temperature was set at 150°C. All gas analyses were performed by injecting 200 μ L gas sample.

3.2.2. Scanning Electron Microscopy of *Pseudomonas* sp. BIOMIG1

A high resolution (2 nm) Environmental Scanning Electron Microscopy (ESEM) equipped with a full range energy dispersive spectroscopy (EDS) Detector-Image Processing and a high temperature attachment (Philips XL30 ESEM-FEG) was used to visualize microorganisms. Sample preparation prior to visualization was as follows; an overnight grown culture of *Pseudomonas* sp. BIOMIG1 in LB-BAC was rinsed with 1X phosphate buffer saline (PBS) and fixed with 2.5% glutaraldehyde prepared in 1X PBS at 4°C for 4 hours. The sample was rinsed again with 1X PBS and resuspended in deionized water. 10 mL of the cell suspension with an OD_{600} adjusted to 0.25 AU was passed through a 0.45 μ millipore filter. Subsequently, the filter was dehydrated in an increasing ethanol series (%25-%50-%75-%100) and air-dried overnight. Appropriate sections of the filter were further used for ESEM analysis.

3.2.3. Determination of the Carbon Utilization Patterns of Microorganisms using BIOLOG GENIII™ Micro Plates

To characterize the phenotypic properties of *Pseudomonas* sp. BIOMIG1 strains isolated from different enrichment cultures (ecotypes), carbon utilization patterns were identified using BIOLOG™ GEN III microplates. The manufacturers instructions were followed. Briefly, an overnight grown colony of *Pseudomonas* sp. BIOMIG1 was transferred into the inoculation fluid provided by the manufacturer, where the turbidity of the fluid was approximately 0.1 AU at OD₆₀₀. 100 µL aliquot of this suspension was inoculated into each well of the BIOLOG GEN III microplate. The plates were incubated at 28°C (the optimum growth temperature of *Pseudomonas* sp. BIOMIG1). After 24 hours, the color change in the wells was recorded. If there was a color change in a well, it was assumed that the carbon source was utilized and the result was recorded as “1”, whereas if there was no color change the result was recorded as “0”. A binomial matrix was constructed using the carbon utilization data of each BIOMIG1 ecotype and *Pseudomonas putida*. The results were analyzed using Hierarchical clustering. Distance calculation method was binary and clustering was made according to “unweighted pair group method with arithmetic mean (UPGMA)”. *Stats* package implemented in R was used for the analyses.

3.2.4. Sequencing the Draft Genome of *Pseudomonas* sp. BIOMIG1 and Bioinformatics analysis

To sequence *Pseudomonas* sp. BIOMIG1 whole genome, DNA was extracted from an overnight grown culture using the NucleoSpin™ Soil DNA Extraction Kit (Macherey Nagel, France). Sequencing was performed using the Illumina HiSeq2000 platform in MacroGen Inc. (Amsterdam, Netherlands). Same methods used for assembling the metagenome shotgun sequences and predicting genes were used to process whole genome shotgun sequences. After gene prediction, the protein sequences were annotated using the uniprot database. The corresponding functional classes were identified using the SEED subsystems.

To reveal the relationship of *Pseudomonas* sp. BIOMIG1 with related microorganisms, the draft genome of *Pseudomonas* sp. BIOMIG1 was aligned with the genomes of fourteen different microorganisms (Table 3.1), which were downloaded from the NCBI's genome database. MAUVE algorithm implemented in Geneious® R7.1 was used for alignment (Darling et al., 2004) and calculating the distances. To identify the unique features in the genome of BIOMIG1, proteins of BIOMIG1 was compared with *P.protegens* using the “reciprocal best match (RBM)” blast method. Briefly, using an in-house script the two protein sets were blasted in a pairwise manner. The cutoffs for the minimum alignment length and identity were 30% of the query length and 30% sequence and identity, respectively. The matched proteins were identified as common and were subtracted from the total set of proteins of BIOMIG1.

Table 3.1. Accession numbers of the genome sequences used in phylogenetic analysis

Organism	RefSeq Accession Number
<i>P.protegens</i> Pf5	NC_004129.6
<i>P.fluorescence</i>	NC_016830.1
<i>P.putida</i> K2244	NC_002947.4
<i>P.nitroreducens</i>	NZ_AZRU00000000.1
<i>P.sp.</i> BIOMIG1	MCRS00000000
<i>P.fluorescence</i> Pf1	NC_007492
<i>P.putida</i> BIRD1	NC_017530.1
<i>P.putida</i> F1	NC_009512.1
<i>P.protegens</i> CHA0	NC_021237.1
<i>P.chlororaphis</i>	NZ_CP008696.1
<i>P.montelii</i>	NC_023075.1
<i>P.fulva</i>	NC_015556.1
<i>P.stutzeri</i>	NC_015740.1
<i>E.coli</i>	NC_000913.3

3.3. Results and Discussion

3.3.1. *Pseudomonas* sp. BIOMIG1 is the Prevalent BAC Degradar in the Environment

There was a correlation between the abundance of Pseudomonads and BAC biodegradation rates of the enrichment communities, indicating that *Pseudomonas* spp. was responsible for BAC degradation in the microbial communities developed in this study. To test this hypothesis, the specific *Pseudomonas* population corresponding to OTU12 was isolated using selective plating on ChromAgar *Pseudomonas*TM. In total, 40 blue/green colored colonies on the selective agar indicative of *Pseudomonas* strains were obtained from each enrichment community and their BAC biotransformation capabilities were measured. Almost all isolates utilized BACs within 3 days. Although none of the BAC biotransformation by-products were detected in the samples taken from most of the tubes, indicating complete mineralization, BDMA was detected at a molar concentration equal to the initial BAC concentration amended in the samples in a few tubes (~2-3 out of 40). The isolates obtained from the enrichment cultures originating from different environments are referred as ecotypes, hereafter. The descriptions of the abbreviations used for isolate labeling is given in Table 3.2.

Table 3.2. Description of the abbreviations used for isolate labeling

Abbreviation	Description
SEW,AS, SOIL, SEA	Indicates origin of the enrichment culture from which the microorganism was isolated
BAC	BAC degrader
BDMA	BDMA Accumulator
BD	Only BDMA degrader
N	Can not degrade BAC or BDMA

The 16S rRNA genes of all *Pseudomonas* spp. isolates recovered from the communities were sequenced. All sequences were identical to each other and OTU12. Therefore, 16S rRNA gene sequencing confirmed that the isolates represented OTU12, which was denoted as *Pseudomonas* sp. BIOMIG1. 16S rRNA gene sequence of BIOMIG1 was then aligned with the sequences of other BAC/QAC degraders, including *Pseudomonas putida* ATCC 1233 (Liffourrena and Lucchesi, 2014), *Pseudomonas* sp. 7-6 (Takenaka et al., 2007), and other selected *Pseudomonas* species. Based on phylogenetic analysis of 16S rRNA gene BIOMIG1 was significantly different from other BAC/QAC degraders and formed a distinct clade close to *P. putida* group (Figure 3.1).

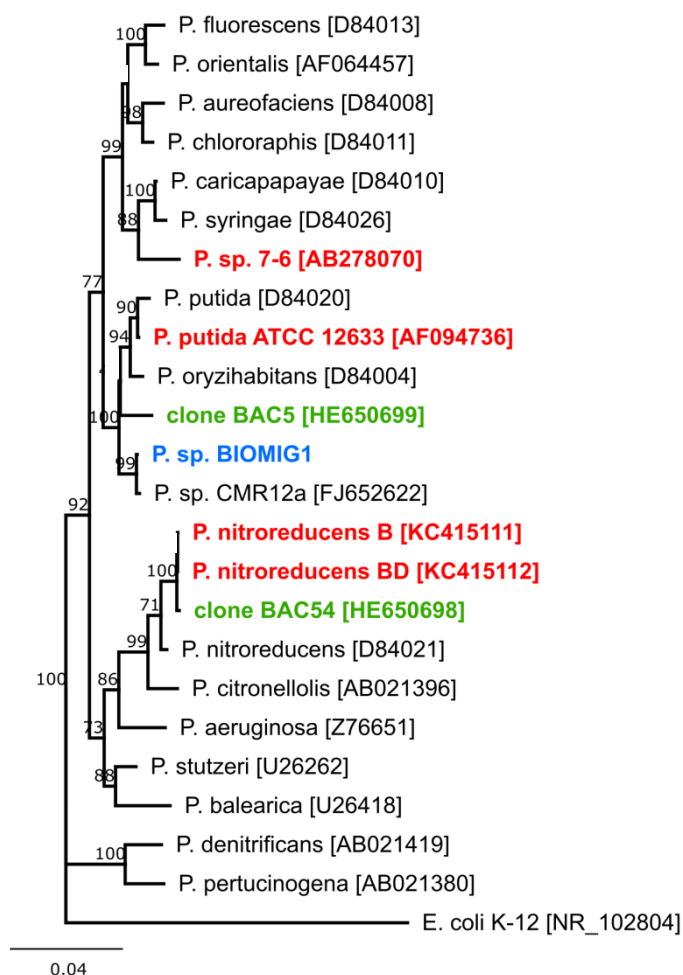


Figure 3.1. Phylogenetic relationship of *P. sp. BIOMIG1* (blue) with other QAC degrading species (red)

3.3.2. Phenotypic Characterization of *Pseudomonas* sp. BIOMIG1

Pseudomonas sp. BIOMIG1 was an aerobic rod shaped microorganism that was catalase and oxidase positive (Figure 3.2). All BIOMIG1 ecotypes except the ones isolated from the AS community produced a fluorescent pigment when growing on LB-BAC and *Pseudomonas* selective agar. All BIOMIG1 ecotypes were also highly resistant to BAC with an MIC of at least 1024 mg/L.

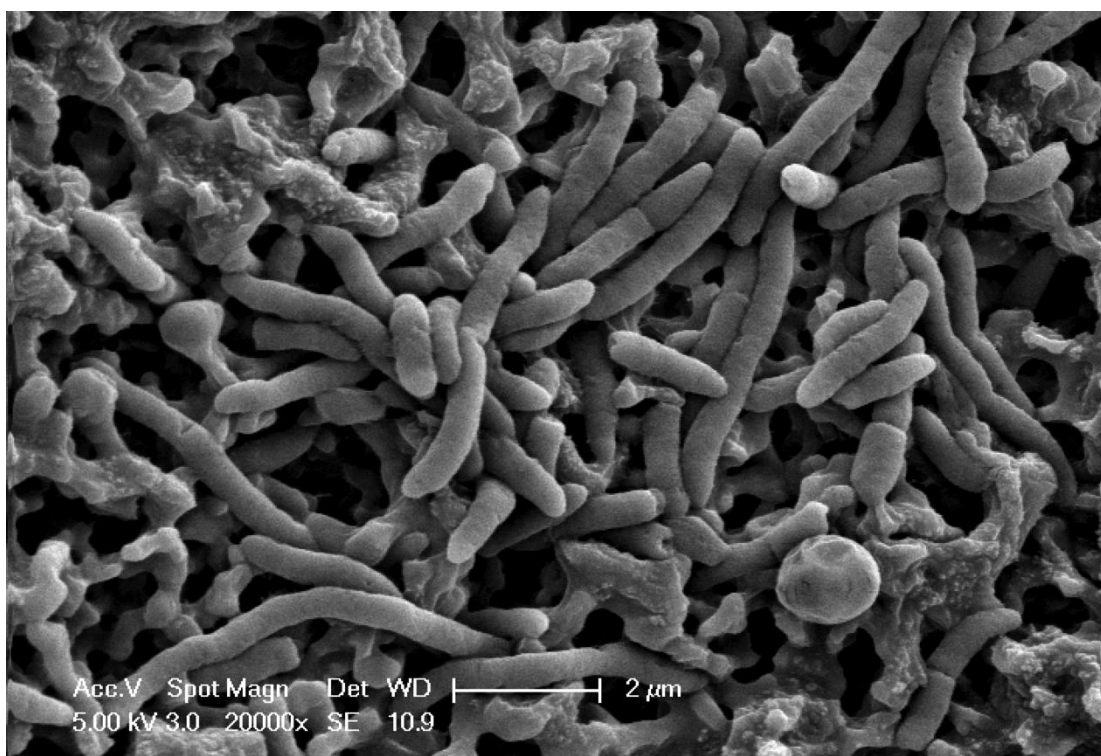


Figure 3.2. Scanning Electron Micrograph of *Pseudomonas* sp. BIOMIG1

In order to elucidate the BAC biodegradation pathway, *Pseudomonas* sp. BIOMIG1 was inoculated into serum bottles containing SM with 200 μM C₁₄BDMA-Cl under oxygen limiting conditions, to assure accumulation of metabolites. C₁₄BDMA-Cl concentration decreased to 75 μM within 3 days (Figure 3.3). During this period, O₂ concentration dropped from 0.45 atm to 0.15 atm and 0.015 atm CO₂ was detected in the headspace (Figure 3.3B). Both C₁₄BDMA-Cl and O₂ utilization slowed down afterwards.

Only 50 μM $\text{C}_{14}\text{BDMA-Cl}$ was utilized within 6 days as O_2 concentration fell below 0.1 atm (Figure 3.3B). Given the linear relationship of O_2 utilization with $\text{C}_{14}\text{BDMA-Cl}$ utilization (Figure 3.4A), and CO_2 formation (Figure 3.4B), $\text{C}_{14}\text{BDMA-Cl}$ biotransformation is an oxidation reaction that results in mineralization of the BACs. An experiment with the same set up was further conducted with BDMA. BIOMIG1 was able to grow on 1000 μM BDMA, the first intermediate of BAC transformation, as the sole carbon and energy source. BDMA was metabolized to equimolar concentration of dimethylamine (DMA) within 1 day (Figure 3.5). DMA was utilized and trace amounts of methyl amine was detected during the biodegradation suggesting that *Pseudomonas sp.* BIOMIG1 metabolized BAC through a series of dealkylation, debenzoylation and a multiple demethylation reactions, as also proposed by van Ginkel et al. (1992) and Tezel et al. (2012) (

Figure 3.6).

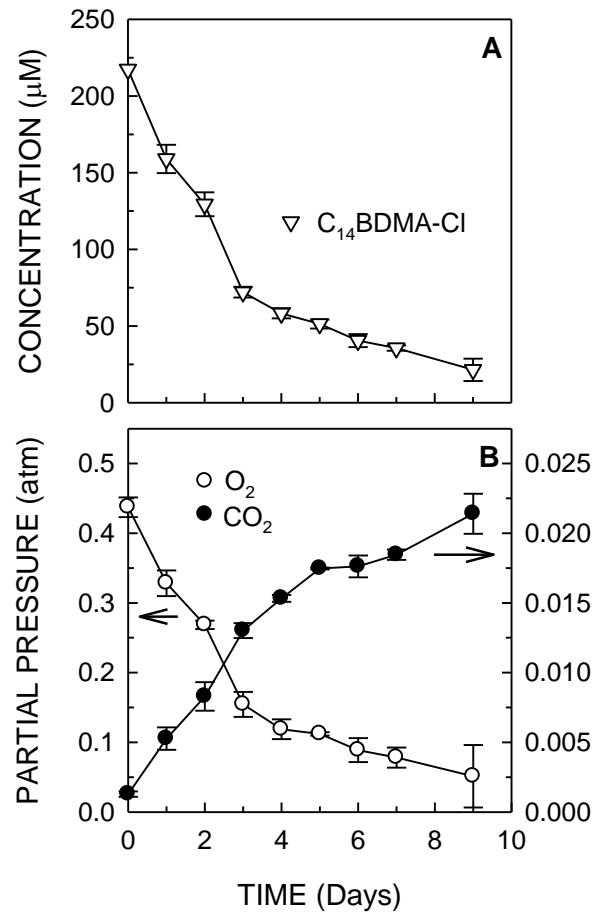


Figure 3.3. Profiles of (A) $C_{14}BDMA-Cl$ utilization and (B) O_2 utilization and CO_2 formation by *Pseudomonas* sp. BIOMIG1 under O_2 limiting conditions in a closed serum bottle. Arrows show the y-axis of data points.

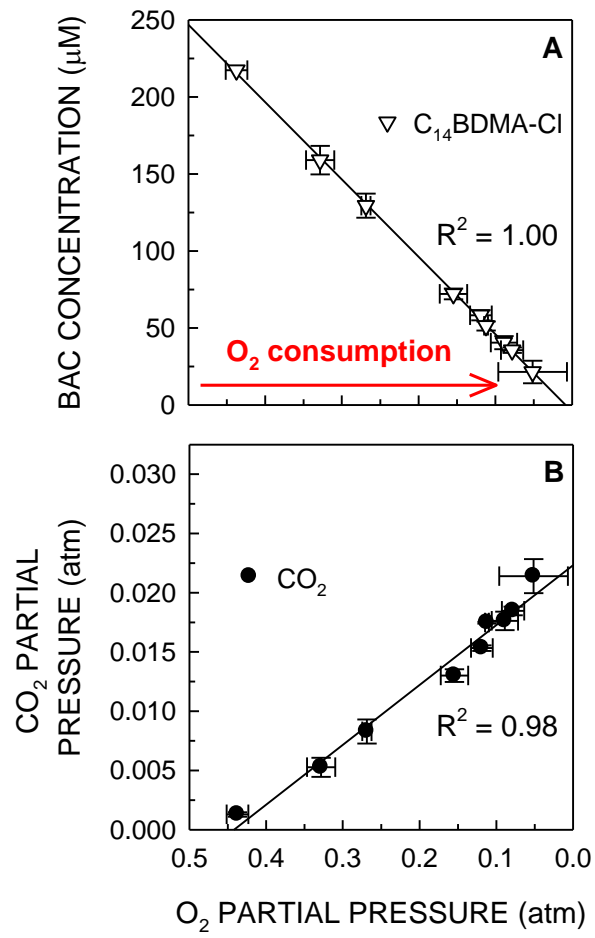


Figure 3.4. Correlation of O₂ consumption with (A) BAC utilization and (B) CO₂ formation by *Pseudomonas sp.* BIOMIG1

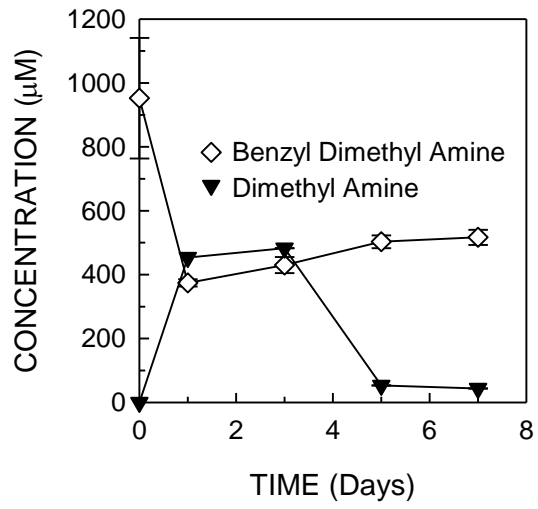


Figure 3.5. Profile of benzyl dimethyl amine (BDMA) utilization and dimethyl amine (DMA) formation by *Pseudomonas sp.* BIOMIG1

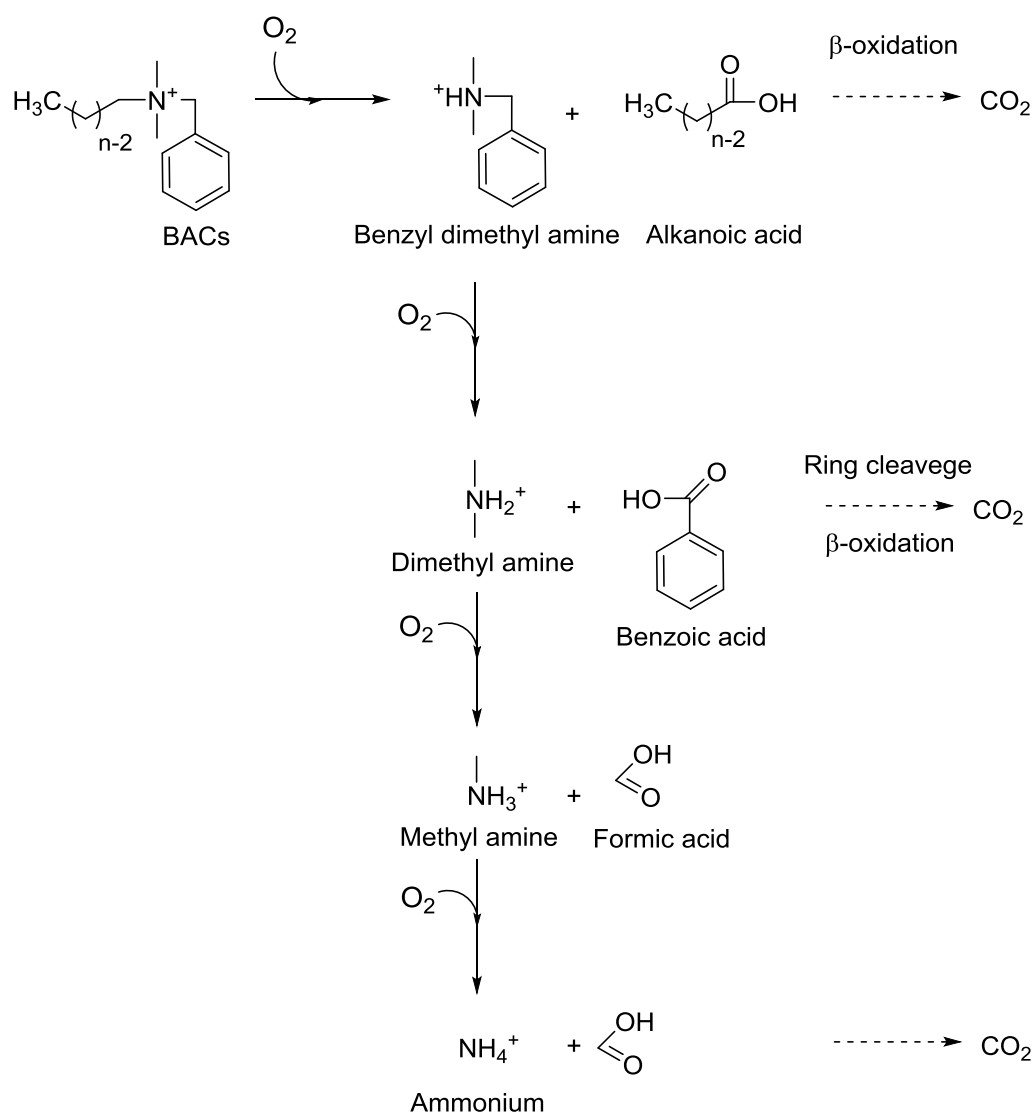


Figure 3.6. Pathway of BACs biodegradation by *Pseudomonas sp.* BIOMIG1

BAC biotransformation rates of complete degrader and BDMA accumulator strains selected from each microbial community were determined using 10 μM C₁₂BDMA as the initial concentration. The initial cell concentration was 10⁸ CFU/mL. The rates under these circumstances were between 0.79 and 2.40 $\mu\text{mol hr}^{-1} 10^{-11}$ cells. Tezel et al. (2012) reported the biotransformation rate of C₁₄BDMA by a BAC-enriched mixed culture, which was mainly dominated by *Pseudomonas putida* and *Pseudomonas nitroreducens*, as 0.09 $\mu\text{mol mg volatile suspended solids (VSS}^{-1}) \text{ hr}^{-1}$. There was no significant difference between the complete degrader and BDMA accumulator strains ($p > 0.05$) in terms of catalyzing the first dealkylation step of the pathway (Figure 3.7). This is expected as conversion of BAC to BDMA is the rate-limiting step and reduces the toxicity of BAC significantly. Also, at this concentration BIOMIG1 could not produce cells but could only use BAC for maintaining its metabolism.

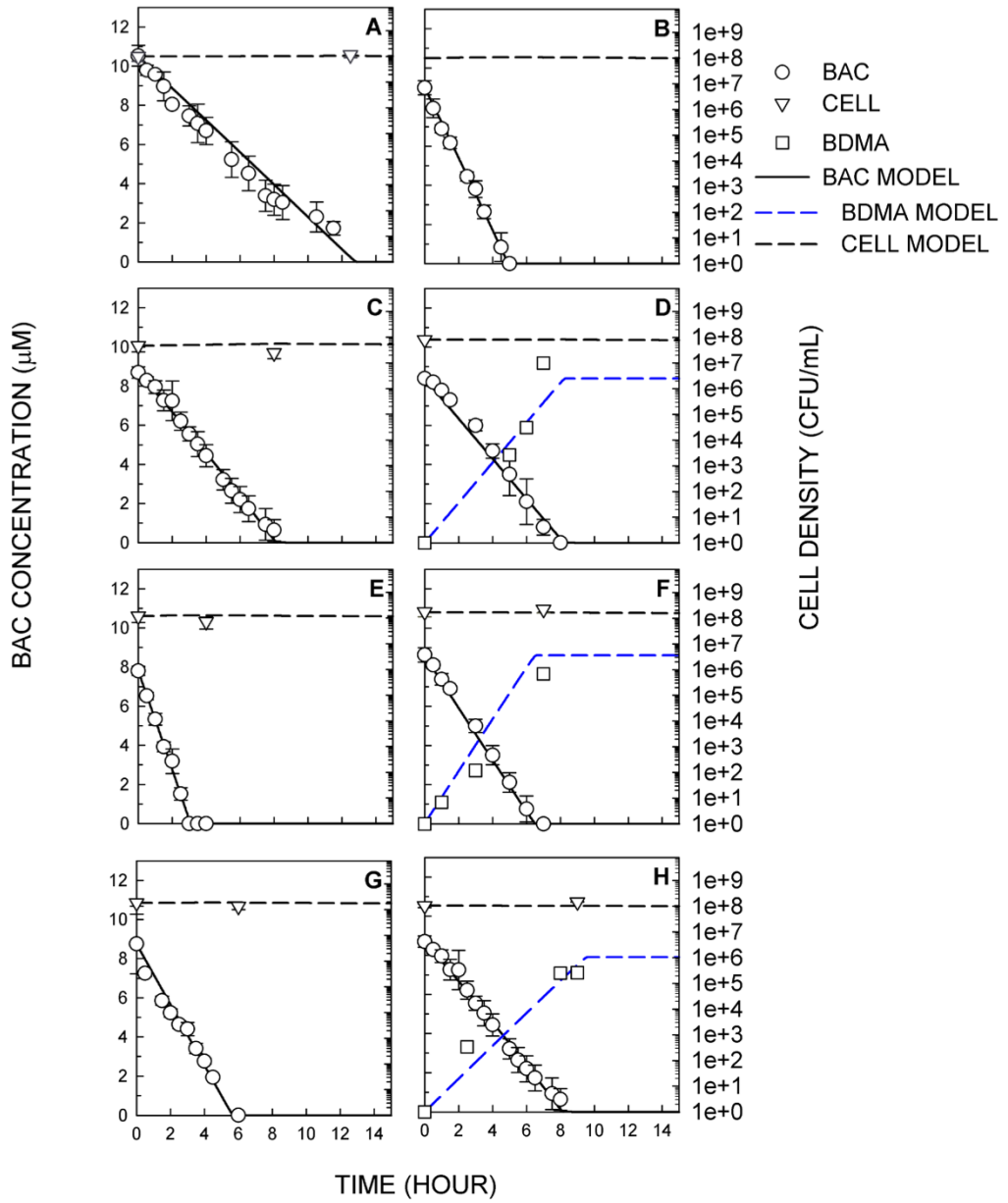


Figure 3.7. BAC degradation kinetics of *Pseudomonas. sp.* BIOMIG1 isolates. (A) *P. sp.* BIOMIG1-AS^{BAC1} (B) *P.sp.* BIOMIG1-AS^{BAC2} (C) *P.sp.* BIOMIG1-SEW^{BAC} (D) *P.sp.* BIOMIG1-SEW^{BDMA} (E) *P.sp.* BIOMIG1-SOIL^{BAC} (F) *P.sp.* BIOMIG1-SOIL^{BDMA} (G) *P.sp.* BIOMIG1-SEA^{BAC} (H) *P.sp.* BIOMIG1-SEA^{BDMA}

To find out if there were significant physiological differences between BIOMIG1 ecotypes and with relative species, the C utilization patterns of each strain was compared with that of *Pseudomonas putida* (Table 3.3). The C utilization fingerprints determined by BIOLOG GenIII microplates, were combined with BAC degradation capability as well as physiological properties and a hierarchical clustering was made to identify distinct groups (Figure 3.8). On the BIOLOG microplates, there were 94 phenotypic tests in which 71 of them were C utilization assays and 23 were chemical sensitivity assays. On average BIOMIG1 strains gave positive results to 59.4 of the 96 test wells compared to 54 of *P. putida*. Within BIOMIG1 strains, few differences in terms of C utilization and chemical sensitivity were observed that could be attributed to experimental error. BIOMIG1 could efficiently utilize sugars like D-trehalose, N-Acetyl-D-glucoseamine and D-glucose-6 phosphate that could not be utilized by *P. putida*. On the contrary, *P. putida* could metabolize organic acids like mucic acid, quinic acid and D-saccharic acids whereas BIOMIG1 could not. The hierarchical clustering analysis showed that there was no significant ecological differentiation between BIOMIG1 ecotypes. On the other hand BIOMIG1 was phenotypically distinct from *Pseudomonas putida*.

Table 3.3. C utilization and chemical sensitivity patterns of BIOMIG1 and *P.putida*. + Indicates a positive and - indicates a negative result.

Well No	C Source	SEW BAC	SEW BDMA	AS N	AS BAC 2	AS BAC 2	SOIL BAC	SOIL BDMA	SEA BAC	SEA BDMA	<i>P. putida</i>
A1	Negative control	-	-	-	-	-	-	-	-	-	-
A2	Dextrin	-	-	-	-	-	-	-	-	-	-
A3	D-maltose	-	-	-	-	-	-	-	-	-	-
A4	D-Trehalose	+	+	+	+	+	+	+	+	+	-
A5	D-cellobiose	-	-	-	-	-	-	-	-	-	-
A6	Gentibiose	-	-	-	-	-	-	+	-	-	-
A7	Sucrose	-	-	-	-	-	-	-	-	-	-
A8	D-Turanose	-	-	-	-	-	-	-	-	-	-
A9	Stachyose	-	-	-	-	-	-	-	-	-	-
A10	Positive control	+	+	+	+	+	+	+	+	+	+
A11	ph 6	+	+	+	+	+	+	+	+	+	+
A12	ph 5	+	+	+	+	+	+	+	+	+	+
B1	D-raffinose	-	-	-	-	-	-	-	-	-	-
B2	alpha D-Lactose	-	-	-	-	-	-	-	-	-	-
B3	D-Melibiose	-	-	-	-	-	-	-	-	-	-
B4	beta-methyl-D-glucoside	-	-	-	-	-	-	-	-	-	-
B5	D-Salicin	-	-	-	-	-	-	-	-	-	-
B6	N-Acetyl-D-glucoseamine	+	+	+	+	+	+	+	+	+	-
B7	N-Acetyl beta-D-mannosamine	-	-	-	-	-	-	-	-	-	-
B8	N-Acetyl-D-glucoseamine	-	-	-	-	-	-	-	-	-	-
B9	N-Acetyl Neurominic Acid	-	-	-	-	-	-	-	-	-	-
B10	1% NaCl	+	+	+	+	+	+	+	+	+	+
B11	4% NaCl	+	+	+	+	+	+	+	+	+	+
B12	8% NaCl	-	-	+	-	-	-	-	-	-	+

Table 3.3 Continued

Well No	C Source	SEW BAC	SEW BDMA	AS N	AS BAC 2	AS BAC 2	SOIL BAC	SOIL BDMA	SEA BAC	SEA BDMA	<i>P. putida</i>
C+	alpha-D-Glucose	+	-	+	+	+	+	+	+	+	+
C2	D-Mannose	+	+	+	+	+	+	+	+	+	+
C3	D-Fructose	+	+	+	+	+	+	-	+	+	+
C4	D-Galactose	-	-	+	-	+	-	+	-	-	-
C5	3-Methyl Glucose	-	-	+	-	-	-	-	-	-	-
C6	D-Fucose	+	+	+	+	+	+	+	+	+	+
C7	L-Fucose	+	+	+	+	+	+	+	+	+	+
C8	L-Rhamnose	-	-	+	-	-	-	-	+	-	-
C9	Inosine	+	+	+	-	+	+	+	+	+	+
C+-	+% Sodium Lactate	+	+	+	+	+	+	+	+	+	+
C++	Fusidic Acid	+	+	+	+	+	+	+	+	+	+
C+2	D-Serine	+	+	+	+	+	+	+	+	+	+
D+	D-sorbitol	-	-	-	-	-	-	-	-	-	-
D2	D-Mannitol	-	-	-	-	-	-	-	-	-	-
D3	D-Arabitol	-	-	-	-	-	-	-	-	-	-
D4	myo-Inositol	+	+	+	+	+	+	+	+	+	-
D5	Glycerol	+	+	+	+	+	+	+	+	+	+
D6	D-Glucose-6-PO4	+	+	+	+	+	+	+	+	+	-
D7	D-Fructose-6-PO4	+	+	+	+	+	+	+	+	+	+
D8	D-Aspartic Acid	-	-	-	-	-	-	-	-	-	-
D9	D-Serine	+	+	-	+	+	-	-	+	-	+
D+-	Troleandomycin	+	+	+	+	+	+	+	+	+	+
D++	Rifamycin SV	+	+	+	+	+	+	+	+	+	+
D+2	Minocycline	+	+	+	+	+	+	+	+	+	+

Table 3.3 Continued

Well No	C Source	SEW BAC	SEW BDMA	AS N	AS BAC 2	AS BAC 2	SOIL BAC	SOIL BDMA	SEA BAC	SEA BDMA	<i>P. putida</i>
E+	Gelatin	-	-	-	-	-	-	-	-	-	-
E2	Glycyl-L-proline	+	-	+	+	+	+	+	+	+	-
E3	L-Alanine	+	-	+	+	+	+	+	+	+	+
E4	L-Arginine	+	+	+	+	+	+	+	+	+	+
E5	L-aspartic acid	+	+	+	+	+	+	+	+	+	+
E6	L-glutamic acid	+	+	+	+	+	+	+	+	+	+
E7	L-histidine	+	+	+	+	+	+	+	+	+	+
E8	L-pyruglutamic acid	+	+	+	+	+	+	+	+	+	+
E9	L-serine	+	+	+	+	+	+	-	+	+	+
E+-	linsomycine	+	+	+	+	+	+	+	+	+	+
E++	guanidine hcl	+	+	+	+	+	+	+	+	+	+
E+2	nia proof 4	+	+	+	+	+	+	+	+	+	+
F+	pectine	+	+	+	-	+	+	+	+	+	+
F2	D-galacturonic acid	+	-	+	-	+	+	+	-	-	+
F3	L-galactonic acid lactone	-	-	-	-	-	-	-	-	-	-
F4	D-Gluconic acid	+	+	+	+	+	+	+	+	+	+
F5	D- Glucuronic aicd	+	+	-	-	+	-	+	-	-	+
F6	glucoranomide	+	+	+	+	+	+	+	+	+	+
F7	mucic acid	-	-	-	-	-	-	-	-	-	+
F8	quinic acid	-	-	-	-	-	-	-	-	-	+
F9	D-saccharic acid	-	-	-	-	-	-	-	-	-	+
F+-	vancomycin	+	+	+	+	+	+	+	+	+	+
F++	terazolium violet	+	+	+	+	+	+	+	+	+	+
F+2	tetrazoliumblue	+	+	+	+	+	+	+	+	+	+

Table 3.3 Continued

Well No	C Source	SEW BAC	SEW BDMA	AS N	AS BAC 2	AS BAC 2	SOIL BAC	SOIL BDMA	SEA BAC	SEA BDMA	<i>P. putida</i>
G+	p-hydroxyphenil acetic acid	+	+	+	+	+	+	+	+	+	+
G2	methyl pyruvate	-	-	+	+	-	-	+	-	-	-
G3	d-lactic acid methyl ester	-	-	+	-	-	-	+	-	-	-
G4	l-lactic acid	+	+	+	+	+	+	+	+	+	+
G5	citric acid	+	+	+	+	+	+	+	+	+	+
G6	alpha keto glutaric acid	+	+	+	+	+	+	+	+	+	+
G7	D-malic acid	+	+	+	+	+	+	+	+	+	+
G8	L-malic acid	+	+	+	+	+	+	+	+	+	+
G9	bromo- succinic acid	-	-	+	-	-	-	+	-	-	-
G+-	nalidixic acid	+	+	+	+	+	+	+	+	+	+
G++	lithium chloride	+	-	+	+	+	+	+	-	-	+
G+2	potassium tellurite	+	+	+	+	+	+	+	+	+	+
H+	tween4-	-	-	-	-	-	-	-	-	-	-
H2	gamma amino butyric acid	+	+	+	+	+	+	+	+	+	+
H3	alpha hydroxy butiric acid	-	-	+	-	-	+	+	-	-	-
H4	beta hydroxy D,L butyric acid	+	+	+	+	+	+	+	+	+	+
H5	alpha keto butyric acid	-	-	-	+	-	-	+	-	-	-
H6	acetoacetic acid	-	-	+	-	-	-	-	-	-	-
H7	propionic acid	+	+	+	+	+	+	+	+	+	+
H8	acetic acid	+	+	+	+	+	+	+	+	+	+
H9	formic acid	+	+	+	+	-	+	+	+	+	+
H+-	astreonom	+	+	+	+	+	+	+	+	+	+
H++	sodium butyrate	+	+	-	-	+	-	-	+	-	+
H+2	sodium bromate	+	-	+	-	-	-	-	+	-	+

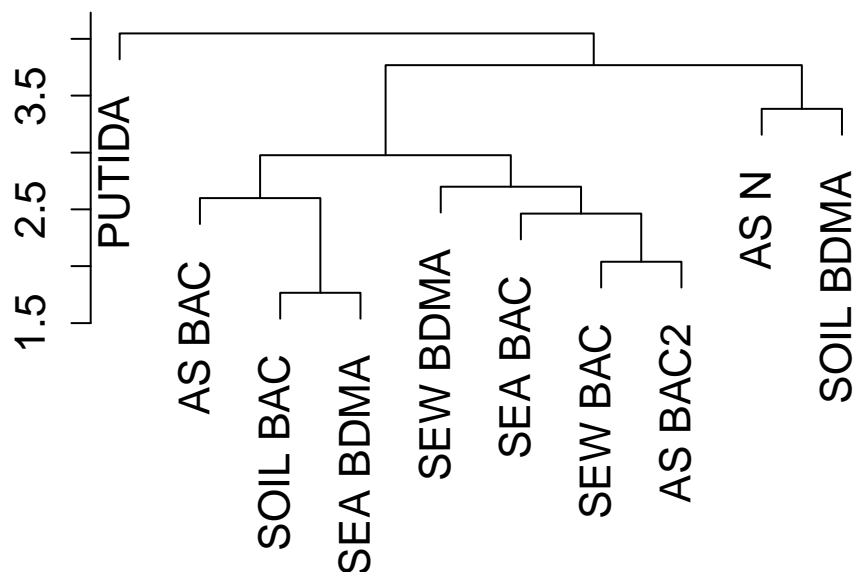


Figure 3.8. Dendrogram showing the hierarchical clustering made according to the carbon utilization profiles of BIOMIG1.

3.3.3. Genome features of *Pseudomonas* sp. BIOMIG1

After assembly, the draft genome of *Pseudomonas* sp. BIOMIG1 consisted of 7 million base pairs of which 88.5% were protein coding genes. This genome size can be considered quite large among the genomes of Pseudomonads, which is consistent with BIOMIG1's metabolic capabilities. Based on the universal single copy essential genes, BIOMIG1's genome was 92.8% complete. A total of 7151 genes that encoded proteins could be identified. Comparison of the general genome features of sequenced Pseudomonads with BIOMIG1 is given in Table 3.4. To determine the taxonomic identity of BIOMIG1, a recently developed tool named Microbial Genomes Atlas (MIGA) was used (<http://enve-omics.ce.gatech.edu:3000>). Briefly, the genome of BIOMIG1 was queried within the 1662 microbial genomes in the RefSeq database and amino acid similarities between the sets of conserved amino acid sequences were calculated (referred as amino acid identity (AAI)). Based on this measure, the closest relatives of BIOMIG1 were *Pseudomonas protegens* Pf5 (88.5% AAI) and *Pseudomonas fluorescence* F113 (80.96%

AAI). Moreover, these estimations indicated that BIOMIG1 was a novel species (p value = 0.018). A phylogenetic tree constructed with the genome sequence of BIOMIG1 and fifteen related microorganisms also showed that BIOMIG formed a distinct clade close to *Pseudomonas protegens*, despite the fact that BIOMIG1's 16S rRNA sequence clustered within the *Pseudomonas putida* group (Figure 3.9). This shows that 16S rRNA gene sequence can be misleading for assigning a taxonomic label to microorganisms at the species level, thus using whole genomes should be preferred when applicable.

Table 3.4. Genome features of sequenced Pseudomonads and BIOMIG1

	<i>P.sp</i> BIOMIG1	<i>P.putida</i> KT2244	<i>P.fluorescens</i> F113	<i>P.protegens</i> Pf5	<i>P.nitroreducens</i>
Size (Mbp)	7.5	6.2	6.8	7.0	7.4
GC content (%)	62.2	61.6	63.3	63.2	64.2
Number of protein coding genes	7,151	5,420	6,040	6,303	6,197

To identify the abundant functions in the genome of BIOMIG1, the proteins were annotated and categorized using the SEED subsystems. Around 45% of the proteins of BIOMIG1 could be assigned to a functional category in the SEED subsystems. The most abundant fifteen functions and their subcategories are shown in Figure 3.10. Based on these functions, it can be seen that the metabolism of BIOMIG1 was mostly devoted to synthesis and destruction of amino acids, synthesis of proteins and degradation of low carbon intermediates, tolerating oxidative stress, antibiotic resistance and transcriptional regulation of gene expression (Figure 3.10).

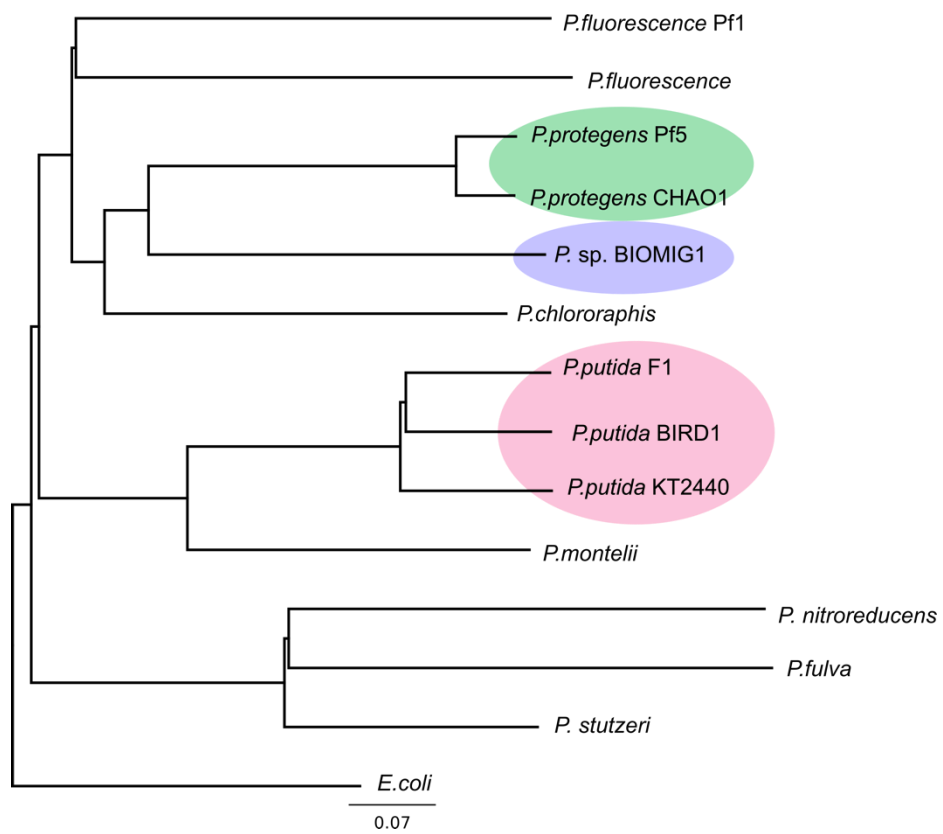


Figure 3.9. Phylogenetic tree constructed with the genome sequences of *P. sp. BIOMIG1* and related microorganisms

Table 3.5. SEED categories represented in the genome of BIOMIG1

SEED Category	Number of hits	Percentage in annotated fraction
Amino Acids and Derivatives	379	12.2
Cofactors, Vitamins, Prosthetic Groups, Pigments	340	10.9
Protein Metabolism	312	10.0
Carbohydrates	246	7.9
Stress Response	186	6.0
RNA Metabolism	166	5.3
Miscellaneous	156	5.0
Virulence	145	4.7
Cell Wall and Capsule	142	4.6
DNA Metabolism	128	4.1
Respiration	122	3.9
Regulation and Cell signaling	111	3.6
Fatty Acids, Lipids, and Isoprenoids	110	3.5
Nucleosides and Nucleotides	94	3.0
Membrane Transport	77	2.5
Metabolism of Aromatic Compounds	68	2.2
Motility and Chemotaxis	62	2.0
Sulfur Metabolism	55	1.8
Cell Division and Cell Cycle	41	1.3
Nitrogen Metabolism	40	1.3
Iron acquisition and metabolism	36	1.2
Potassium metabolism	32	1.0
Phosphorus Metabolism	31	1.0
Phages, Prophages, Transposable elements, Plasmids	23	0.7
Dormancy and Sporulation	6	0.2
Photosynthesis	4	0.1
Secondary Metabolism	2	0.1

Pseudomonas sp. BIOMIG1 can use a variety of carbon sources including amino acids and sugars. Consistently, a substantial number of genes were involved in amino acid and sugar metabolism as well as synthesis of coenzymes/cofactors required in those pathways. A total of 379 genes that corresponded to 12.2% of BIOMIG1's annotated genome encoded for synthesis and catabolism of amino acids. Among them, the most abundant group was involved in lysine, threonine, methionine and cysteine metabolism

(4.5%) followed by arginine metabolism (2.6%). degradation of branched chain amino acids (1.8%) and synthesis of aromatic amino acids (1.8%) were also among abundant amino acid metabolisms. Protein synthesis was the most abundant sub-group within protein metabolism. 66 genes related with single copy ribosomal protein synthesis and 79 genes related with ribosome large and small subunit synthesis were present in the genome of BIOMIG1. 25 genes were involved in post- translational modification of proteins. Genes associated with heat shock response, specifically dnaK gene cluster, was also abundant, represented with 24 genes. A total of 340 genes constituting 10% of the annotated fraction of BIOMIG1s genome were related with synthesis of coenzymes, cofactors and vitamins. The most abundant sub-groups were associated with YgfZ and YggS like proteins encoded by a number of 55 and 40 genes respectively. YgfZ type proteins participate in repair and synthesis of iron-sulfur clusters (Waller et al., 2011), which are crucial components of many catabolic enzymes. YggS proteins have been suggested to take part in osmotic regulation (Ito et al., 2014). 246 genes constituting 7.9% of the annotated fraction of BIOMIG1s genome belonged to carbohydrate metabolism. Central carbohydrate metabolism was especially highly represented (103 genes) along with one carbon compound metabolism (44 genes). Genes encoding for dehydrogenase enzymes was the most abundant among genes associated with central carbohydrate metabolism (Figure 3.10).

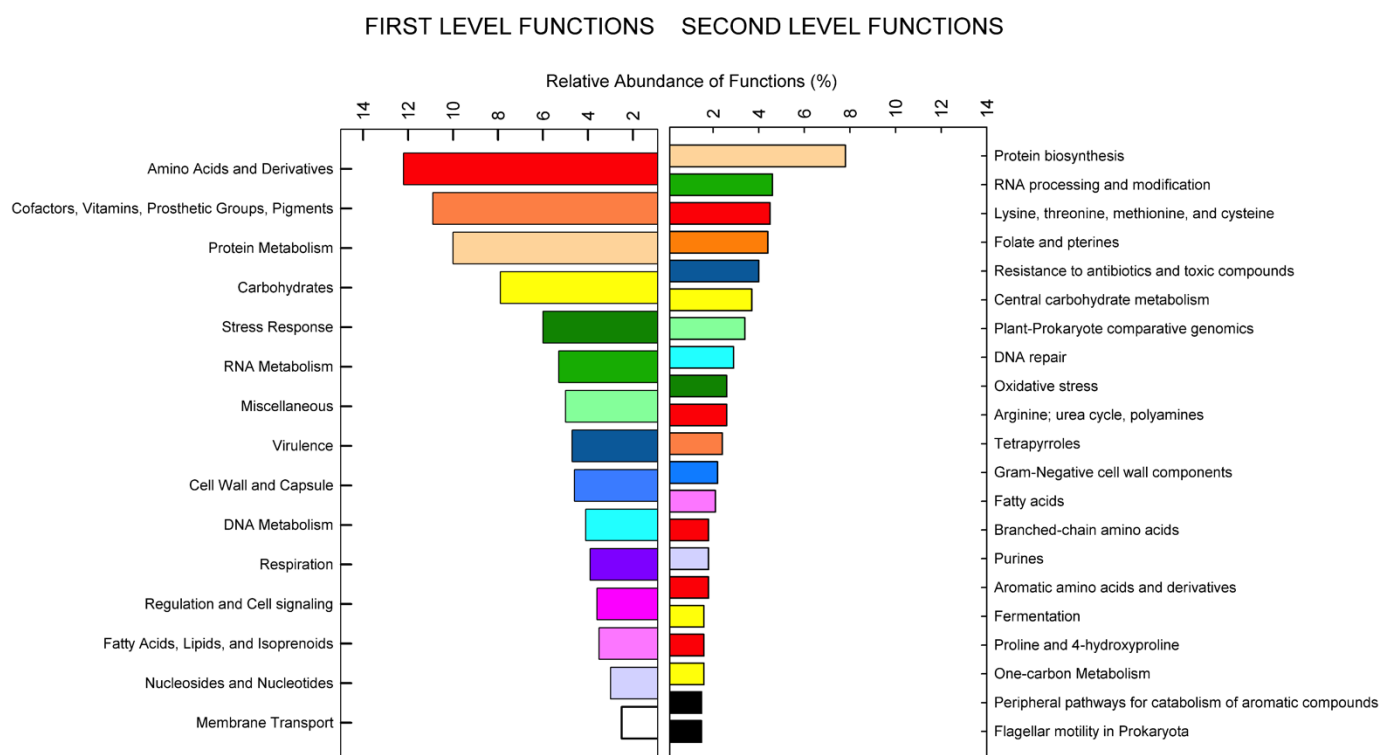


Figure 3.10. Relative abundance of Level 1 and level 2 functional categories in the genome of BIOMIG1

The genome of BIOMIG1 contained a number of multidrug efflux pump encoding operons and their regulators, which was expected given its low susceptibility to BACs. Among them RND and MDR type efflux systems were most abundant along with the *mex* and *mtr* operons. These efflux pump determinants have been well characterized in terms of how they confer resistance against various types of QACs and BACs (Tezel and Pavlostathis, 2015). Additionally genome of BIOMIG1 also contained operons encoding for antibiotic resistance such as fluoroquinolone and streptothricine resistance determinants. Combined with multidrug efflux systems, this genetic evidence proposed that BIOMIG1 was probably highly tolerant to various antimicrobials. A recent study confirmed this assumption by experimentally showing that BIOMIG1 was highly resistant to more than 10 clinically important antibiotics (Gul, 2016). Several oxidative stress response gene clusters, which most likely contributed to the protection of cells against oxidative damage caused by BACs, were present in the genome of BIOMIG1. Most of them encoded for glutathione and

rubredoxin based enzyme systems, which were characterized for scavenging free radicals formed after exposure to oxidants. The metagenome comparison analysis presented in chapter 3.3.1, as well as previous studies, similarly revealed that glutathione reductase systems played an important part for community-wide adaptations to BAC exposure. A total of 80 genes encoded for DNA repair systems in the genome of BIOMIG1. Of these, 30 encoded for the general bacterial DNA repair proteins including *radC* and *recA*. 15 genes encoded for base excision DNA repair systems and 13 genes encoded for the bacterial RecFOR pathway.

To identify the unique features in BIOMIG1s genome, its proteins were compared with those of *Pseudomonas protegens*, which was the closest relative of BIOMIG1 (80% amino acid identity on average). There was 2000 proteins, which were present in the genome of BIOMIG1 but absent in the genome of *P.protegens*, therefore considered as distinct to BIOMIG1. These proteins were classified according to their protein families as annotated in PFAM database.

Multidrug efflux transporters and proteins related to oxidative stress response were among distinct proteins of BIOMIG1 that were associated with BAC resistance. Major facilitator superfamily (MFS) transporters were the most abundant class in multidrug efflux transporters, followed by ABC transporters and small multidrug resistance (SMR) proteins (Figure 3.11A). These groups have been shown to specifically contribute to QAC/BAC resistance by exporting them out of the cell (Tezel and Pavlostathis, 2012). An increasing body of evidence shows that these proteins are also effective against various antibiotics (Buffet-Bataillon et al., 2012b; Buffet-Bataillon et al., 2012a). Moreover, the results presented in Chapter 2 demonstrated that similar proteins contributed to community-wise resistance against BACs.

A number of proteins specific to BIOMIG1 were associated with oxidative stress response and modification of the outer membrane (Figure 3.11B). Glutathione peroxidases and glutathione-S-transferases were the main groups of proteins that were associated with alleviating oxidative stress caused by BAC exposure (Tezel and Pavlostathis, 2015) along

with paraquat inducible protein A. Outer membrane porin family (OprD) and outer membrane efflux family proteins were associated with modification of the cell membrane as a response to QAC exposure.

Proteins associated with catabolic functions, transport of solutes and gene expression regulation were also represented among the distinct features of BIOMIG1 (Figure 3.12). A group of oxygenases including the Rieske and phytanoyl CoA type dioxygenases were potentially involved in catalyzing the initial attack to BAC and BDMA. Other catabolic enzymes such as aldehyde and short chain dehydrogenases as well as hydrolases possibly degraded products such as benzaldehydes and alkanolic acids (Figure 3.12A). Additionally, several transporter proteins likely facilitated transport of these organics into the cell (Figure 3.12B).

A number of transcriptional regulators were included in the distinct features of BIOMIG1 (Figure 3.12C). Among them a group of LysR and LysE type regulators existed, which has been linked with the expression of ABC, MFS and SMR multidrug efflux pumps (Chen et al., 2013). Hence, these regulators most likely contributed to QAC resistance in BIOMIG1. Other important transcriptional regulators linked with regulation of antimicrobial resistance were TetR and MerR family proteins (Cuthbertson and Nodwell, 2013). Moreover, AraC and IcIR family type regulators that control the expression of catabolism of organic compounds were identified among the distinct features of BIOMIG1 (Chen et al., 2013; Shimizu and Nakamura, 2014). These potentially contributed to the regulation of BAC and BDMA transformation. Interestingly, a number of helix-turn-helix family proteins were abundant in the distinct features of BIOMIG1. These proteins have been proposed to regulate phage repression and immunity, suggesting BIOMIG1 specifically harbored phage defense mechanisms.

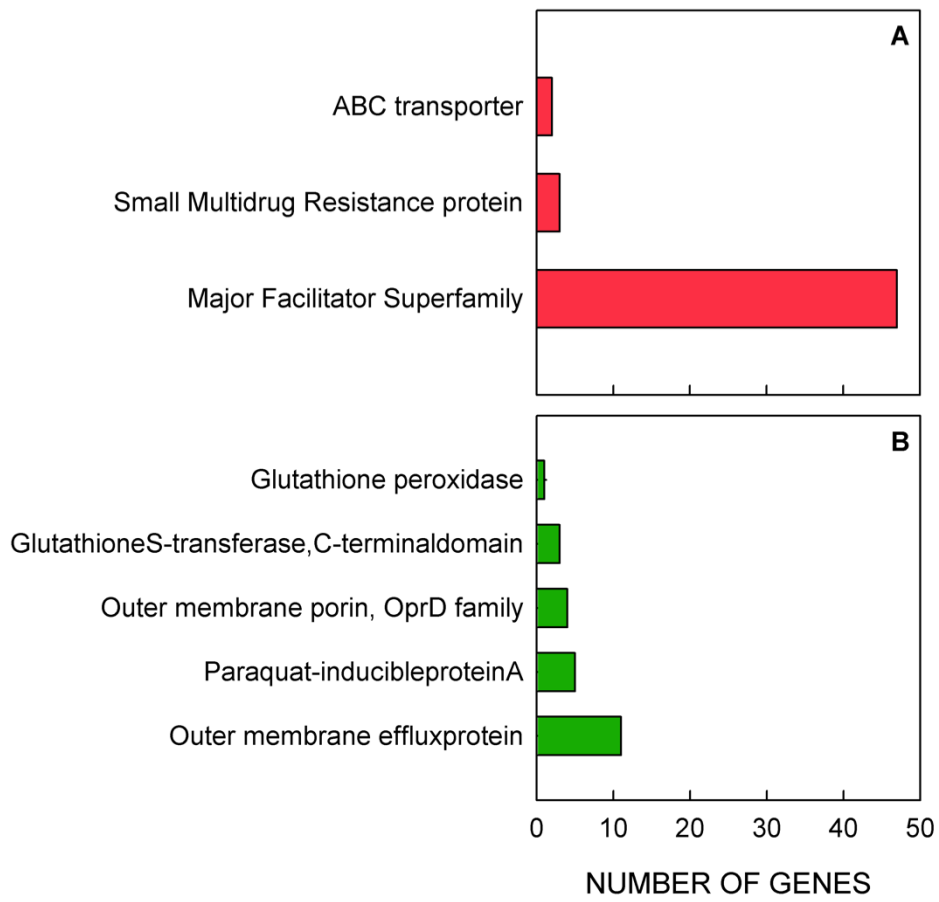


Figure 3.11. Distinct proteins of BIOMIG1 that are related to (A) Multidrug efflux pumps
(B) Oxidative stress response

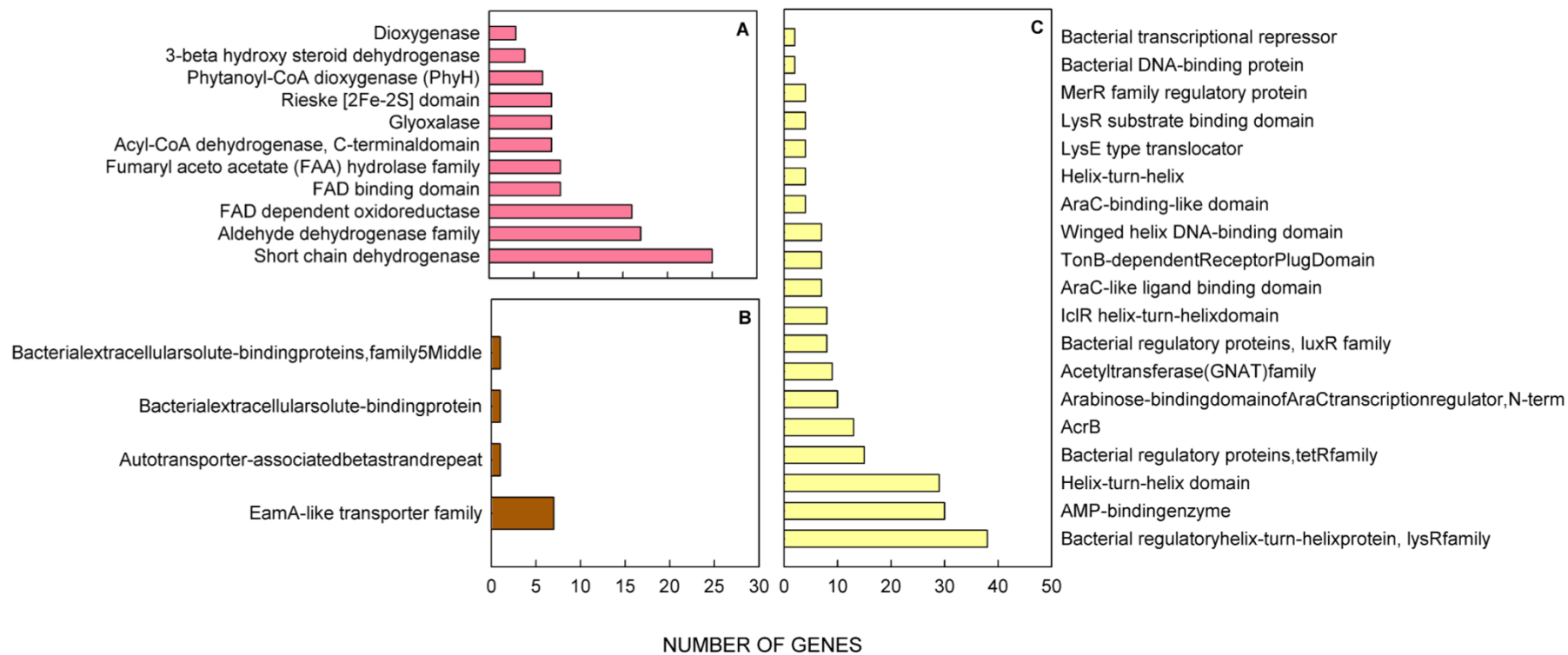


Figure 3.12. Distinct proteins of BIOMIG1 related to (A) Catabolism of organics (B) Transfer of solutes (C) Regulation of gene expression

A substantial number of proteins related with phages were distinctly present in the genome of BIOMIG1, indicating it was possibly infected by a phage (Figure 3.13). Although it is unknown whether or not a phage mediated horizontal gene transfer contributed to the acquirement of the specific features of BIOMIG1 such as BAC degradation and high levels of BAC resistance, this assumption is probable, given that phages play a significant part for the transfer of catabolic genes (van der Meer et al., 2001). Other protein families related to horizontal gene transfer were several integrases and transposases as well as type IV secretory system and conjugative transfer proteins (Figure 3.13). This suggests that certain unique features of BIOMIG1 were likely acquired via transposons. Moreover, BIOMIG1 is capable of conjugation thus disseminating genes among other microorganisms.

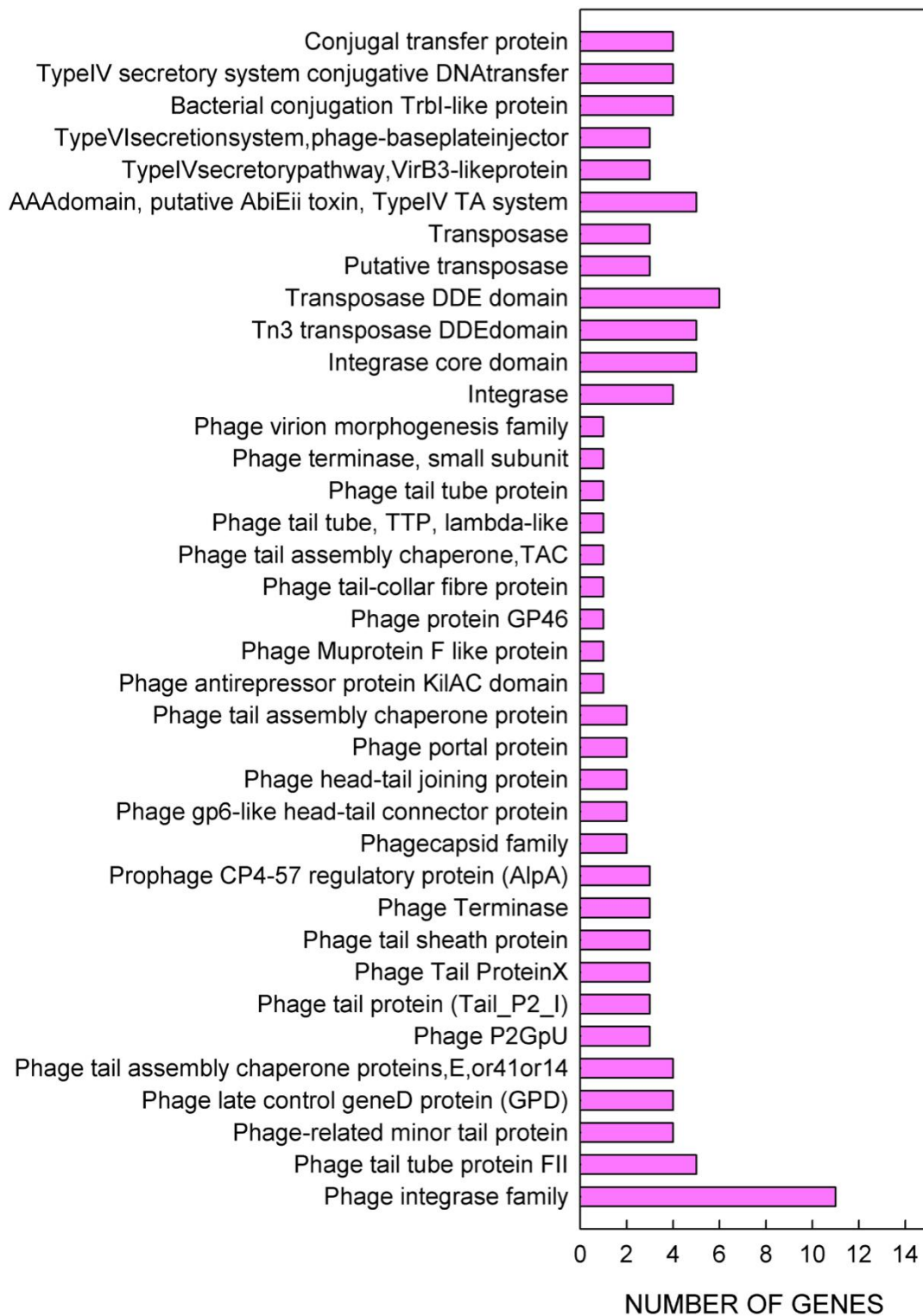


Figure 3.13. Distinct proteins of BIOMIG1 that are related with horizontal gene transfer

4. CHARACTERIZATION OF THE GENES INVOLVED IN BENZALKONIUM CHLORIDE BIOTRANSFORMATION

A part of this chapter was published in “Environmental Science and Technology” journal entitled “Similar Microbial Consortia and Genes Are Involved in the Biodegradation of Benzalkonium Chlorides in Different Environments” (Ertekin et al., 2016). Another part was published in “Environmental Science and Technology” journal, entitled “A Rieske-Type Oxygenase of *Pseudomonas* sp. BIOMIG1 Converts Benzalkonium Chlorides to Benzyl dimethyl Amine” (Ertekin et al., 2017). Disclosure of both articles is permitted by Hatt, J.; Konstantinidis, K. T. and Tezel, U.

4.1. Introduction

As discussed earlier, BACs are the most commonly used group of QACs (Tezel and Pavlostathis, 2012) and their contamination of the environment can cause severe ecological and public health problems such as eco-toxicity and dissemination of antimicrobial resistance (Tezel and Pavlostathis, 2012; Tezel and Pavlostathis, 2015). Despite their antimicrobial properties, some microorganisms in the environment can degrade BACs and convert them to non-toxic end products (van Ginkel et al., 1992; Patrauchan and Oriel, 2003; Liffourrena and Lucchesi, 2014; Oh et al., 2014). The biochemistry of BAC degradation has been described in detail; first the alkyl chain is cleaved with an attack to central the C-N bond. This N-dealkylation reaction results in the formation of benzyl dimethyl amine (BDMA) which is further mineralized (Tezel et al., 2012). It was observed that the initial N-dealkylation was oxygen dependent, therefore presumed to be catalyzed by a monooxygenase. However, there is relatively limited information on the genes underlying the pathway.

To date, tetradecyl trimethyl ammonium bromide monooxygenase (TTABMO) of *Pseudomonas putida* ATCC 12633 (Liffourrena and Lucchesi, 2014) and amine oxidase of a *Pseudomonas nitroreducens* B (Oh et al., 2014) which converted QAC homologs to tertiary amines have been characterized. TTABMO was a typical flavoprotein that used

nicotinamide adenine dinucleotide phosphate (NADPH) and flavin adenine dinucleotide (FAD) as cofactors, whereas the amine oxidase of *Pseudomonas nitroreducens* B required only FAD. Phylogenetically, AOx-BAC was more closely related to another pseudooxynicotine amine oxidase (Qiu et al., 2013) compared to TTABMO, although both of them are QAC N-dealkylating enzymes. In addition, three genes encoding oxygenases that metabolized naturally occurring QACs such as; glycine betaine (*gbcA*), stachydrine (*stc2*) (Daughtry et al., 2012) and carnitine (*cntA*) (Zhu et al., 2014) have been identified. Those enzymes were Rieske non-heme iron dependent oxygenases that catalyze the N-dealkylation of naturally occurring QACs. Among them, *stc2* and *gbcA* removed methyl group from quaternary N whereas *cntA* cleaved the C-N⁺ bond between the ester and the quaternary N. However none of these enzymes were shown to attack on C-N⁺ between a saturated alkane and quaternary N that is present in synthetic QACs such as BACs. This phylogenetic and functional diversity shows that multiple genetic mechanisms may underlie BAC detoxification in the environment. A better understanding of these mechanisms should be provided to produce feasible solutions to the problems caused by their improper use. Previous chapter described the isolation of a novel BAC-degrader, *Pseudomonas* sp. BIOMIG1 and characterization of this microorganism in terms of BAC degradation and genomic features. This chapter reports on the specific genes involved in the BAC degradation pathway, revealed by comparing the genomes of four different BIOMIG1 phenotypes. The function of an oxygenase, which was identified by the aforementioned genome comparison to convert BAC to BDMA, was also experimentally verified.

4.2. Materials and Methods

4.2.1. Microorganisms

Pseudomonas sp. BIOMIG1^{BAC} which has been shown to mineralize BACs and BDMA, and *Pseudomonas* sp. BIOMIG1^{BDMA} which converts BACs to BDMA but cannot utilize BDMA was isolated from the BAC degrading enrichment community originating from sewage (SEW) (see section 4.2.1). Two additional phenotypes such as *Pseudomonas* sp. BIOMIG1^{BD} which utilized BDMA but not BACs and *Pseudomonas* sp. BIOMIG1^N

generated from *Pseudomonas* sp. BIOMIG1^{BAC} and BIOMIG1^{BDMA}, respectively. *Pseudomonas* sp. BIOMIG1^{BAC} was cultured in SM that contained BDMA as the sole carbon source to produce *Pseudomonas* sp. BIOMIG1^{BD}. *Pseudomonas* sp. BIOMIG1^{BDMA} was cultured in LB, containing neither BACs nor BDMA to produce *Pseudomonas* sp. BIOMIG1^N. *E.coli* BL21(DE3) pLysS (Invitrogen, Thermo Fisher Scientific, USA) was used in heterologous expression experiments. Summary of the strains and their characteristics are given in Table 4.1.

Table 4.1. Strains, plasmids and primers used in this study

Strains, plasmids and primers	Description	Source
<i>Pseudomonas</i> sp. BIOMIG1	A strain isolated from sewage taken from an urban wastewater treatment plant in Istanbul, TR	This study
::BAC	Can utilize both BACs and BDMA	This study
::BDMA	Can convert BACs to BDMA but cannot utilize BDMA	This study
::BD	Cannot utilize BACs but can utilize BDMA	This study
::N	Can utilize neither BACs nor BDMA	This study
<i>Escherichia coli</i> BL21 (DE3)pLysS	Heterologous expression of <i>oxyBAC</i> under the T7 promoter	Invitrogen
:: <i>oxyBAC</i>	Contains pET29+ with <i>oxyBAC</i>	This study
::N	Contains pET29+ with no <i>oxyBAC</i>	This study
Plasmids pET29a+	For overexpression of <i>oxyBAC</i>	Merc Millipore
Primers <i>oxyBAC</i> -F	5' -TTATATGCAACAGATCCATCCCCT-3'	This study
<i>oxyBAC</i> -R	5' -TTATGTACGCCGTAGGCGGGGCC-3'	This study

:: Appears as superscripts

4.2.2. Identification of the Genes Involved in BAC Biotransformation Pathway

In order to identify the genes involved in BAC biodegradation, genomes of the aforementioned four BIOMIG1 phenotypes were compared. For whole genome sequencing,

assembly and gene prediction, the methods described in Chapter 4.2.5 were exactly followed. Accession numbers and assembly statistics of the BIOMIG1 genomes are given in Table 4.2. The gene sequences of the BIOMIG1 strains were compared in a pairwise manner using “reciprocal best match blast”. The set of genes that was present in the genome of the *Pseudomonas sp.* BIOMIG1^{BAC} and *Pseudomonas sp.* BIOMIG1^{BDMA} but absent in the *Pseudomonas sp.* BIOMIG1^{BD} and *Pseudomonas sp.* BIOMIG1^N was determined as the candidate genes involved in BAC to BDMA transformation. Likewise, the genes that were present in BIOMIG1^{BDMA} and BIOMIG1^{BD} but absent in BIOMIG1^{BDMA} and BIOMIG1^N were identified as candidate genes for degrading BDMA.

Table 4.2. Assembly statistics of the whole genomes used in this study

Strain	Accession number	Total number of contigs	Number of large contigs (>500bp)	N50 contig length (bp)	Total number of basepairs
<i>Pseudomonas sp.</i> BIOMIG-1 ^{BAC}	MCRS000000000	472	316	57,441	7.5 x 10 ⁶
<i>Pseudomonas sp.</i> BIOMIG-1 ^{BDMA}	MCRT000000000	466	304	60,737	7.5 x 10 ⁶
<i>Pseudomonas sp.</i> BIOMIG-1 ^{BD}	MCRU000000000	454	338	46,394	7.5 x 10 ⁶
<i>Pseudomonas sp.</i> BIOMIG-1 ^N	MCRV000000000	383	286	57,495	7.5 x 10 ⁶

The amino acid sequences of all the discovered genes were annotated using BLASTP in the non-redundant protein sequence database of National Center of Biotechnology Information (NCBI, <http://www.ncbi.nlm.nih.gov/protein>). For phylogenetic classification, protein sequences of homolog proteins were aligned using ClustalW implemented in Geneious[®] 7.1 (Amsterdam, Netherlands) and Jukes-Cantor neighbor joining method was used for clustering. Certain genes identified by whole genome comparison, were amplified

in BIOMIG1 phenotypes as well as in the *E.coli* host used in heterologous expression experiments. Using these genes as templates, PCR primers were designed with *Primer 3* tool implemented in Geneious® 7.1 (Amsterdam, Netherlands). The primer sequences are provided in Table 1. The amplification conditions were as follows; denaturation at 95°C for 10 seconds, annealing at 60°C for 30 seconds and elongation at 72°C for 1 minute, for 30 cycles.

4.2.3. BAC Biotransformation Experiments with *Pseudomonas sp.* BIOMIG1

Pseudomonas sp. BIOMIG1^{BAC} and *Pseudomonas sp.* BIOMIG1^{BDMA} were grown in LB containing 50 mg/L BACs (Barquat 80, Lonza Inc., Switzerland). An overnight grown culture of each phenotype was resuspended in SM and spiked with 150 µM BAC containing equimolar amounts of dodecyl benzyl dimethyl ammonium chloride (C₁₂BDMA-Cl, TCI Chemicals, Japan) and tetradecyl benzyl dimethyl ammonium chloride (C₁₄BDMA-Cl, TCI Chemicals, Japan). After all of the BACs were consumed, cultures were diluted to OD₆₀₀ of 0.02 AU (~10⁶ cells/mL) in SM and respiked with 300 µM BACs. The cultures were incubated at room temperature on a rotary shaker at 130 rpm. Samples were taken intermittently to monitor BAC concentration by HPLC (Chapter 3.2.2) and cell growth was measured by plate counting. On the other hand, BIOMIG1^{BD} and BIOMIG1^N were grown in LB with 1000 mg/L BDMA or only in LB, respectively. The overnight grown cultures were resuspended in SM to an OD₆₀₀ of 0.2 AU, and spiked with 300 µM BAC. BAC concentration and cell density were measured as described above.

4.2.4. Heterologous Expression of Genes in *E. coli*

The *oxyBAC* gene was chemically synthesized by GenScript and inserted into pet29a+ vector (Merck Millipore, Germany), between the NdeI/NcoI sites, respectively (Figure 27). The *E.coli* BL21(DE3) pLysS strain (Invitrogen, Thermo Fisher Scientific, USA) was transformed with plasmid containing *oxyBAC* (*E. coli*^{oxyBAC}) (Table 4.1). For protein overexpression, *E.coli* cells were grown in LB broth containing 30 µg/mL

kanamycin (Sigma-Aldrich, Germany) and 34 $\mu\text{g}/\text{mL}$ chloramphenicol (Sigma-Aldrich, Germany) at 37°C. After the turbidity reached at OD_{600} of 0.5, 0.5 mM isopropyl β -D-1-thiogalactopyranoside (IPTG) (Sigma-Aldrich, Germany) was added to initiate induction, which was carried out at room temperature for 24 hours. Representation of the plasmid map is shown in Figure 4.1.

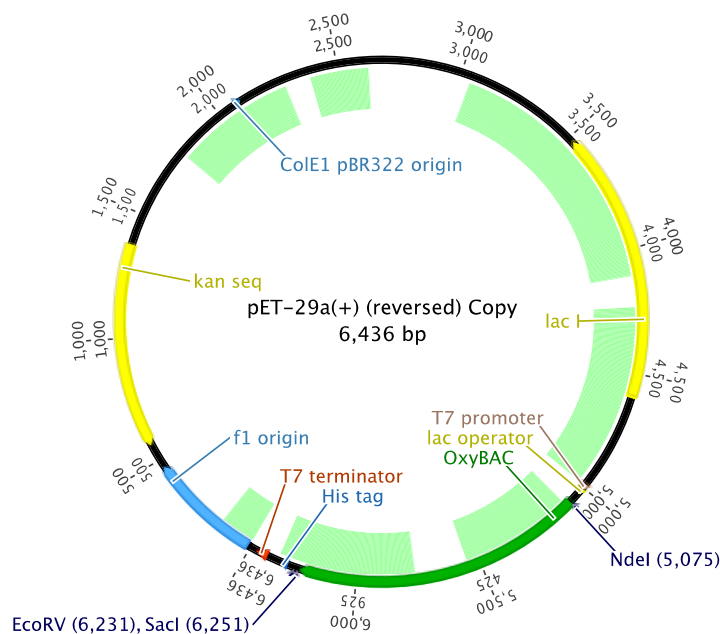


Figure 4.1. Plasmid map used in the heterologous expression experiments

Following induction, *E. coli*^{oxyBAC} cells were harvested and inoculated into 20 mL SM containing either 20 μM of $\text{C}_{12}\text{BDMA-Cl}$ at a final O.D. of 2.0. At determined intervals, $\text{C}_{12}\text{BDMA-Cl}$ utilization and BDMA production were monitored by HPLC (see Chapter 3.2.2). A control assay was performed with *E. coli* cells transformed with the pet29a+ plasmid not containing *oxyBAC* gene (*E. coli*^N, Table 4.1). To calculate biotransformation rates, experimental data was fitted to Michaelis-Menten growth model using Berkeley-Madonna software employing Runge-Kutta 4 integration method.

4.3. Results and Discussion

4.3.1. Potential Genetic Determinants of BAC Biotransformation

A comparative genomic approach was used in order to identify the genes involved in the BAC biodegradation pathway which consist of two steps; conversion of BAC to BDMA and further degradation of BDMA. For this, whole genome sequences of four *Pseudomonas* sp. BIOMIG1 phenotypes such as a complete BAC degrader (BIOMIG1^{BAC}), a BDMA accumulator (BIOMIG1^{BDMA}), an only BDMA degrader (BIOMIG1^{BD}) and a BAC non-degrader (BIOMIG1^N) were compared (Isolation of the strains and generation of the phenotypes are described in the materials and methods section of this chapter). It was hypothesized that the genes present in the genomes of BIOMIG1^{BAC} and BIOMIG1^{BDMA} but absent in BIOMIG1^{BD} and BIOMIG1^N would be involved in converting BAC to BDMA. Likewise, the genes present in the genomes of BIOMIG1^{BAC} and BIOMIG1^{BD} but not in BIOMIG1^{BDMA} and BIOMIG1^N would be involved in converting BDMA to DMA.

Comparing the whole genomes of the described four BIOMIG1 strains showed that the genomes had >99.9% average nucleotide identity (ANI), suggesting that any difference was most likely associated with BAC degradation. The genes that were present in the genomes of BIOMIG1^{BAC} and BIOMIG1^{BDMA} but absent in the genomes of BIOMIG1^{BD} and BIOMIG1^N were clustered in a single contig (Contig_BAC1) (Figure 4.2). The genes on this contig were: two major facilitator superfamily transporters, a TetR family transcriptional regulator, a dioxygenase, a SCP-2 sterol transfer protein and an integrase (Figure 4.2A). There were also three hypothetical genes with no previously known function.

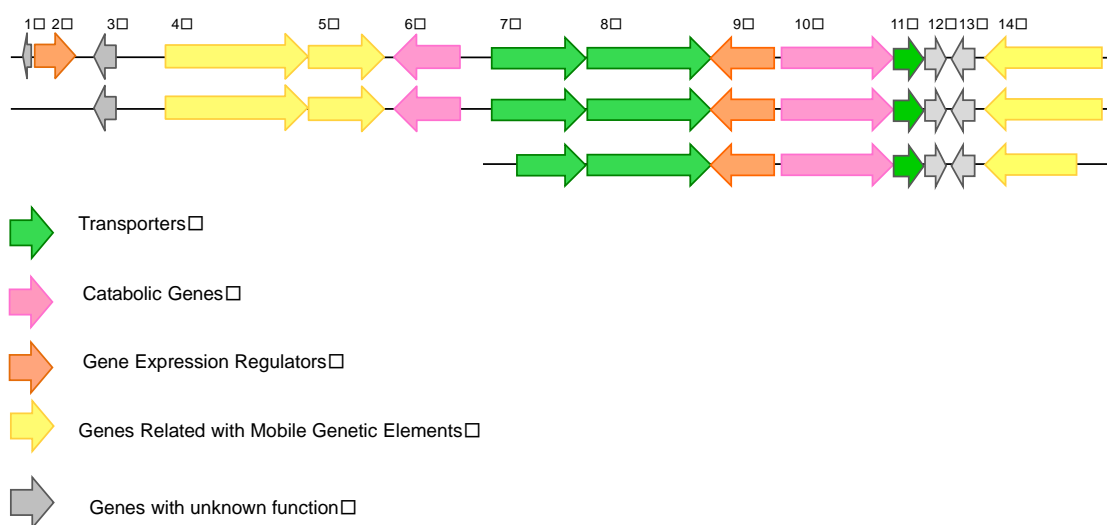


Figure 4.2. Comparison of (A) Contig_BAC1 with a similar contig in metagenome datasets of (B) SEW, SOIL and SEA, (C) AS and (D) river sediment (Contig B_{43d}_01683) communities. Genes are: (1) Hypothetical protein; (2) Single strand DNA binding protein; (3) Hypothetical protein; (4) IS21 family transposase; (5) IS21 family transposase; (6) Amine oxidase; (7) MFS transporter; (8) MFS transporter; (9) TetR family transcriptional regulator; (10) Rieske oxygenase; (11) Sterol binding domain protein; (12) Hypothetical protein; (13) LysR family transcriptional regulator and (14) Phage integrase family protein

To understand the significance of Contig_BAC1 for BAC biotransformation, its sequence was searched in the BAC-enriched metagenomes. Three contigs 100% identical to Contig_BAC1 was present in SEW, SOIL and SEA metagenomes respectively (Figure 4.2B), however Contig_BAC1 was assembled slightly different in the AS metagenome and contained 4 additional genes; a hypothetical protein, two IS21 family transposases and an amine oxidase (Figure 4.2C). Furthermore, Contig_BAC1 was highly abundant in the metagenomes, and there was a linear relationship between the abundance of Contig_BAC1 and abundance of *Pseudomonas* sp. (Figure 4.3) in the metagenomes. This indicated that BIOMIG1 played a major part for BAC degradation in the consortia and the genes present on Contig_BAC1 were involved in biotransformation BACs to BDMA.

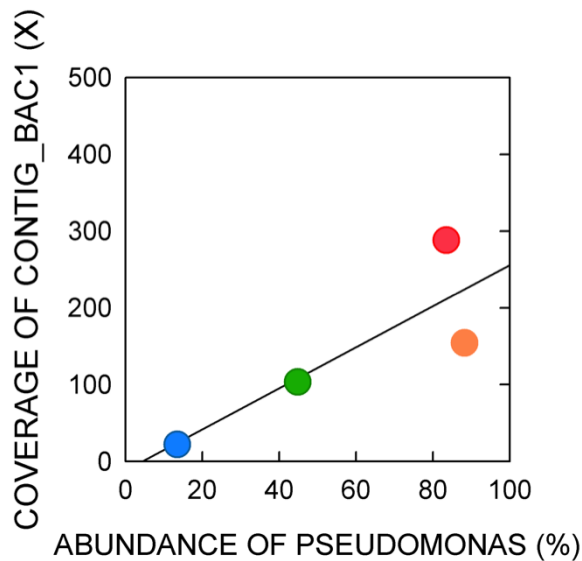


Figure 4.3. Relationship between the abundance of *Pseudomonas* sp. and abundance of Contig_BAC1 represented as coverage. (Red) AS (Yellow) SEW (Green) SOIL (Blue) SEA

Recently, Oh et al. (2013) reported an array of genes that were encoded on a contig (Contig B_{43d}_01683, GenBank Accession Number: SRR643894) that became significantly enriched in the metagenome of a microbial consortium selected on BACs. We found that Contig B_{43d} was remarkably similar to Contig_BAC1 (Figure 21D) (>96% of the length of Contig_BAC1 was aligned with >97% identity). Aside from minor nucleotide substitutions, gene content and arrangements of Contig B_{43d} and Contig_BAC1 were identical. Based on comparative genomic and experimental results combined with previous results from the literature, it was suggested that genes encoded by Contig_BAC1 played a key role in the biotransformation of BACs in various habitats. Among the common genes in Contig_BAC1 and Contig B_{43d}_01683, a putative oxygenase was the only catabolic gene and therefore was the candidate gene for conversion of BAC to BDMA. This oxygenase was denoted as *oxy-BAC* hereafter. In addition, the presence of transposases and integrases indicated that the Contig_BAC1 possibly resided on a mobile element such as a transposon or a plasmid (Figure 4.2).

Fifteen genes located on four contigs (Figure 4.4) were present in the genomes of *Pseudomonas* sp. BIOMIG1^{BAC} and BIOMIG1^{BD} but absent in the genomes of *Pseudomonas* sp. BIOMIG1^{BDMA} and BIOMIG1^N. A Blastp search in the protein database of NCBI revealed that on that four contigs there were two catabolic genes. First one was a putative phytanoyl Co-A dioxygenase (look at figure 2.10), what does it do???? from the 2- α glutarate and FeII dependent (2OG-FeII) oxygenase group. Second one was a salicylaldehyde dehydrogenase. BDMA degradation experiments have shown that degradation ceases when oxygen is depleted, hence can be considered O₂ dependent. Therefore between the aforementioned two enzymes, it is more likely that the putative dioxygenase catalyzed debenzoylation of BDMA. This enzyme will be referred as oxyBDMA hereafter. 2OG-FeII dependent oxygenases comprise a diverse group of enzymes that can catalyze various reactions including hydroxylation of amines like proline (Schofield and Zhang, 1999). Although BDMA is also a tertiary amine, there are no previous reports identifying a 2OG-FeII oxygenase related to its degradation. The candidate BDMA degrading oxygenase identified here had 50% amino acid identity to a phytanoyl Co-A oxygenase of *Novosphingobium* sp. B7 (GenBank Accession number: WP_022675950.1). Another example tertiary amine is trimethylamine (TMA), which is formed as a result of natural QAC degradation, thus a ubiquitous compound in the environment. A recent study showed that TMA was first oxidized to trimethyl amine N oxide (TMAO) by a flavin monooxygenase (Tmm) in *Methylocella silvestris* that thrived in oceans (Chen et al., 2011). A complementary report revealed that TMAO was further converted to dimethyl amine (DMA) by a TMAO demethylase (Tdm) in *Ruegeria pomeroyi*, and further to methyl amine (Lidbury et al., 2014). This pathway differs from BDMA degradation as it requires five steps until mineralization whereas BDMA degradation requires four steps, although some intermediates are produced. It can be suggested that oxyBDMA bypasses the second step generating a more efficient tertiary amine degradation pathway.

The salicylaldehyde dehydrogenase identified here probably catalyzed degradation of produced intermediates such as benzaldehyde. Additionally, there were four transporter genes and five transcriptional regulators on the four contigs identified as related to BDMA degradation. These likely contributed to the uptake of substrates and regulation of gene

expression during BDMA degradation. Testing the hypothetical functions of the genes identified here is part of future studies. Tertiary amines are the ultimate intermediates in both naturally occurring and synthetic QAC degradation pathways. Mineralization of tertiary amines have been observed in enrichment cultures, however is rarely accomplished by pure cultures. In fact, the only the microorganism other than BIOMIG1, which could mineralize BDMA was an *Aeromonas* species, although through an atypical pathway (Patrauchan and Oriel, 2003).

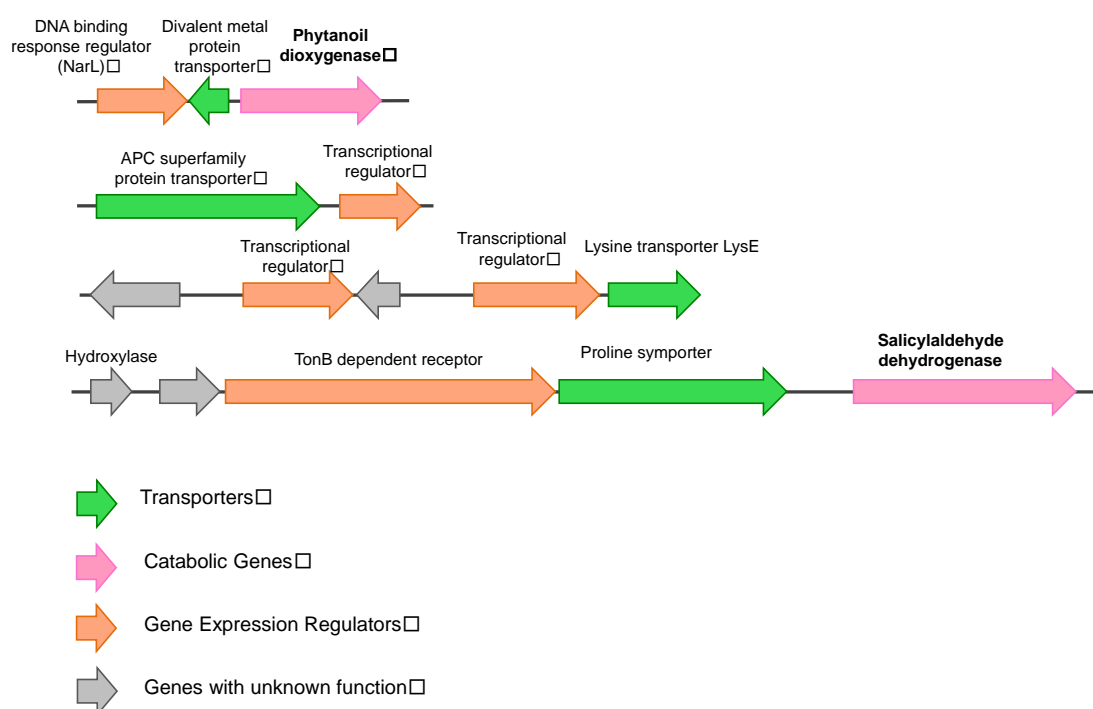


Figure 4.4. Contigs involved in BDMA degradation

4.3.2. Phylogenetic Analysis and Classification of the Genes Involved in BAC Degradation Pathway

Analysis of the amino acid sequence of oxyBAC confirmed that it had a conserved Rieske domain [2Fe-2S] and an iron containing catalytic active site, therefore this protein was likely a Rieske oxygenase (RO) (Nam et al., 2001) classified ROs into four distinct groups according to the amino acid sequence patterns of their oxygenase subunits. Those four RO groups (Group I-IV, Figure 4.5) mainly catalyze *cis* and *trans* hydroxylation of a benzene ring. However, it was recently reported that some of the newly discovered ROs did not cluster with any of these groups, thus representing a novel group. The ROs that belonged to the latter group include enzymes like stachydrine demethylase (*stc2*) (Daughtry et al., 2012), glycine demethylase (*gbcA*) (Stover et al., 2000) and carnitine oxygenase (*cntA*) (Zhu et al., 2014) which could catalyze non-ring hydroxylating reactions. The latter enzymes attack on C-N⁺ bond between a methyl or ester groups and quaternary N of natural QACs resulting in removal of these groups from the N atom and formation of a tertiary amine (Figure 4.6). In order to delineate the evolutionary relationship of oxyBAC with the previously characterized ROs, a phylogenetic tree was constructed using the amino acid sequences of its closest homologs along with two recently identified QAC degrading enzymes (Figure 4.5). Our results demonstrated that oxyBAC belonged to a distinct clade including *stc2*, *gbcA* and *cntA*. This group was denoted as Group V ROs in this study. The previously identified enzymes degrading QAC disinfectants such as the amine oxidase of *Pseudomonas nitroreducense* B (Oh et al., 2014) and tetradecyltrimethylammonium bromide monooxygenase of *Pseudomonas putida* ATCC 12633 (TTBMO) Liffourrena (Liffourrena and Lucchesi, 2014), are non-RO enzymes and were more closely related to Group II ROs as opposed to Group V enzymes. Furthermore, among ROs, Group V was more closely related to monooxygenases such as the choline monooxygenase (*cmo*). On the other hand, *cmo* cannot catalyze a N-dealkylation reaction but can oxidize the terminal C of the alcohol group attached to the quaternary N of the choline. (Rathinasabapathi et al., 1997). Within this group, the closest homolog of oxyBAC was *stc2* with 26% amino acid identity. This relatively low homology to previously characterized enzymes doing N-dealkylation of short saturated and un-saturated alkyl groups suggested that oxyBAC was

a novel enzyme, potentially involved in the N-dealkylation of a long-chain saturated alkyl group from a quaternary N. The previously identified BAC dealkylating amine oxidase (Oh et al., 2014) and TTABMO (Liffourrena and Lucchesi, 2014) showed substantially lower homology to oxyBAC (13% and 17% amino acid identity, respectively) compared to cntA, gbcA and stc2. The most similar amino acid sequence (~97% amino acid similarity) to oxyBAC was present in the draft genome of *Novosphingobium sp. B7* (GenBank Accession Number: WP_022676119.1). The gene encoding this protein was located on a 3 kbp long contig. The sequence of this contig was almost identical to the gene cluster containing oxyBAC (98% nucleotide similarity). However, neither *Novosphingobium sp. B7*, nor the aforementioned protein has been previously tested for QAC degradation. The flanking regions of oxyBAC in our *Pseudomonas sp. BIOMIG1* strain consisted of two MFS transporters, a tetR family type transcriptional regulator, a sterol binding domain protein, a hypothetical protein, a Lyrs family transcriptional regulator and a phage integrase. This structure was also conserved in the genome of *Novosphingobium sp. B7*, where the homolog oxygenase was flanked with a tetR family transcriptional regulator, a sterol binding protein and two hypothetical proteins. In the latter gene cluster, a reductase gene next to oxyBAC was not identified which is not usual for ROs. The latter finding indicated that oxyBAC could function without a specific reductase or recruit a non-specific reductase for electron transfer.

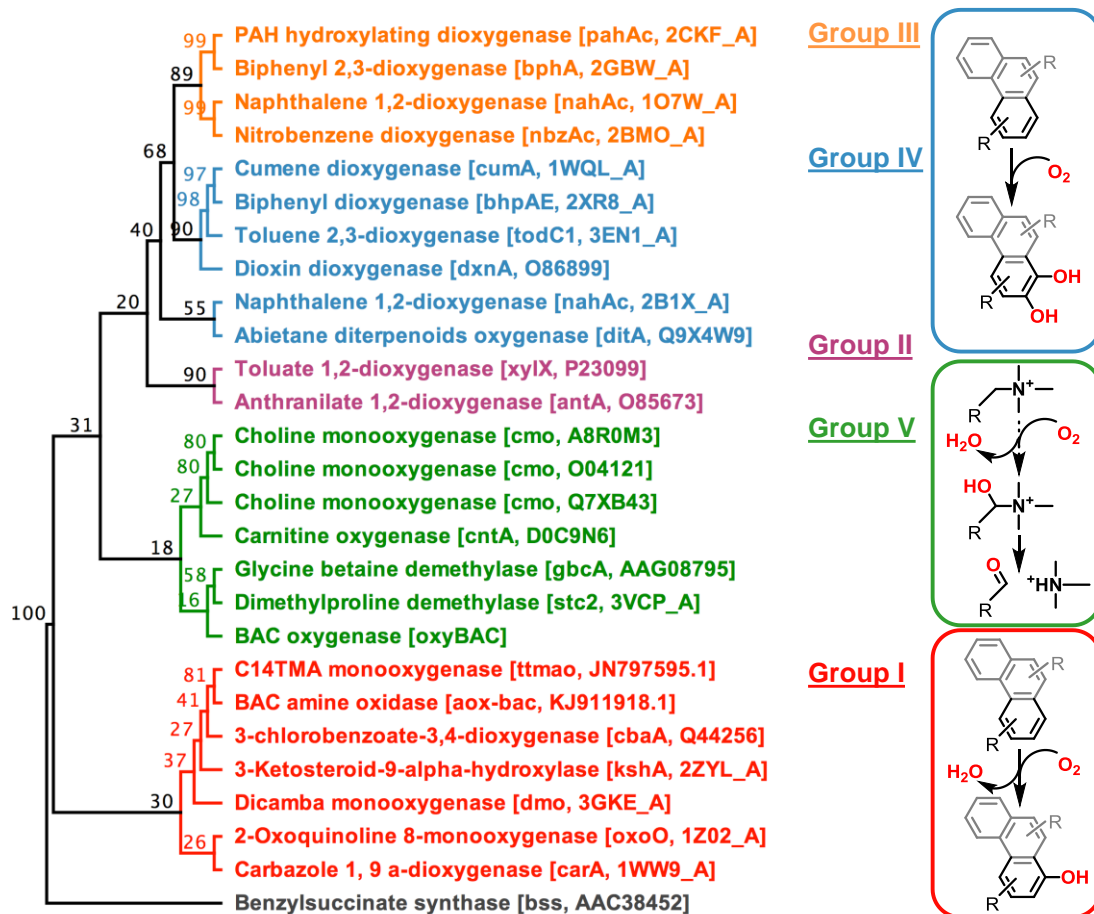
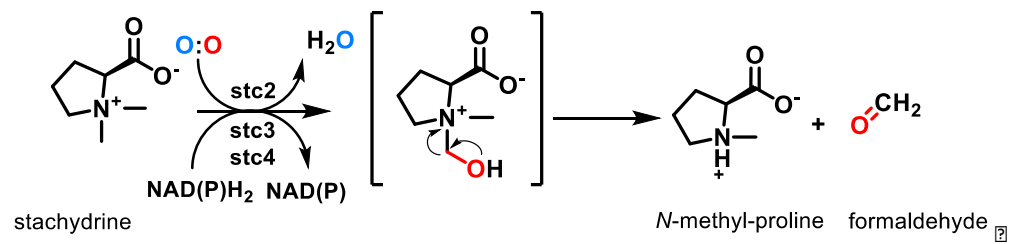
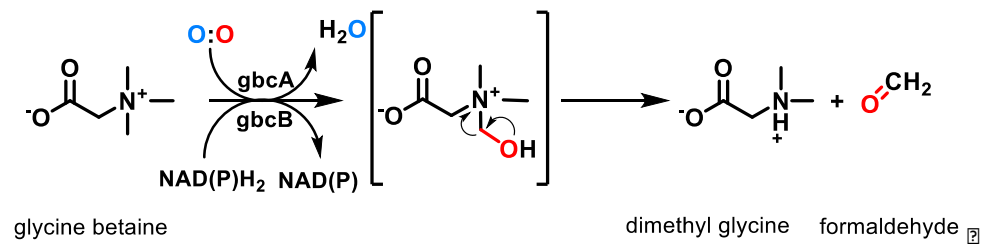


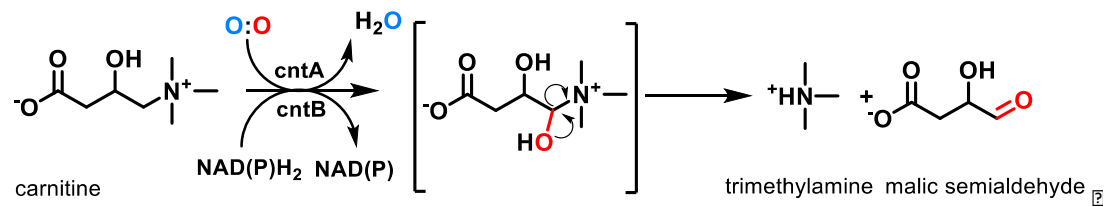
Figure 4.5. Phylogenetic relationship of oxyBAC, ttmao, aox-bac, microbial Rieske type terminal oxygenases (Groups I-IV) and eukaryotic Rieske type choline monooxygenases. Benzy succinate synthase was used as the outgroup. Reactions show generalized mechanisms of oxidation of substrates by Rieske type oxygenases.



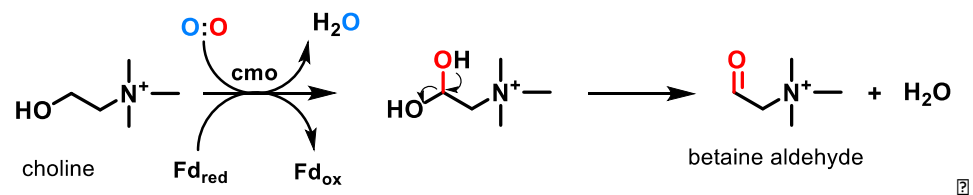
(A)



(B)



(C)



(D)

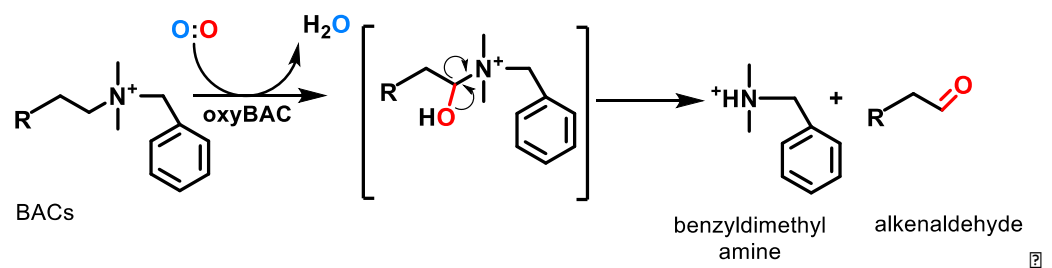


Figure 4.6. Reactions catalyzed by QAC degrading enzymes

4.3.3. *Pseudomonas* sp. BIOMIG1 with *oxyBAC* grows on BACs

Using specific primers, a ~700 bp region of *oxyBAC* was amplified from BIOMIG1 strains to confirm its presence in the genomes of *Pseudomonas* sp. BIOMIG1^{BAC} and BIOMIG1^{BDMA}, and absence in the genomes of *Pseudomonas* sp. BIOMIG1^{BD} and *Pseudomonas* sp. BIOMIG1^N (Figure 4.7). Given that BIOMIG1^{BD} and BIOMIG1^N were generated from BIOMIG1^{BAC} and BIOMIG1^{BDMA}, respectively by selective cultivation in BAC free media, it can be assumed that *oxyBAC* was lost from the genome of the former two strains. A biodegradation assay was further conducted with the four BIOMIG1 strains. Both BIOMIG1^{BAC} and BIOMIG1^{BDMA} completely utilized 250 μ M BAC within 50 hours (Figure 4.8). Given the fact that BDMA transformation rate is faster than BAC conversion to BDMA (Tezel et al., 2012), BDMA was not detected in the flasks inoculated with BIOMIG1^{BAC}. Moreover, the cell density increased by approximately 200 folds (Figure 4.8B). The results suggested that BIOMIG1^{BAC} transformed BACs to BDMA which was quickly utilized as a carbon and energy source promoting cell growth. On the other hand, equimolar amount of BDMA was produced when BACs were utilized by BIOMIG1^{BDMA}. However, cell density increased only 10 folds which was less than that of BIOMIG1^{BAC} (Figure 4.8B). These results suggested that *oxyBAC* was only involved in the BAC to BDMA conversion and does not support growth on the BDMA. In contrast, BIOMIG1^{BD} and BIOMIG1^N, which did not contain *oxyBAC*, neither utilized BACs nor grew in the SM containing BACs (Figure (Figure 4.8D and E). In conclusion, absence of *oxyBAC* in BIOMIG1 resulted in subsequent loss of BAC transformation to BDMA.

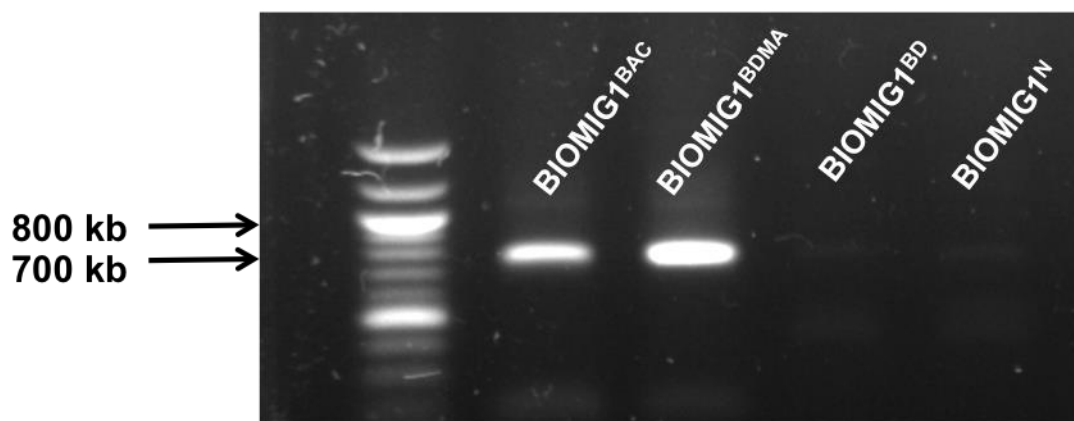


Figure 4.7. Amplification of *oxy*-BAC from *P. sp.* BIOMIG1 phenotypes.

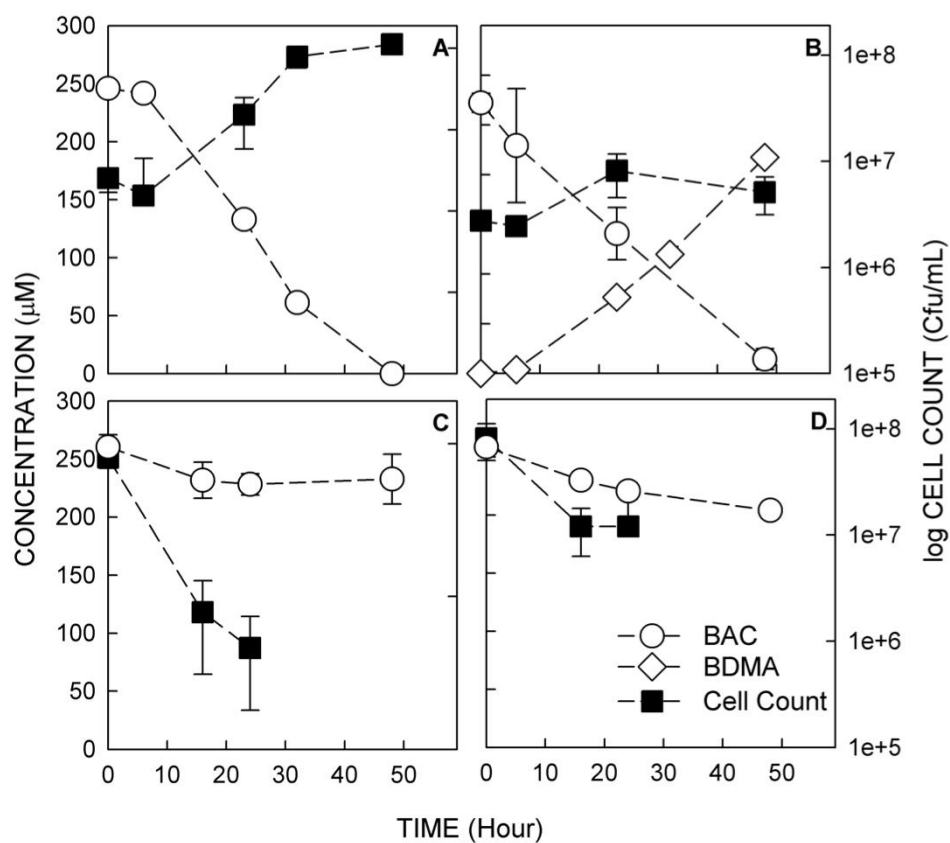


Figure 4.8. Profile of C₁₂BDMA-Cl utilization, BDMA formation and cell growth by (A) BIOMIG1^{BAC}, (B) BIOMIG1^{BDMA}, (C) BIOMIG1^{BD} and (D) BIOMIG1^N (Error bars represent one standard deviation of the means, $n = 3$)

4.3.4. *E. coli* overexpressing *oxyBAC* gene converts BACs to BDMA

In order to confirm the function of *oxyBAC* experimentally, biotransformation experiments were conducted with *E. coli* cells heterologously expressing the gene (*E.coli^{oxyBAC}*). A control assay was prepared with *E. coli* cells transformed with an empty plasmid (*E.coli^N*). The presence of *oxyBAC* in *E. coli^{oxyBAC}* and absence in *E.coli^N* were confirmed by PCR (Figure 4.7) In the biotransformation assay, C₁₂BDMA-Cl was used as the substrate at 20 μM concentration. *E. coli^N* did not utilize C₁₂BDMA-Cl in the course of incubation (Figure 4.9). On the other hand, C₁₂BDMA-Cl was completely converted to BDMA within 1.5 h in the flasks inoculated with *E. coli^{oxyBAC}* (Figure 4.9A). The rate of C₁₂BDMA-Cl biotransformation was predicted as 14 μM/hr. These results confirmed that *oxyBAC* was the enzyme responsible for the conversion of BAC to BDMA via N-dealkylation reaction and it could function effectively outside of its original host. The high efficiency in integrating *oxyBAC* into a heterologous expression system (e.g., *E. coli*), indicates that the gene might be promiscuous in horizontal gene transfer and easy to manipulate in further biotechnological applications.

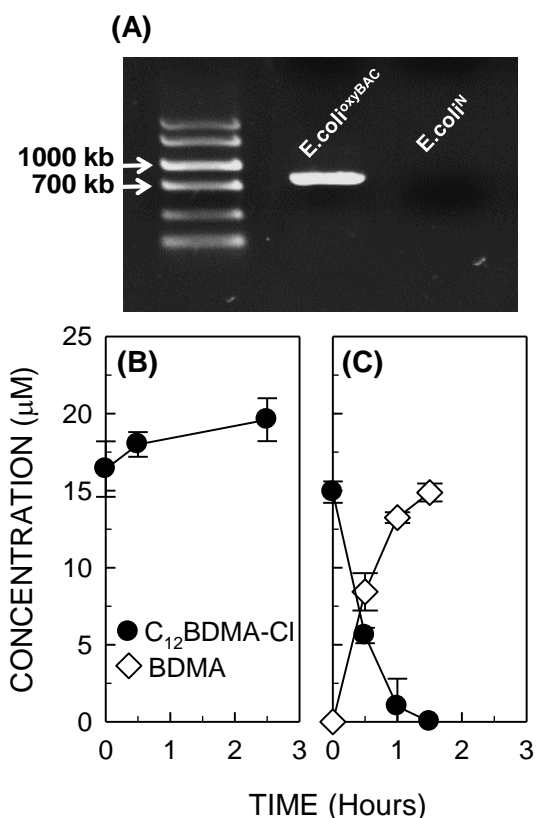


Figure 4.9. (A) *oxyBAC* PCR amplicons of two *E. coli* phenotypes on agarose gel. Profile of C₁₂BDMA-Cl utilization and BDMA formation by (B) *E. coli*^N and *E. coli*^{oxyBAC} (Error bars represent one standard deviation of the means, $n = 3$)

As previously mentioned, two other enzymes capable of biotransforming QAC disinfectants have been identified. Aox-Bac of *Pseudomonas nitroreducens* B (Oh et al., 2014) could convert C₁₂BDMA-Cl and C₁₄BDMA-Cl to BDMA with ~50% efficiency and a rate of 20 nmol substrate/mg of protein/min and 7 nmol substrate mg of protein⁻¹ min⁻¹, respectively and TTABMO of *Pseudomonas putida* ATCC 12633 could convert tetradecyltrimethylammonium bromide with a rate of 128.6 nmol TMA min⁻¹ mg protein⁻¹. Despite catalyzing similar reactions, those previously identified QAC degrading enzymes were phylogenetically distant to *oxyBAC* and group V ROs. The most closely related enzyme to amine oxidase of *Pseudomonas nitroreducens* B was a pseudooxynicotine amine oxidase (pao, GenBank accession number: AFD54463.1) (Qiu et al., 2013). Both amine oxidases could attack the C-N bond and catalyze a dealkylation reaction. Additionally, the

closest homolog of TTABMO was a type V secretion protein; Rhs of *Pseudomonas* sp. (GenBank accession no: WP_049586647.1) These results imply that there might be multiple genetic mechanisms and enzymes capable of biotransforming QAC disinfectants in the environment.

4.3.5. OxyBAC is a unique N-dealkylating RO

Rieske type oxygenases (ROs) are growing group of oxygenase enzymes which are important for biodegradation of xenobiotic pollutants (Neilson and Allard, 2008). As explained in the previous sections, the presence of a conserved Rieske motif (-CXHX₁₅₋₁₇CXXH-) and mononuclear iron center qualified oxyBAC as an RO. Moreover, oxyBAC cleaved the C-N⁺ bond between a long saturated alkyl chain and a quaternary N, which is a unique reaction type compared to other N-dealkylating ROs, because the other N-dealkylating ROs either targets a methyl group and demethylate an amine (Gu et al., 2013; Chen et al., 2014) or a quaternary ammonium (Daughtry et al., 2012), or an unsaturated short alkyl chain (Zhu et al., 2014). In addition, ROs are multicomponent enzymes, consisting of an oxygenase, reductase and sometimes also a ferredoxin subunit (Ferraro et al., 2005). OxyBAC could function without a specific reductase, which suggests that it probably recruited one from *E.coli*. Although this is uncommon, multicomponent ROs with promiscuous oxygenase subunits have been identified (Ferraro et al., 2005).

In order to understand the unique features of oxyBAC that gives its novel reaction capabilities, Rieske domain and the mononuclear iron center of oxyBAC was compared to other N-dealkylating ROs (Figure 31). Rieske domain of oxyBAC was 51, 46 and 43% similar to those of cntA, gbcA and stc2, respectively. The key difference between the Rieske domains of oxyBAC and other N-dealkylating ROs was the presence of 19 residues, instead of 17 between CXH and CXXH conserved regions. The reason for this was the insertion of two glycines (G) into this region (Figure 31A). In addition, adjacent 2 amino acids (LR) before and 3 amino acids (RIL) after the two glycine are unique to oxyBAC where as they are VA and KLV in both stc2 and gbcA (Figure 31A). Thus, LR-GG-RIL motif is unique for oxyBAC Rieske domain and might underlie its unique biochemical function. Moreover,

mononuclear iron center of the oxyBAC is 42, 54 and 58% similar to those of cntA, gbcA and stc2, respectively. Substitution of bridging aspartate (D) to bridging glutamate (E) is common to all N-dealkylating ROs compared to other ROs including cmo (Figure 4.10). Zhu et al (2014) suggested that this substitution is the main reason for the attack on C-N⁺ in the N-dealkylation reaction which can be achieved by all Group V ROs except cmo which cannot attack on C-N⁺ bond. On the other hand, substitution of tyrosine (Y) with leucine (L) adjacent to first conserved histidine (H) in mononuclear iron center is unique to oxyBAC (Figure 4.10B). These unique features of oxyBAC peptide sequence may result in the N-dealkylation of saturated long-chain alkyl groups from QACs without a need of a specific reductase for the reaction. This hypothesis should be verified by testing the BAC biotransformation ability of amino acid variant mutants.



Figure 4.10. Multiple sequence alignment of (A) Rieske domain and (B) mononuclear iron center of oxyBAC with other Group V Rieske oxygenases and oxyBAC of *Novosphingobium sp.* B7. ↑ and Δ denote amino acid insertion and substitution, respectively

In this study, a number of genes involved in both BAC to BDMA transformation and BDMA degradation were predicted. Among them, the function of a RO denoted as oxy-BAC could convert BAC to BDMA, which was experimentally proven. This enzyme

was used by *Pseudomonas* sp. BIOMIG1 to utilize BACs as an energy source and to produce cells. OxyBAC enzyme can be used to develop advanced wastewater treatment technologies where BACs are problem such as poorly treated wastewater and effluents originating from hospitals and pharmaceutical facilities. In addition, oxyBAC based biotechnology could have applications in bioremediation of environments contaminated with BACs. For instance, the primers developed here can be used to evaluate the BAC treatment potential of activated sludge treating domestic, industrial and agricultural wastewater as well as of the natural environments contaminated with BACs. On the other hand, microorganisms having *oxyBAC* gene are not desirable in medical environments since they would decrease the efficacy of disinfectant most of which have BACs as active ingredients and thus could cause proliferation of pathogens. Systematically analyzing the abundance of oxyBAC in the medical settings, and taking the necessary precautions to avoid contamination of indoor environment by microorganisms harboring oxyBAC gene may minimize such threats.

Protein based experiments are necessary for further characterization of oxyBAC. The multicomponent structure can be fully resolved once the reductase and ferredoxin subunits of the enzyme are identified and analyzed via crystallography. Additionally, Protein characteristics such as substrate specificity and binding efficiency, optimum working temperature, pH, etc. should be determined for implementing technology applications. Also, the stoichiometry of the N-dealkylation reaction needs to be defined by identifying the total repertoire of metabolites. All of these matters are crucial for better understanding of how oxyBAC functions, which is critical for BAC degradation in the environment. The enzymes degrading BACs and QACs are diverse in terms of structure and phylogeny. This suggests that there are possibly a number of enzymes in the environment yet to be discovered. Candidate QAC degrader strains and enzymes can be identified and tested using ongoing whole genome sequencing projects. In summary, the discovery of oxyBAC as a novel RO enzyme expands our knowledge on the biotransformation mechanisms of disinfectants in the environment and applications and complications it provides.

5. CONCLUSIONS AND PERSPECTIVES

Benzalkonium chlorides (BACs) are disinfectants that are toxic to the ecosystem and promote dissemination of antimicrobial resistance. Biodegradation of BACs is a unique metabolic capability which is the ultimate mechanism to alleviate the impact of BAC contamination in the environment. In this study, the understanding of BAC biodegradation in the environment has been expanded, using an approach combining enrichment cultures and isolation of BAC degraders with high-throughput sequencing.

Using metagenome sequencing and analysis of enrichment cultures originating from natural environments such as activated sludge, sewage, soil and sea sediment; it was shown that a specific BAC degrader *Pseudomonas* sp. was the key role player for emergence of a rapidly BAC degrading community. This microorganism was a novel *Pseudomonas* species that could mineralize BACs through a series of dealkylation, debenzoylation and demethylation reactions and was denoted as *Pseudomonas* sp. BIOMIG1. Whole genome of *Pseudomonas* sp. BIOMIG1 was further sequenced and analyzed. Even though it was draft, this was the first available genome sequence originating from a BAC/QAC degrader. The genome sequence of BIOMIG1 was significantly distant to its closest relatives and supported the assumption that it represented a novel species.

The biodegradation experiments with BIOMIG1 demonstrated that some strains could not mineralize BAC, but stopped after an intermediate; benzyl dimethyl amine (BDMA) was produced. Furthermore, if BAC was excluded from the cultivation media, BIOMIG1 lost its ability to degrade BACs. Following these observations, it was hypothesized that by comparing the genomes of BIOMIG1 phenotypes that could do different steps of the biodegradation pathway, the specific genes underlying each step could be identified. This hypothesis was tested by comparing the whole genomes of four BIOMIG1 phenotypes such as a complete degrader, a BDMA accumulator, an only BDMA degrader and a BAC non-degrader. This analysis revealed that a gene encoding a Rieske oxygenase (oxyBAC) was responsible for converting BAC to BDMA. Moreover, *E.coli* heterologously expressing oxyBAC could also convert BAC to equimolar amounts of BDMA, which experimentally

confirmed the function of this gene. In addition, putative catabolic genes have been identified as involved in BDMA degradation. Function of these genes can be similarly tested in the future and provide valuable insights, since there is even fewer information on BDMA degradation pathway.

The findings of this study revealed that OxyBAC was a new enzyme detoxifying BACs in the environment. This enzyme can potentially be used to clean-up wastewater from BACs. Additionally the abundance and expression levels of oxyBAC can be monitored in wastewater treatment plants as well as hospitals and indoor environments, where presence of such a gene can cause health hazards. Appropriate precautions can be promptly taken to prevent dissemination of oxyBAC in non-target environments. The results of this study also showed that *oxyBAC* was distantly related to homolog ROs degrading naturally occurring QACs, suggesting it formerly diverged from a common ancestor. Furthermore, *oxyBAC* was found in the close vicinity of integrases and IS elements, which indicated that horizontal gene transfer contributed to its evolution and dissemination in the environment. New hypotheses formulated from these assumptions hopefully will be tested in future studies.

The outcomes of this study have brought forth new questions that would be attempted in the future. Genomic evidence suggests oxyBAC is located on a mobile genetic element. The structure of that element would be revealed and whether or not oxyBAC can be transferred to other microorganisms would be tested in-vitro. The function of the putative BDMA degrading enzymes proposed in this study can be verified by heterologous overexpression in *E.coli* which would completely characterize the pathway. Finally, the purified proteins encoded by both oxyBAC and oxyBDMA can be used in bioreactors to eliminate BAC and BDMA from wastewater influents.

REFERENCES

- Ahn, Y., Kim, J.M., Kweon, O., Kim, S.J., Jones, R.C., Woodling, K. et al. (2016) Intrinsic Resistance of Burkholderia cepacia Complex to Benzalkonium Chloride. *MBio* **7**.
- Alexander, M. (1981) Biodegradation of Chemicals of Environmental Concern. *Science* **211**: 132-137.
- Barnhart, M.M., Pinkner, J.S., Soto, G.E., Sauer, F.G., Langermann, S., Waksman, G. et al. (2000) PapD-like chaperones provide the missing information for folding of pilin proteins. *Proc Natl Acad Sci U S A* **97**: 7709-7714.
- Barry, S.M., and Challis, G.L. (2013) Mechanism and Catalytic Diversity of Rieske Non-Heme Iron-Dependent Oxygenases. *ACS Catal* **3**.
- Bergero, M.F., and Lucchesi, G.I. (2015) Immobilization of Pseudomonas putida A (ATCC 12633) cells: A promising tool for effective degradation of quaternary ammonium compounds in industrial effluents. *International Biodeterioration & Biodegradation* **100**: 38-43.
- Blazquez, J., Couce, A., Rodriguez-Beltran, J., and Rodriguez-Rojas, A. (2012) Antimicrobials as promoters of genetic variation. *Curr Opin Microbiol* **15**: 561-569.
- Bucheli-Witschel, M., and Egli, T. (2001) Environmental fate and microbial degradation aminopolycarboxylic acids. *FEMS Microbiology Reviews* **25**: 69-106.
- Buffet-Bataillon, S., Tattevin, P., Bonnaure-Mallet, M., and Jolivet-Gougeon, A. (2012a) Emergence of resistance to antibacterial agents: the role of quaternary ammonium compounds--a critical review. *Int J Antimicrob Agents* **39**: 381-389.
- Buffet-Bataillon, S., Le Jeune, A., Le Gall-David, S., Bonnaure-Mallet, M., and Jolivet-Gougeon, A. (2012b) Molecular mechanisms of higher MICs of antibiotics and quaternary ammonium compounds for Escherichia coli isolated from bacteraemia. *J Antimicrob Chemother* **67**: 2837-2842.
- Chen, Q., Hong-Cheng, W., Shi-Kai, D., Ya-Dong, W., Yi Li, L., Li, Y. et al. (2014) Novel Three-Component Rieske Non-Heme Iron Oxygenase System Catalyzing the N-Dealkylation of Chloroacetanilide Herbicides in Sphingomonads DC-6 and DC-2. *Applied and Environmental Microbiology* **80**: 5078-5085.
- Chen, S., Wang, H., Katzianer, D.S., Zhong, Z., and Zhu, J. (2013) LysR family activator-regulated major facilitator superfamily transporters are involved in Vibrio cholerae antimicrobial compound resistance and intestinal colonisation. *Int J Antimicrob Agents* **41**: 188-192.
- Chen, Y., Patel, N.A., Crombie, A., Scrivens, J.H., and Murrell, J.C. (2011) Bacterial flavin-containing monooxygenase is trimethylamine monooxygenase. *Proc Natl Acad Sci U S A* **108**: 17791-17796.
- Copley, S.D. (2000) Evolution of a metabolic pathway for degradation of a toxic xenobiotic: the patchwork approach. *Trends in Biochemistry* **25**: 261-265.
- Cox, M., Peterson, D., and Biggs, P.J. (2010) SolexaQA: At-a-glance quality assessment of Illumina second-generation sequencing data. *BMC Bioinformatics* **11**: 1471-2105.

- Cuthbertson, L., and Nodwell, J.R. (2013) The TetR family of regulators. *Microbiol Mol Biol Rev* **77**: 440-475.
- Darling, A.C., Mau, B., Blattner, F.R., and Perna, N.T. (2004) Mauve: multiple alignment of conserved genomic sequence with rearrangements. *Genome Res* **14**: 1394-1403.
- Daughtry, K.D., Xiao, Y., Stoner-Ma, D., Cho, E., Orville, A.M., Liu, P., and Allen, K.N. (2012) Quaternary ammonium oxidative demethylation: X-ray crystallographic, resonance Raman, and UV-visible spectroscopic analysis of a Rieske-type demethylase. *J Am Chem Soc* **134**: 2823-2834.
- Dennis, J.J. (2005) The evolution of IncP catabolic plasmids. *Curr Opin Biotechnol* **16**: 291-298.
- Diaz, E., Jimenez, J.I., and Nogales, J. (2013) Aerobic degradation of aromatic compounds. *Curr Opin Biotechnol* **24**: 431-442.
- Edgar, R.C. (2010) Search and clustering orders of magnitude faster than BLAST. *Bioinformatics* **26**: 2460-2461.
- Eren, A.M., Maignien, L., Sul, W.J., Murphy, L.G., Grim, S.L., Morrison, H.G., and Sogin, M.L. (2013) Oligotyping: Differentiating between closely related microbial taxa using 16S rRNA gene data. *Methods Ecol Evol* **4**.
- Fatta-Kassinos, D., Kalavrouziotis, I.K., Koukoulakis, P.H., and Vasquez, M.I. (2011) The risks associated with wastewater reuse and xenobiotics in the agroecological environment. *Sci Total Environ* **409**: 3555-3563.
- Ferraro, D.J., Gakhar, L., and Ramaswamy, S. (2005) Rieske business: structure-function of Rieske non-heme oxygenases. *Biochem Biophys Res Commun* **338**: 175-190.
- Fuchs, G., Boll, M., and Heider, J. (2011) Microbial degradation of aromatic compounds - from one strategy to four. *Nat Rev Microbiol* **9**: 803-816.
- Gai, Z., Wang, X., Liu, X., Tai, C., Tang, H., He, X. et al. (2010) The Genes Coding for the Conversion of Carbazole to Catechol Are Flanked by IS6100 Elements in *Sphingomonas* sp. Strain XLDN2-5. *PLoS One* **5**: 1-9.
- Gibson, D.T., and Parales, R.E. (2000) Aromatic hydrocarbon dioxygenases in environmental biotechnology. *Current Opinion in Biotechnology* **11**: 236-243.
- Gillings, M.R. (2014) Integrons: past, present, and future. *Microbiol Mol Biol Rev* **78**: 257-277.
- Gu, T., Zhou, C., Sorensen, S.R., Zhang, J., Jian, H., Yu, P. et al. (2013) The novel Bacterial N-Demethylase PdmAB is Responsible for the initial step of N,N-Dimethyl-Substituted Phenylurea Herbicide Degradation. *Applied and Environmental Microbiology* **79**: 7846-7856.
- Harbers, J.V., Huijbregts, M.A.J., Posthuma, L., and Van De Meent, D. (2006) Estimating the Impact of High-Production-Volume Chemicals on Remote Ecosystems by Toxic Pressure Calculation. *Environmental Science and Technology* **40**: 1573-1580.

- He, Z., Deng, Y., Van Nostrand, J.D., Tu, Q., Xu, M., Hemme, C.L. et al. (2010) GeoChip 3.0 as a high-throughput tool for analyzing microbial community composition, structure and functional activity. *ISME J* **4**: 1167-1179.
- Iovdijova, A., and Benchko, V. (2010) Potential Risk of Exposure to Selected Xenobiotic Residues and Their Fate in the Food Chain-Part I: Classification of Xenobiotics. *American Academy of Environmental Medicine* **17**: 183-192.
- Janssen, D.B., Dinkla, I.J., Poelarends, G.J., and Terpstra, P. (2005) Bacterial degradation of xenobiotic compounds: evolution and distribution of novel enzyme activities. *Environ Microbiol* **7**: 1868-1882.
- Jimenez, J.I., Minambres, B., Garcia, J.L., and Diaz, E. (2002) Genomic analysis of the aromatic catabolic pathways from *Pseudomonas putida* KT2440. *Environmental Microbiology* **4**: 824-841.
- Johnson, G.R., and Spain, J.C. (2003) Evolution of catabolic pathways for synthetic compounds: bacterial pathways for degradation of 2,4-dinitrotoluene and nitrobenzene. *Appl Microbiol Biotechnol* **62**: 110-123.
- Johri, A.K., Dua, M., Singh, A., Sethunathan, N., and Legge, R.L. (1999) Characterization and regulation of catabolic genes. *Crit Rev Microbiol* **25**: 245-273.
- Kawai, F., and Hu, X. (2009) Biochemistry of microbial polyvinyl alcohol degradation. *Appl Microbiol Biotechnol* **84**: 227-237.
- Kivisaar, M. (2011) Evolution of catabolic pathways and their regulatory systems in synthetic nitroaromatic compounds degrading bacteria. *Mol Microbiol* **82**: 265-268.
- Koeth, A.K., Wang, A., Levison, B.S., Buffa, J.A., Org, E., Sheehy, B.T. et al. (2013) Intestinal microbiota metabolism of L-carnitine, a nutrient in red meat, promotes atherosclerosis *Nature medicine* **19**: 576-585.
- Kolvenbach, B.A., Helbling, D.E., Kohler, H.P., and Corvini, P.F. (2014) Emerging chemicals and the evolution of biodegradation capacities and pathways in bacteria. *Curr Opin Biotechnol* **27**: 8-14.
- Li, R., Zhu, H., Ruan, J., Qian, W., Fang, X., Shi, Z. et al. (2010) De novo assembly of human genomes with massively parallel short read sequencing. *Genome Res* **20**: 265-272.
- Lidbury, I., Murrell, C.J., and Chen, Y. (2014) Trimethylamine N-oxide metabolism by abundant marine heterotrophic bacteria. *Proceeding of the National Academy of Sciences* **111**: 2710-2715.
- Liffourrena, A.S., and Lucchesi, G.I. (2014) Identification, cloning and biochemical characterization of *Pseudomonas putida* A (ATCC 12633) monooxygenase enzyme necessary for the metabolism of tetradecyltrimethylammonium bromide. *Appl Biochem Biotechnol* **173**: 552-561.
- Liffourrena, A.S., Lopez, F.G., Salvano, M.A., Domenech, C.E., and Lucchesi, G.I. (2008) Degradation of tetradecyltrimethylammonium by *Pseudomonas putida* A ATCC 12633 restricted by accumulation of trimethylamine is alleviated by addition of Al³⁺ ions. *J Appl Microbiol* **104**: 396-402.

- Loos, R., Carvalho, R., Antonio, D.C., Comero, S., Locoro, G., Tavazzi, S. et al. (2013) EU-wide monitoring survey on emerging polar organic contaminants in wastewater treatment plant effluents. *Water Res* **47**: 6475-6487.
- Luo, C., Rodriguez, R.L., and Konstantinidis, K.T. (2013) A user's guide to quantitative and comparative analysis of metagenomic datasets. *Methods Enzymol* **531**: 525-547.
- Martinez, S., and Hausinger, R.P. (2015) Catalytic Mechanisms of Fe(II)- and 2-Oxoglutarate-dependent Oxygenases. *J Biol Chem* **290**: 20702-20711.
- Mc Cay, P.H., Ocampo-Sosa, A.A., and Fleming, G.T. (2010) Effect of subinhibitory concentrations of benzalkonium chloride on the competitiveness of *Pseudomonas aeruginosa* grown in continuous culture. *Microbiology* **156**: 30-38.
- Moen, B., Rudi, K., Bore, E., and Langsrud, S. (2012) Subminimal inhibitory concentrations of the disinfectant benzalkonium chloride select for a tolerant subpopulation of *Escherichia coli* with inheritable characteristics. *Int J Mol Sci* **13**: 4101-4123.
- Nakata, K., Tsuchido, T., and Matsumura, Y. (2011) Antimicrobial cationic surfactant, cetyltrimethylammonium bromide, induces superoxide stress in *Escherichia coli* cells. *J Appl Microbiol* **110**: 568-579.
- Nam, J.W., Nojiri, H., Yoshida, T., Habe, H., Yamane, H., and Omori, T. (2001) New classification system for oxygenase components involved in ring-hydroxylating oxygenations. *Biosci Biotechnol Biochem* **65**: 254-263.
- Neilson, A.H., and Allard, A.-S. (2008) *Environmental Degradation and Transformation of Organic Chemicals*. 6000 Broken Sound Parkway NW, Suite 300 Boca Raton, FL 33487-2742: CRC Press
Taylor & Francis Group.
- Nunoshiba, T., Hidalgo, E., Cuevas, C.F.A., and Demple, B. (1992) Two-Stage Control of an Oxidative Stress Regulon: the *Escherichia coli* SoxR Protein Triggers Redox-Inducible Expression of the soxS Regulatory Gene. *Journal of Bacteriology* **174**: 6054-6060.
- Oh, S., Tandukar, M., Pavlostathis, S.G., Chain, P.S., and Konstantinidis, K.T. (2013) Microbial community adaptation to quaternary ammonium biocides as revealed by metagenomics. *Environ Microbiol* **15**: 2850-2864.
- Oh, S., Kurt, Z., Tsemenzi, D., Weigand, M.R., Kim, M., Hatt, J. et al. (2014) Microbial Community Degradation of Widely Used Quaternary Ammonium Disinfectants. *Applied and Environmental Microbiology* **80**: 5892-5900.
- Patrauchan, M.A., and Oriel, P.J. (2003) Degradation of benzyldimethylalkylammonium chloride. *Journal of Applied Microbiology* **94**: 266-272.
- Perneel, M., Heyrman, J., Adiobo, A., De Maeyer, K., Raaijmakers, J.M., De Vos, P., and Hofte, M. (2007) Characterization of CMR5c and CMR12a, novel fluorescent *Pseudomonas* strains from the cocoyam rhizosphere with biocontrol activity. *J Appl Microbiol* **103**: 1007-1020.
- Phillips, D.A., Joseph, C.M., and Maxwell, C.A. (1992) Trigonelline and Stachydrine Released from Alfalfa Seeds Activate NodD2 Protein in *Rhizobium meliloti*. *Plant Physiology* **99**: 1526-1531.

- Pieper, D., Gonzalez, B., Camara, B., Perez-Pantoja, D., and Reineke, W. (2010) Aerobic Degradation of Chloroaromatics. In *Handbook of Hydrocarbon and Lipid Microbiology*. Timmis, K.N. (ed). Berlin, Heidelberg 978-3-540-77587-4: Springer Berlin Heidelberg, pp. 839-864.
- Qiu, J., Yun, M., Zhang, J., Wen, Y., and Weiping, L. (2013) Cloning of a Novel Nicotine Oxidase Gene from *Pseudomonas* sp. Strain HZN6 Whose Product Nonenantioselectively Degrades Nicotine to Pseudonicotine. *Applied and Environmental Microbiology* **79**: 2164-2171.
- Rathinasabapathi, B., Burnet, M., Russell, B.L., Gage, D.A., Liao, P.-C., Nye, G.J. et al. (1997) Choline monooxygenase, an unusual iron-sulfur enzyme catalyzing the first step of glycine betaine synthesis in plants: Prosthetic group characterization and cDNA cloning. *Proceeding of the National Academy of Sciences* **94**: 3454-3458.
- Rieger, P.G., Meier, H.M., Gerle, M., Vogt, U., Groth, T., Knackmuss, H.J. et al. (2002) Xenobiotics in the environment: present and future strategies to obviate the problem of biological persistence. *Journal of Biotechnology* **94**: 101-123.
- Rodriguez, R.L., and Konstantinidis, K.T. (2014) Nonpareil: a redundancy-based approach to assess the level of coverage in metagenomic datasets. *Bioinformatics* **30**: 629-635.
- Sarand, I., Haario, H., Jorgensen, K.S., and Romantschuk, M. (2000) Effect of inoculation of a TOL plasmid containing mycorrhizosphere bacterium on development of Scots pine seedlings, their mycorrhizosphere and the microbial flora in m-toluolate-amended soil. *FEMS Microbiology Ecology* **31**: 127-141.
- Schofield, S.J., and Zhang, Z. (1999) Structural and mechanistic studies on 2-oxoglutarate dependent oxygenases and related enzymes. *Current Opinion in Structural Biology* **9**: 722-731.
- Selbes, M., Kim, D., Ates, N., and Karanfil, T. (2013) The roles of tertiary amine structure, background organic matter and chloramine species on NDMA formation. *Water Res* **47**: 945-953.
- Shimizu, T., and Nakamura, A. (2014) Characterization of LgnR, an IclR family transcriptional regulator involved in the regulation of L-gluconate catabolic genes in *Paracoccus* sp. 43P. *Microbiology* **160**: 623-634.
- Springael, D., Peys, K., Ryngaert, A., Van Roy, S., Hooyberghs, L., Ravatn, R. et al. (2002) Community shifts in a seeded 3-chlorobenzoate degrading membrane biofilm reactor: indications for involvement of in situ horizontal transfer of the *clc*-element from inoculum to contaminant bacteria. *Environmental Microbiology* **4**: 70-80.
- Stover, C.K., Pham, X.Q., Erwin, A.L., Mizoguchi, S.D., Warrener, P., Hickey, M.J. et al. (2000) Complete genome sequence of *Pseudomonas aeruginosa* PA01, an opportunistic pathogen. *Nature* **406**: 959-964.
- Su, X., Pan, W., Song, B., Xu, J., and Ning, K. (2014) Parallel-META 2.0: Enhanced Metagenomic Data Analysis with Functional Annotation, High Performance Computing and Advanced Visualization. *PLoS One* **9**: 1-13.

- Takenaka, S., Tonoki, T., Taira, K., Murakami, S., and Aoki, K. (2007) Adaptation of *Pseudomonas* sp. strain 7-6 to quaternary ammonium compounds and their degradation via dual pathways. *Applied and Environmental Microbiology* **73**: 1797-1802.
- Tan, H.M. (1999) Bacterial catabolic transposons. *Appl Microbiol Biotechnol* **51**: 1-12.
- Tandukar, M., Oh, S., Tezel, U., Konstantinidis, K.T., and Pavlostathis, S.G. (2013) Long-term exposure to benzalkonium chloride disinfectants results in change of microbial community structure and increased antimicrobial resistance. *Environ Sci Technol* **47**: 9730-9738.
- Tezel, U., and Pavlostathis, U. (2012) Role of quaternary ammonium compounds on antimicrobial resistance in the environment In *Antimicrobial Resistance in the Environment*. Keen, P.L., and Montforts, M.H.M.M. (eds). New Jersey: Wiley-Blackwell, pp. 349-388.
- Tezel, U., and Pavlostathis, S.G. (2015) Quaternary ammonium disinfectants: microbial adaptation, degradation and ecology. *Curr Opin Biotechnol* **33**: 296-304.
- Tezel, U., Tandukar, M., Martinez, R.J., Sobocky, P.A., and Pavlostathis, S.G. (2012) Aerobic biotransformation of n-tetradecylbenzyltrimethylammonium chloride by an enriched *Pseudomonas* spp. community. *Environ Sci Technol* **46**: 8714-8722.
- Top, E.M., and Springael, D. (2003) The role of mobile genetic elements in bacterial adaptation to xenobiotic organic compounds. *Current Opinion in Biotechnology* **14**: 262-269.
- Ufarte, L., Laville, E., Duquesne, S., and Potocki-Veronese, G. (2015) Metagenomics for the discovery of pollutant degrading enzymes. *Biotechnol Adv* **33**: 1845-1854.
- van der Meer, J.R., Ravatn, R., and Sentchilo, V. (2001) The *clc* element of *Pseudomonas* sp. strain B13 and other mobile degradative elements employing phage-like integrases. *Archives of Microbiology* **175**: 79-85.
- Van Ginkel, C.G. (2004) Biodegradation of Cationic Surfactants. 523-549.
- van Ginkel, C.G., van Dijk, J.B., and Kroon, A.G.M. (1992) Metabolism of Hexadecyltrimethylammonium chloride in *Pseudomonas* strain B1. *Applied and Environmental Microbiology* **58**: 3083-3087.
- von der Ohe, P.C., Dulio, V., Slobodnik, J., De Deckere, E., Kuhne, R., Ebert, R.U. et al. (2011) A new risk assessment approach for the prioritization of 500 classical and emerging organic microcontaminants as potential river basin specific pollutants under the European Water Framework Directive. *Sci Total Environ* **409**: 2064-2077.
- Wackett, L.P. (2002) Mechanism and applications of Rieske non-heme iron dioxygenases. *Enzyme and Microbial Technology* **31**: 577-587.
- Wackett, L.P., and Hershberger, C.D. (2001) *Biodegradation and Biocatalysis*. 1752 N St., N.W., Washington, DC 20036-2904, U.S.A.: ASM Press.
- Xu, M., Wu, W.M., Wu, L., He, Z., Van Nostrand, J.D., Deng, Y. et al. (2010) Responses of microbial community functional structures to pilot-scale uranium in situ bioremediation. *ISME J* **4**: 1060-1070.

- Zelezniak, A., Andrejev, S., Ponomarova, O., Mende, D.R., Bork, P., and Patil, K.R. (2015) Metabolic dependencies drive species co-occurrence in diverse microbial communities. *Proc Natl Acad Sci U S A* **112**: 6449-6454.
- Zerbino, D.R., and Birney, E. (2008) Velvet: algorithms for de novo short read assembly using de Bruijn graphs. *Genome Res* **18**: 821-829.
- Zhu, W., Lomsadze, A., and Borodovsky, M. (2010) Ab initio gene identification in metagenomic sequences. *Nucleic Acids Res* **38**: e132.
- Zhu, Y., E., J., Croasatti, M., Schafer, H., Rajakumar, K., Bugg, T.D., and Chen, Y. (2014) Carnitine metabolism to trimethylamine by an unusual Rieske-type oxygenase from human microbiota. *Proceeding of the National Academy of Sciences* **111**: 4268-4273.